FINAL REPORT

Estimated Exposure and Lifetime Cancer Incidence Risk from 903 Area Plutonium Releases at the Rocky Flats Plant

Part of Task 3: Independent Analysis of Exposure, Dose, and Health Risk to Offsite Individuals

August 1999

Submitted to the Colorado Department of Public Health and Environment, Disease Control and Environmental Epidemiology Division, Rocky Flats Health Studies in partial fulfillment of Contract No. 100APPRCODE 391

"Setting the standard in environmental health"

RAC

Radiological Assessments Corporation
417 Till Road Neeses, South Carolina 29107
phone 803.536.4883 fax 803.534.1995

FINAL REPORT

Estimated Exposure and Lifetime Cancer Incidence Risk from 903 Area Plutonium Releases at the Rocky Flats Plant

Part of Task 3: Independent Analysis of Exposure, Dose, and Health Risk to Offsite Individuals

August 1999

Authors

Arthur S. Rood, K-Spar, Inc.
Helen A. Grogan Ph.D., Cascade Scientific Inc.

Principal Investigator

John E Till, Ph.D., *Radiological Assessments Corporation*

EXECUTIVE SUMMARY

The Rocky Flats Environmental Technology Site is owned by the U.S. Department of Energy (DOE) and is currently contractor-operated by Kaiser-Hill Company. For most of its history, the site was called the Rocky Flats Plant (RFP) and was operated by Dow Chemical Company as a nuclear weapons research, development, and production complex. The RFP is located about 8–10 km from the cities of Arvada, Westminster, and Broomfield, Colorado, and 26 km (16 mi). northwest of downtown Denver, Colorado.

Through a 1989 Agreement in Principle between DOE and the State of Colorado, DOE provided the State with funding and technical support for health-related studies. The purpose of the Historical Public Exposures Studies on Rocky Flats is to estimate exposure to nearby residents from past toxic and radioactive releases from the plant.

This report documents fate and transport calculations and lifetime cancer incidence risk estimates for inhalation of plutonium[1]-contaminated soil suspended from the 903 Area for the period 1964–1969. Risk estimates are reported in terms of probability distributions that reflect the uncertainty in the calculation. It presents estimates of time-averaged plutonium airborne concentrations for three different particle sizes at selected receptor locations within the model domain. Lifetime cancer incidence risks are then calculated for hypothetical individuals residing in the model domain who inhale plutonium-contaminated dust. Behavior and physical attributes of hypothetical individuals are characterized by exposure scenarios that are discussed in detail. Details of atmospheric transport modeling and uncertainty estimates are described. Atmospheric transport calculations and risk estimates made in Phase I are summarized, and an overview of the source term developed for Phase II and documented in Weber et al. (1999) is provided. Lifetime cancer incidence risks using risk coefficients and associated uncertainty developed by Grogan et al. (1999) are summarized.

903 Area Background and Source Term. The 903 Area is located in the eastern part of the main production area of the RFP. The 903 Area served as a waste storage area for barrels containing plutonium-laden cutting oil and degreasing agents during the late 1950s and 1960s. The barrels were stored outside on a grassy area that became known as the 903 Area. Four thousand seven hundred and twenty-nine barrels were reported to have been stored at the 903 Area. By 1964, there was evidence of large-scale corrosion and subsequent leakage of barrel contents onto the soil. In 1967, efforts were made to remove the barrels from the 903 Area, repackage the contents, and ship the waste offsite. Drum removal was completed in 1968 and 1969, and the now empty area was cleared of vegetation, graded, and paved.

During the removal and subsequent paving operations, plutonium-contaminated soil was suspended by wind and mechanical disturbance. Suspension of plutonium-contaminated soil was most prevalent during high wind events and evidenced by high count rates observed at ambient air samplers, especially at S-8 sampler, which is located downwind (east) from the 903 Area.

Plutonium activity released from the barrels onto the soil was investigated by Phase II researchers (Meyer et al. 1996). This investigation reviewed Dow Chemical Company's (the site

[1] In this context, the word plutonium means weapons grade plutonium, which consists primarily of ^{239}Pu (~93.8%) ^{240}Pu (≈5.8%), and ^{241}Pu (~0.36%) by weight percent. Specific activity of weapons grade plutonium is 0.072 Ci g^{-1}.

contractor) estimate of the amount of plutonium released from the barrels (~85 g or 6.1 Ci) along with an alternative upper bound estimate of 800 g (58 Ci). Airborne suspension of contaminated soil particles from the 903 Area was investigated by Weber et al. (1999). The investigation revealed that high count rates observed at the S-8 sampler were strongly correlated with high wind events reported at the Jefferson County Airport and portable meteorological recording stations located near the RFP. In addition, the samplers surrounding the 903 Area and the S-8 sampler, in particular, had generally higher counts rates from 1964 to 1969 compared to other years. These higher counts suggest suspension of plutonium-contaminated soil was occurring somewhat regularly during this period.

Wind speed-dependent soil suspension models were investigated: however, data needed to characterize soil conditions during suspension events were lacking. Therefore, releases from the suspension model were calibrated to daily S-8 sampler measurements. Deficiencies in the sampling apparatus were accounted for in the calculations. Releases were calculated for particles up to 30-μm aerodynamic equivalent diameter (AED) because particles larger than that generally went undetected by the sampler. Release of plutonium-contaminated particles larger that 30-μm AED is of interest for offsite contamination, but larger particles do not pose the inhalation health risk that smaller particles do because they are nonrespirable. Furthermore, larger particles do not behave like smaller particles during erosion and atmospheric transport. The principal transport mechanism of particles >50 μm physical diameter is saltation. Particles in this size range tend to deposit quickly because their gravitational settling velocities are greater than the turbulent motions of the air (Whicker and Schultz 1982). The nearest site boundary is about 2.5-km east of the 903 Area.

Total activity released on particles <30-μm AED ranged from 1.4 Ci (5th percentile value) to 15 Ci (95th percentile value). Releases were calculated for the 24 days in 1968 and 1969 with the highest count rates observed at the S-8 sampler and annually for releases that occurred more-or-less continuously. We called the former of these releases discrete releases and the latter baseline releases.

Environmental Transport Modeling. Five atmospheric transport models, ranging from a simple straight-line Gaussian plume model to a complex terrain model, were evaluated for use in this study (Rood 1999a). Models were compared to tracer measurements taken in the winter of 1991 at Rocky Flats. The results of this evaluation indicated no one model clearly outperformed the others. However, the puff trajectory models (RATCHET, TRIAD, and INPUFF2) generally had lower variability and higher correlation to observed values compared to the other models. The RATCHET model was chosen for these calculations because it incorporates spatially varying meteorological and environmental parameters. Additionally, the model includes modules that perform random sampling of the meteorological parameters, allowing for Monte Carlo analysis of uncertainty.

The model domain encompassed a 2200-km^2 area (50 km north-south × 44 km east-west). The domain extended 28 km south, 12 km west, 22 km north, and 32 km east from the RFP. Most of the Denver metropolitan area and the city of Boulder were included in the domain.

Transport calculations were simplified by considering only 6 of the 24 discrete events explicitly. The remainder of the estimated activity released during discrete events was added to the baseline releases for their respective years. The six highest discrete events accounted for ~ 90% of the total activity attached to particles <30-μm AED estimated to have been released from the 903 Area.

Reliable meteorological data from RFP for the time frame of interest were lacking (1964 to 1969). However, strip charts from portable meteorological stations set up north of the RFP during 1968 through 1969 were obtained and used to define hourly average wind speed and direction for the discrete events. These were also the same data used to calibrate the wind speed-dependent suspension model to S-8 sampler data. We supplemented these data with cloud cover and ceiling height data from Jefferson County Airport and Denver Stapleton International Airport to derive atmospheric stability class estimates.

Baseline releases were treated as steady-state annual releases. Because meteorological data spanning the entire time frame of interest were lacking (1964–1969), a recent 5-year (1989–1993) meteorological data set was used to determine annual average *X*/Q (air concentration divided by release rate) values for baseline releases. Meteorological data taken at the Denver Stapleton International Airport during the same period were also incorporated into the simulations. Annual average concentrations for each year were then determined by multiplying the annual baseline release rate by the appropriate *X*/Q value.

Risk calculations were performed for three different particle size fractions: <3 μm, 3—10 μm, and 10–15 μm. Particles >15-μm AED do not pose the same inhalation health risk as smaller particles. These particles do not even penetrate as far as the bronchial region of the respirable tract and are eliminated from the body rapidly via transfer to the gastrointestinal tract and subsequent excretion or direct expulsion (i.e., nose blowing) to the environment (ICRP 1994). Particles >15 μm, therefore, are considered nonrespirable.

Treatment of Uncertainty. Risk estimates were reported as probability distributions that reflect our current state of knowledge of the problem. They do not represent the probability of seeing a health effect within the population of potential receptors. Uncertainty for discrete releases was calculated differently than for baseline releases. Uncertainty for discrete events employed the Monte Carlo sampling features of the RATCHET code, which considered uncertainty in the wind speed, wind direction, Monin-Obukhov scaling length, and mixing height. This allowed for mass balance of material within the model domain for every Monte Carlo trial.

For baseline releases, model prediction uncertainty was accounted for using several multiplicative stochastic correction factors that accounted for uncertainty in the dispersion estimate, the meteorology, and deposition and plume depletion. Dispersion uncertainty was based on distributions of predicted-to-observed ratios from field tracer experiments using the Gaussian plume and other models, including RATCHET. These values were derived from literature reviews and results from studies specific to this project. Meteorological uncertainty arises because we used 5 years of meteorological data spanning a recent time period (1989–1993) to define an annual average *X/Q* value that was applied to the specific years of the assessment period (1964–1969). This correction factor was derived from studies performed for the Fernald Dosimetry Reconstruction Project (Killough et al. 1998) and additional comparisons made at Rocky Flats. Deposition and plume depletion uncertainty factors were calculated using the Monte Carlo sampling features of RATCHET. All correction factors were distributed lognormally and were combined with the source term uncertainty to yield distributions of predicted concentrations at selected receptor locations. Monte Carlo techniques were used to propagate model prediction uncertainty through to the final risk calculations.

Predicted Air Concentrations. Median value predicted time-integrated concentration (*TIC*) of plutonium attached to respirable soil particles (<15-μm AED) east of the plant along Indiana

Street were around 1 fCi-y m^{-3}. Discrete events were responsible for about 50% of the airborne activity concentration at this location. At almost all other locations, the baseline releases had the greatest contribution. The relative importance of discrete and baseline events is attributed to two factors. First, the discrete events resulted in relatively narrow plumes of airborne contamination so that receptors outside the plume were unaffected by the release. Second, the high wind events that were responsible for suspension of relatively large amounts of plutonium-contaminated soil also contributed to greater dilution and dispersion of the airborne plume, resulting in lower airborne concentrations.

Exposure Scenarios. The risk that a person experiences depends upon a number of factors, such as

- Where the person lived and worked in relation to the RFP
- When and how long that person lived near the RFP (for example, during the key release events in 1960s or in the 1970s when releases were less)
- Lifestyle (that is, did the person spend a great deal of time outdoors or doing heavy work on a farm)
- Age and gender of the person.

To consider these features of a person's life, we developed profiles (or exposure scenarios) of hypothetical, but realistic, residents of the RFP area for which representative risk estimates could be made. Risks were calculated for seven hypothetical exposure scenarios. These scenarios incorporate typical lifestyles, ages, genders, and lengths of time in the area, and they can help individuals determine risk ranges for themselves by finding a lifestyle profile that most closely matches their background. The scenarios are not designed to include all conceivable lifestyles of residents who lived in this region during the time of the RFP operations. Rather, they provide a range of potential profiles of people in the area.

The seven exposure scenarios were distributed at 18 locations within the model domain. Seven rancher scenarios were located east of the RFP along Indiana Avenue to intercept all possible discrete event plume paths. Scenarios also included a housewife, infant, child, student, and laborer who lived in communities surrounding the RFP (Broomfield, Westminster, Arvada, and Boulder) and office worker who lived in downtown Denver.

Inhalation of activity suspended directly from the 903 Area was the only pathway considered in the evaluation. We made this decision based on the Phase I results (ChemRisk 1994a) that showed soil ingestion and inhalation of *resuspended* plutonium to be minor pathways when considering the long-term exposure to Rocky Flats effluent. We recognize that these two later pathways become increasingly important for the later years of exposure because of the accumulation of deposited plutonium in soil and the lower airborne emissions. However, doses during this period (1971–1989) were several orders of magnitude smaller than doses for earlier years (1952–1970). The inhalation of resuspended plutonium will be addressed later in a comprehensive risk report covering all releases from the RFP.

Each receptor scenario incorporates inhalation rates that reflect their lifestyle. For example, the rancher's breathing rate reflects one who performs manual labor for part of the day. Uncertainty was not incorporated into the exposure scenarios; that is, the physical attributes and behavior of the receptors were assumed to be fixed. The calculated risks were not intended to represent a population of receptors who exhibit a given behavior.

Plutonium Risk Coefficients. Lifetime cancer incidence risk coefficients (risk per unit intake) with uncertainty for plutonium were developed by Grogan et al. (1999) for the four critical organs: lung, liver, bone surface, and bone marrow (leukemia). Where feasible, gender- and age-specific risk coefficients were determined. Risk coefficients were reported for three different particle size distributions having geometric mean values of 1 μm, 5 μm, and 10 μm activity median aerodynamic diameter and a geometric standard deviation of 2.5 in all cases.

Incremental Lifetime Cancer Incidence Risk Estimates. Geometric mean incremental lifetime cancer incidence risk estimates for plutonium inhalation were greatest for lung followed by liver, bone surface, and bone marrow. The Rancher #4 scenario exhibited the highest inhalation risks. Lifetime cancer incidence risk for this scenario ranged from 4.4×10^{-8} (2.5 percentile) to 3.3×10^{-5} (97.5 percentile), with a geometric mean value of 1×10^{-6}. Using this rancher scenario as an example, these risks may be interpreted as follows:

- There is a 95% probability that incremental lifetime cancer incidence risk was between 4.4×10^{-8} (2.5% value) and 3.3×10^{-5} (97.5% value).
- There is a 2.5% probability that incremental lifetime cancer incidence risk was greater than 3.3×10^{-5} and a 2.5% probability the risk was less than between and 4.4×10^{-8}.

We may also interpret this as, given an exposure history and lifestyle similar to that of the Rancher #4 scenario, there is a 97.5% probability that the expected number of cancer cases attributed to inhalation of plutonium originating from the 903 Area would be no greater than 33 persons in a population of 1million similarly exposed individuals.

The magnitude of the lifetime cancer incidence risk was dependent mainly on the location of the receptor. Plumes from the discrete events, which account for most of the 903 Area releases, were confined to a relatively narrow corridor east of the 903 Area. Receptors located outside the plume trajectory generally received little or no exposure. The high winds responsible for suspension during discrete events also resulted in greater dilution and dispersion of airborne material, resulting in lower air concentrations. Consequently, exposure attributed to baseline releases made up a substantial portion of the overall exposure received by the receptors in the model domain. In general, the discrete events only contributed substantially to rancher scenario exposures. The calculated risks were within the U.S. Environmental Protection Agency point of departure for acceptable lifetime cancer incidence risk of 1 in 1,000,000 to 1 in 10,000 people.

ACRONYMS

AED	aerodynamic equivalent diameter
AMAD	activity median aerodynamic diameter
ASCOT	Atmospheric Studies in Complex Terrain
CDPHE	Colorado Department of Public Health and Environment
CI	confidence interval
DOE	U.S. Department of Energy
EPA	U.S. Environmental Protection Agency
FDM	Fugitive Dust Model
GM	geometric mean
GSD	geometric standard deviation
HAP	Health Advisory Panel
ICRP	International Commission on Radiological Protection
ISC	Industrial Source Complex Short Term Version 2
INPUFF	INtegrated PUFF dispersion code
LET	linear energy transfer
NCAR	National Center for Atmospheric Research
RAC	*Radiological Assessments Corporation*[2]
RATCHET	Regional Atmospheric Transport Code for Hanford Emission Tracking
RFP	Rocky Flats Plant
RBE	relative biological effectiveness
TIC	time-integrated concentration
TRAC	Terrain-Responsive Atmospheric Code
TLLa	total long-lived alpha activity
UTM	universal transverse mercator
WVTS	Winter Validation Tracer Study

[2] In 1998 *Radiological Assessments Corporation* changed its name to *Risk Assessment Corporation*. For consistency throughout the project, all reports were published by *Radiological Assessments Corporation*.

CONTENTS

Figures

Tables

INTRODUCTION

The Rocky Flats Environmental Technology Site is owned by the U.S. Department of Energy (DOE) and is currently contractor-operated by Kaiser-Hill Company. For most of its history, the site was called the Rocky Flats Plant (RFP) and was operated by Dow Chemical Company as a nuclear weapons research, development, and production complex (Figure 1). The RFP is located on approximately 2650 ha (6500 acres) of Federal property, about 8–10 km from the cities of Arvada, Westminster, and Broomfield, Colorado and 26 km northwest of downtown Denver, Colorado. The original 156-ha (385-acre) main production area is surrounded by a 2490-ha (6150-acre) buffer zone that now delineates the RFP boundary.

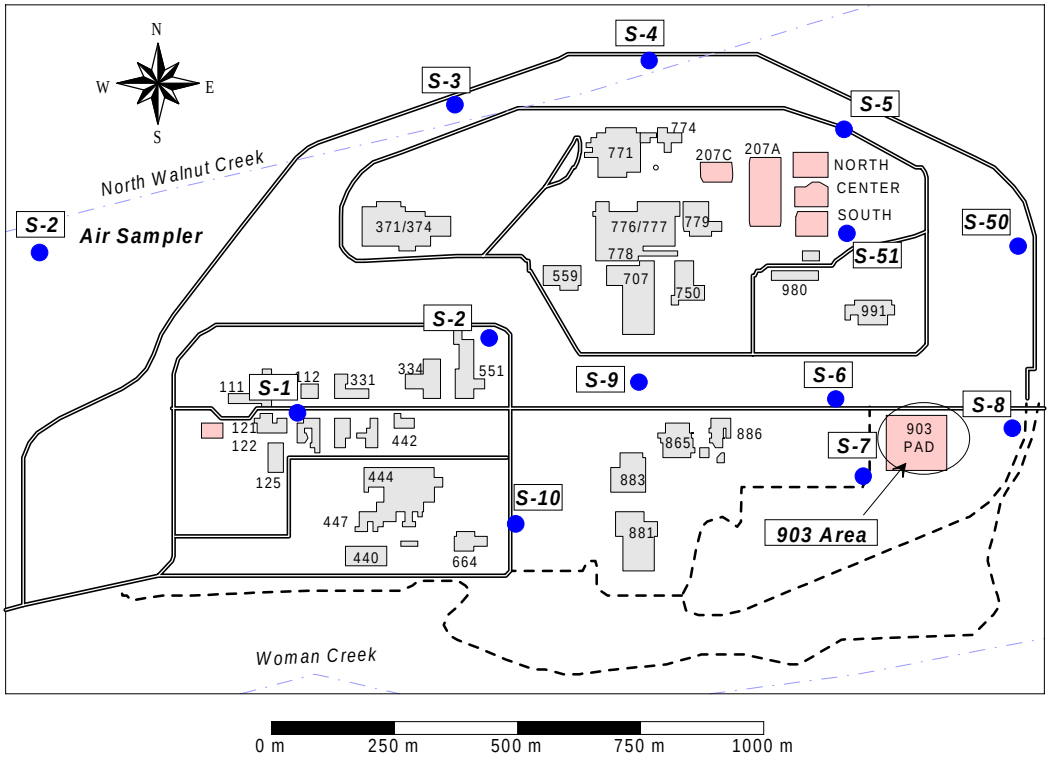

Figure 1. Main production area of the Rocky Flats Plant as it appeared in 1990. Originally, the buildings were identified with two-digit numbers. Later, a third digit was added. The production area, now sometimes called the industrial area, is surrounded by a security perimeter fence. Placement of air samplers is based on air sampler locations and numbers that existed before 1973. See Chapter II and Appendix B in Rope et al. (1999) for maps of air sampler locations as they existed with respect to past features.

Through a 1989 Agreement in Principle between the DOE and the State of Colorado, DOE provided the State with funding and technical support for health-related studies. The purpose of the Historical Public Exposures Studies on Rocky Flats is to estimate exposure to nearby residents from past toxic and radioactive releases from the plant. The Colorado Department of Public Health and Environment (CDPHE) first invited a national panel of experts to help design the health studies. Because of intense public concern about Rocky Flats contamination among

Denver metropolitan area residents following a Federal Bureau of Investigation raid of Rocky Flats in June 1989, the panel decided to stress public involvement and to separate the research into two major phases conducted by two different contractors to enhance accountability and credibility.

Phase I of the study was performed by ChemRisk (a division of McLaren/Hart, Environmental Engineering). In Phase I, ChemRisk conducted an extensive investigation of past operations and releases from the RFP. The Phase I effort identified the primary materials of concern, release points and events, quantities released, transport pathways, and preliminary estimates of dose and risk to offsite individuals. The conclusions from Phase I were released in a public summary document (HAP 1993), a series of task reports by ChemRisk, and several articles in the journal *Health Physics*.

Radiological Assessments Corporation (*RAC*) was awarded the contract to conduct Phase II of the study, which is an in-depth investigation of the potential doses and risks to the public from historical releases from Rocky Flats. Recommendations for work to be performed in Phase II are outlined in the Phase I summary document HAP (1993).

This report documents fate and transport calculations and lifetime cancer incidence risk estimates for inhalation of plutonium[1]-contaminated soil suspended from the 903 Area for the period 1964–1969. Risk estimates are reported in terms of probability distributions that reflect the uncertainty in the calculation. Time-averaged plutonium airborne concentrations for three different particle sizes are estimated at selected receptor locations within the model domain. Lifetime cancer incidence risks are then calculated for hypothetical individuals residing in the model domain who inhale plutonium-contaminated dust. Behavior and physical attributes of hypothetical individuals are characterized by exposure scenarios, which are discussed in detail. This report describes details of atmospheric transport modeling and uncertainty estimates, summarizes atmospheric transport calculations and risk estimates made in Phase I, and provides an overview of the source term developed for Phase II and documented in Weber et al. (1999). Lifetime cancer incidence risks using risk coefficients and associated uncertainty developed by Grogan et al. (1999) are also summarized.

OVERVIEW OF THE 903 AREA

The background and nature of the releases from the 903 Area are described in Meyer et al. (1996). A brief summary of their findings is provided here. The 903 Area is located in the eastern part of the main production area of the RFP (see Figure 1). The 903 Area served as a waste storage area for barrels containing cutting oil and degreasing agents during the late 1950s and 1960s. This oil became contaminated with plutonium during its use at the plant as a lubricant for plutonium-machining tools. Degreasing agents primarily consisted of carbon tetrachloride. This combination of radiological and hazardous chemicals precluded its storage in traditional waste disposal locations at the RFP. Consequently, waste was transferred to 55-gal barrels and the barrels were stored outside on a grassy area that became known as the 903 Area. Four thousand seven hundred and twenty-nine barrels were reported to have been stored at the 903 Area.

[1] In this context, the word plutonium means weapons grade plutonium, which consists primarily of ^{239}Pu (~ 93.8%) ^{240}Pu (≈5.8%),and ^{241}Pu (~0.36%) by weight percent. Specific activity of weapons grade plutonium is 0.072 Ci g^{-1}.

As early as 1962, evidence of barrel corrosion and subsequent leakage onto the soil was detected by site personnel. In 1964, the first evidence of large-scale leakage was reported, and fences were constructed to limit the spread of contamination by intruding wildlife. In 1967, efforts were made to remove the barrels from the 903 Area, repackage the contents, and ship the waste to the Idaho National Engineering Laboratory. Barrel removal was completed in June of 1968. A total of 4826 repackaged barrels containing uranium, plutonium, and trash or tars were removed from the 903 Area. This number was inconsistent with the number of barrels reported to have been delivered to the area (5237). This difference (411 barrels) is assumed to be due to the fact that a number of barrels were not full, either originally or due to leakage, and were combined with the contents of other barrels during the repackaging processes. By late 1968, there was evidence that plutonium-contaminated soil had been transported outside the 903 Area boundaries, primarily by wind suspension. In 1969, efforts were made to place an asphalt surface over the contaminated area. During January of that year, high wind events were reported to have spread the contamination further, as indicated by site survey reports and perimeter air samplers east of the area. In March and April 1969, during surface grading and leveling operations in preparation for paving, large plumes of dust were visible 0.8 km past the perimeter security fence. In July 1969, the first coat of asphalt was applied and paving was completed in November of that year. Meyer et al. (1996) estimated the mass of plutonium released to the soil from leaking barrels ranged from 85 g to an upper bound of 800 g (6.1 to 58 Ci).

REVIEW OF THE PHASE I 903 AREA RELEASES AND RISK ESTIMATES

In Phase I, the release of plutonium from the 903 Area[2] was believed to have been the largest nonroutine release of plutonium from the RFP. Considerable effort was put into quantifying and characterizing this release.

The Fugitive Dust Model (FDM, Winges 1990) was used to model the atmospheric transport and deposition processes that removed contaminated soil from the 903 Area and deposited it in the surrounding areas. The FDM provided both air and soil concentration predictions. Key input data for the FDM were the meteorological conditions, the particle size distribution of potentially resuspendable soil, and the relationship between the soil particle size and the extent of plutonium contamination. These are summarized as follows.

A meteorological data set for 1987–1991 was used to represent meteorological conditions at Rocky Flats during the 1964–1969 period of release. This surrogate data set was used in the absence of direct meteorological data of adequate quality.

The potentially resuspendable contaminated soil particle size distribution was assumed to be lognormal, with a mass median physical diameter of 200 μm and a geometric standard deviation (GSD) of 6.18. Under these circumstances, 5% of the soil mass is made up of soil particles less than 5-μm physical diameter (8-μm aerodynamic equivalent diameter [AED]). The amount of plutonium contamination was assumed to be directly proportional to the mass of airborne soil particles.

Soil sample measurements of plutonium taken between 1969 and 1973 were compiled and checked for consistency and accuracy. Three sources of uncertainty in the soil sampling data were treated in the analysis: analytic, soil dry bulk density, and soil plutonium inventory

[2] 903 Area is referred to as 903 Pad in Phase I reports.

distribution. These data were central to the analysis because the FDM was used to estimate releases from the pad that would lead to the soil contamination pattern observed in late 1969 and the early 1970s.

Many different release scenarios were analyzed, ranging from assuming the majority of the release was associated with grading activities on just one or more days in 1968 and 1969, to assuming that the releases occurred throughout the 5 years following the first reported observations of deterioration of drums at the 903 Area until the pad area was paved in 1969. Based on the predictions of the FDM, the release scenario that gave the best fit to all the available data and assumptions used in the reconstruction was one that extended over a number of years; thus, the 903 Area was treated as a release event that occurred over a 5-year period. Although actual releases from the pad were likely to have varied daily, it was considered that insufficient information was available to permit evaluation of short time span releases.

Air concentrations measured in onsite air samplers (S-6, S-7, and S-8) were not used to estimate releases from the 903 Area directly. They were compared with the FDM model predictions for two purposes:

1. To evaluate the potential for a wind speed dependency for contaminant release based on relative sampler readings, and
2. To determine whether the observed average air sampling results were consistent with the average air concentrations predicted under the estimated release scenario developed using the soil sampling data set and the FDM.

Based on these comparisons, the plutonium releases were assumed to be proportional to the fifth power of the wind speed (v^5) for the model calculations with the FDM. Also, the air concentrations predicted with the FDM were consistently larger than the observed concentrations. Because the observed concentrations were within the predicted uncertainty estimates, the model predictions were considered satisfactory.

A total release of 25 Ci of plutonium was predicted from the 903 Area. This was considered a best estimate (geometric mean [GM]) of the source term, which had an order of magnitude uncertainty in either direction (GSD 3.3). Of the 25 Ci released,

- 11.4 Ci were redeposited on the pad
- 13.6 Ci escaped from the pad.

Of the 13.6 Ci that escaped,

- 5.6 Ci were deposited between the pad and the plant exclusion boundary
- 1.2 Ci were deposited between the plant exclusion boundary and the buffer zone
- 6.8 Ci escaped from the buffer zone boundary.

To calculate doses to individuals it was assumed that particles <5 μm physical size (8-μm AED) are respirable. A best estimate of 5% of the total activity was associated with particles of 8-μm AED or less. Uncertainty in this parameter was accounted for in the analysis. Furthermore, because the predicted plutonium concentrations in soil were reported on an areal basis, a conversion factor was required to use them in the exposure model.

Risk Estimates for Phase I

To evaluate the releases, ChemRisk divided the study area, which extended between 3.2- and 16-km (2–10 mi respectively) radius from the center of the plant, into 24 relatively uniform sectors in all directions around the plant (see ChemRisk 1994b, Figure 3-4). The exposure within a sector was calculated to vary by about a factor of 3 to 4. Releases from the 903 Area were believed to have occurred over a period of 5 years (1965–1969), and they were distributed in all directions but predominantly to the southeast of the plant. The dose estimates decreased with increasing distance from the site. The highest total dose estimates for airborne releases of $^{239/240}$Pu from the 903 Area during 1965–1969 were predicted for one of the innermost sectors, Sector 4B, in the southeast quadrant. The best estimate was 72 μSv, and the 95 percent confidence interval (CI) about the best estimate was 11–490 μSv. Moving away from the plant in an east-southeasterly direction, the best estimate of dose for Sector 8B was 24 μSv (95% CI: 3.1–190 μSv), and still further away from the plant, the best estimate of dose for Sector 12B was 9.1 μSv (95% CI: 1.2–66 μSv).

However, resuspension of deposited plutonium of 903 Area origin during the period 1970–1989 was calculated to be the largest contributor to the total dose that an individual might have received while living southeast of Rocky Flats during its entire operation history. For Sector 12B, the total dose during 1970–1989 was approximately 135 μSv (approximate 95% CI: 60–310 μSv).

Preliminary cancer risk estimates were also presented in Phase I of the study. A risk factor of 7.3% per sievert was used based on ICRP (1990). This risk factor includes fatal and nonfatal cancers and severe hereditary effects. The highest best estimate of risk was 5.2×10^{-6} (95% CI: 8×10^{-7} to 4×10^{-5}). This corresponds to the dose estimate of 72 μSv (95% CI: 11–490 μSv) for Sector 4B. The dose and risk estimates for the three sectors with the highest exposures to releases from the 903 Area during 1965–1969 are summarized in Table 1.

Table 1. Summary of Largest Phase I Dose and Risk Estimates for Airborne Releases of Plutonium from the 903 Area During 1965 to 1969

Southeast quadrant sector designation	Dose estimate[a] (μSv)	Risk estimate[a]
Sector 4B	72 (11 to 490)	5×10^{-6} (8×10^{-7} to 4×10^{-5})
Sector 8B	24 (3.1 to 190)	2×10^{-6} (2×10^{-7} to 1×10^{-5})
Sector 12B	9.1 (1.2 to 66)	7×10^{-7} (9×10^{-8} to 5×10^{-6})

[a] Best estimate (95% confidence interval about best estimate).

PHASE II SOURCE TERM FOR THE 903 AREA

A considerable effort was made in Phase II to reevaluate the source term for the 903 Area. Research into the nature of the releases from the 903 Area (Meyer et al. 1996; Weber et al. 1999) indicated that the highest releases occurred as discrete events of 1-day duration. It appeared that there was a correlation between high wind days, as measured at the Jefferson County Airport, and high air sampler count rates observed daily at the S-8 sampler (see Figure 1). The S-8 sampler is located east of the 903 Area, which puts it in the plume path of soil particles suspended from the 903 Area by westerly winds. Wind storms on the Colorado Front Range

generally result in westerly winds, and plutonium contamination in soil east of the pad confirm this. In addition, it was noted that monthly average S-8 sampler concentrations were generally higher than the other samplers operating routinely at the plant. The consistently high S-8 measurements were attributed to suspension of plutonium-contaminated soil from the 903 Area. Therefore, analysis of the source term was divided into two parts: releases that occurred from short-term (1 day) high wind events and releases that occurred more-or-less continuously throughout the assessment period (1964–1969). The later of these releases were referred to as baseline releases, and the former were referred to as discrete events. The S-8 sampler data include daily measurements of total long-lived gross alpha activity. The sampler was changed every working day at 8:15 a.m. and allowed to run continuously for 24 hours. The sampler ran continuously throughout weekend and holiday periods.

Suspension models were investigated, and models that incorporated wind speed dependence as described originally by Gillette (1974) were judged to be most applicable to the 903 Area environs. Implementation of Gillette's model by Cowherd et al. (1985) provided a means to quantify release estimates assuming the 903 Area soils and plutonium concentrations could be adequately characterized. Plutonium concentrations in soil could be estimated based on the estimates of quantities released from the barrels and infiltration depth of the cutting oil; however, soil characterization data were lacking. In addition, soil conditions were known to be highly variable because of precipitation and mechanical disturbance. For these reasons, the suspension model was calibrated to measurements made at the S-8 sampler, correcting for the sampling apparatus deficiencies.

Discrete source terms were calculated for 24 individual days that represented about 95% of the total counts observed at the S-8 sampler from 1964–1969. The baseline release source term that comprised the remainder of the days during this period was calculated annually using similar methodology. For the 24-highest S-8 sampler days, wind speed dependent release rates were coupled with an atmospheric transport model capable of dealing with gravitational settling, plume depletion, and area source geometry to calculate concentrations of plutonium-contaminated dust at the S-8 sampler for four different particle sizes: <3-μm, 3—10-μm, 10—15-μm, and 15—30-μm AED. The FDM code (Winges 1990) was chosen for this task. The S-8 sampler was incapable of measuring particles larger than 30 μm; therefore, these results only apply to particles <30 μm. Release of plutonium-contaminated particles >30 μm is of interest for offsite contamination, but larger particles do not pose the inhalation health risk of smaller particles. Particles >15-μm AED do not even penetrate as far as the bronchial region of the respirable tract and are eliminated from the body rapidly via transfer to the gastrointestinal tract and subsequent excretion or direct expulsion (i.e., nose blowing) to the environment (ICRP 1994). Particles >15 μm, therefore, are considered nonrespirable. In addition, larger particles do not behave like smaller particles during erosion and atmospheric transport. The principal transport mechanism of particles >50 μm physical diameter is saltation. Saltation is also a mechanism by which smaller particles are released by the jarring action of larger ones. Particles in this size range tend to deposit quickly because their gravitational settling velocities are greater than the turbulent motions of the air (Whicker and Schultz 1982). The nearest public receptor east of the 903 Area is 3 km away.

Daily net count rates measured at the S-8 sampler were converted to airborne plutonium concentrations. Corrections were made for filter collection efficiency, detector counting efficiency, sampled air volume, and sampler inlet collection efficiency. Airborne activity particle

size distributions were obtained from the onsite measurements made by numerous researchers and considered the variability in those measurements. Ten activity particle size distributions were defined, ranging from those that favored the smaller particles to those that favored the larger particles. The range of the fraction of activity associated with each particle size range (in AED) is as follows: <3 μm, 1–13%; 3–10 μm, 0.3–12%; 10–15 μm, 1–6.7%; 15–30 μm 74–92%. A particle size distribution that favored smaller particles meant that the fraction of activity attached to small particles was selected from the upper end of the distribution for small particles (13%) and the fraction of activity attached to larger particles was selected from the lower end of the distribution assigned to lager particles (74%). The two remaining particle sizes were selected such that the sum of the fraction of activity attached to all four particles sizes equaled 1.0. The ten particles size distributions were then randomly sampled for each Monte Carlo realization. Note that most of the airborne activity was associated with the larger, nonrespirable size fractions. Uncertainty was propagated through the entire calculation.

Meteorological data for the 24 highest S-8 sampler days were obtained from portable meteorological stations operated by the National Center for Atmospheric Research (NCAR) in Boulder. These stations were temporarily installed by NCAR during the late 1960s to study wind evolution on the Front Range. Five-minute average wind speed and direction data were digitized every 5 minutes for each 24-hour S-8 sampler period. The 5-minute periods were designed to capture high wind gusts that were known to have occurred and that drive dust suspension. Atmospheric stability class was determined hourly using the general classification scheme discussed in Pasquill (1961), Gifford (1961), and Turner (1964). This typing scheme employs seven stability categories ranging from A (extremely unstable) to G (extremely stable) and requires estimates of cloud cover and ceiling height. Cloud cover and ceiling height data were obtained from Jefferson County Airport, and from Denver Stapleton International Airport for the periods of time when Jefferson County Airport was closed (11:00 p.m. to 6:00 a.m.).

Meteorological data for baseline release used the 5-year data set (1989–1993) at the 10-m level taken from the 61-m tower located at the RFP. This data set is discussed in more detail in the meteorological data section of this report.

Table 2 presents the 24-hour integrated release quantities for the 24 discrete events, and Table 3 presents the annual baseline release quantities (excluding activity measured during the 24 discrete events) for 1964–1969 including uncertainty. Release quantities in Tables 2 and 3 represent the total for all particle size classes. The subsequent risk calculations only considered particles <15-μm AED, which represent the first three particle size classes. The six highest discrete event days (the shaded rows and the row labeled "Total 6 highest days" in Table 2) account for ~90% of the total discrete event releases[3]. If we add the 50% value from the discrete events (3.1 Ci) to the corresponding total baseline release (0.19 Ci, total ~3.3 Ci), we find that the six highest discrete still account for ~90% of the total estimated releases from the 903 Area from 1964–1969. Because these 6 days accounted for most of the 903 Area releases, and to reduce the computational time, we decided to model only those days as individual discrete events. Consequently, the remainder of the discrete releases were combined with the appropriate baseline release estimates reported in Table 3.

[3] This value cannot be obtained from Table 2. It was arrived at by comparing the distribution of the *sum* of total discrete activity released (last line in Table 2) to the distribution of the *sum* of activity released for the 6 highest discrete days

Table 2. Calibrated 903 Area Release Estimates of Plutonium Attached to < 30-μm AED Soil Particles for the 24 Highest Release Days (Weber et al. 1999)

	Release quantity (Ci)		
Release date	50%	95%	5%
18-Mar-68	1.4×10^{-2}	7.4×10^{-2}	2.9×10^{-3}
11–14-Apr-68	6.4×10^{-2}	3.4×10^{-1}	1.4×10^{-2}
13-May-68	3.0×10^{-2}	1.6×10^{-1}	6.6×10^{-3}
17-Sep-68	6.7×10^{-3}	3.4×10^{-2}	1.2×10^{-3}
22, 23, 24-Nov-68	6.9×10^{-2}	3.4×10^{-2}	1.3×10^{-3}
25-Nov-68	4.9×10^{-3}	2.4×10^{-2}	1.1×10^{-3}
5-Dec-68[a]	5.1×10^{-2}	2.5×10^{-1}	9.7×10^{-3}
11-Dec-68	9.3×10^{-3}	4.6×10^{-2}	2.0×10^{-3}
2-Jan-69	2.9×10^{-3}	1.3×10^{-2}	5.7×10^{-4}
3–5-Jan-69	2.2×10^{-2}	1.0×10^{-1}	4.4×10^{-3}
6 Jan-69[a]	1.8×10^{-1}	8.6×10^{-1}	3.4×10^{-2}
7-Jan-69[a]	8.9×10^{-1}	$4.3 \times 10^{+0}$	1.8×10^{-1}
29-Jan-69	1.3×10^{-2}	6.0×10^{-2}	2.7×10^{-3}
30-Jan-69[a]	5.3×10^{-1}	$2.4 \times 10^{+0}$	9.6×10^{-2}
24-Feb-69	7.3×10^{-3}	3.7×10^{-2}	1.7×10^{-3}
19-Mar-69[a]	5.5×10^{-2}	2.7×10^{-1}	1.2×10^{-2}
7-Apr-69[a]	3.8×10^{-1}	$1.9 \times 10^{+0}$	7.7×10^{-2}
Total 6 highest days[b]	$2.8 \times 10^{+0}$	$1.4 \times 10^{+1}$	$1.2 \times 10^{+0}$
Total[b]	$3.1 \times 10^{+0}$	$1.5 \times 10^{+1}$	$1.4 \times 10^{+0}$

[a] These releases were treated as discrete events in the RATCHET simulations. The activity released from the remainder of the days was added to the baseline releases.

[b] The distribution of total releases was determined by sampling from the distribution of each individual release event and summing. It is not the sum of the given percentile value.

Table 3. Calibrated 903 Area Release Estimates of Plutonium Attached to < 30 μm Soil Particles for the Baseline Releases (1964–1969) and Baseline Plus Discrete Event Remainder

	Baseline release (Ci)			Baseline plus remainder[a] (Ci)		
Year	50th %	95th %	5th %	50th %	95th %	5th %
1964	6.6×10^{-3}	3.8×10^{-2}	8.1×10^{-4}	6.6×10^{-3}	3.8×10^{-2}	8.1×10^{-4}
1965	1.3×10^{-2}	1.0×10^{-1}	9.4×10^{-4}	1.3×10^{-2}	1.0×10^{-1}	9.4×10^{-4}
1966	1.4×10^{-2}	1.1×10^{-1}	1.3×10^{-3}	1.4×10^{-2}	1.1×10^{-1}	1.3×10^{-3}
1967	2.6×10^{-2}	1.6×10^{-1}	3.0×10^{-3}	2.6×10^{-2}	1.6×10^{-1}	3.0×10^{-3}
1968	5.5×10^{-2}	3.0×10^{-1}	1.1×10^{-2}	1.9×10^{-1}	1.0×10^{0}	3.9×10^{-2}
1969	6.4×10^{-2}	3.4×10^{-1}	1.3×10^{-2}	1.1×10^{-1}	5.5×10^{-1}	2.2×10^{-2}
Total[b]	1.9×10^{-1}	9.8×10^{-1}	3.9×10^{-2}	---	---	---

[a] The remainder is the activity released from the 24 highest S-8 sampler days that were not treated as discrete events. This activity was added to the baseline releases for their respective year of occurrence.

[b] The distribution of total releases was determined by sampling from the distribution of each individual release event and summing. It is not the sum of the given percentile value.

Release rates for the 6 highest S-8 sampler days that were used in the transport calculations were further discretized for each hour of the release based on the hourly average wind speed. These and other details are discussed in the "Source Characterization" section of this report. Details of the methodology, calculations, and data for the 903 Area Source term can be found in Weber et al. (1999). A detailed accounting of percentiles for each respirable size fraction is presented in Appendix A.

It is interesting to compare the source term with that derived for Phase I. Of the 13.6 Ci estimated in Phase I to have escaped the pad, 5% of that was assumed to be in the respirable size range (<8-µm AED). Therefore, 0.68 Ci was the respirable activity that was suspended from the 903 Area according to Phase I. The median total release quantity from Phase II (for particles <30-µm AED) was about 3.3 Ci. Of that total, about 10–20% was in the <10-µm AED size range, leaving 0.33 to 0.66 Ci in that size range. These values are very close to the original Phase I estimates. It should be emphasized that derivation of the Phase II source term was independent of the Phase I calculations and used an entirely different approach from Phase I, which relied on fitting the deposition isopleths to measured soil concentration data.

ENVIRONMENTAL MONITORING

In this section, we briefly review environmental monitoring data that may potentially be used for model validation of 903 Area releases. However, direct comparisons cannot be made at this time because *all* potential sources of plutonium must be accounted for in any comparison. Therefore, we summarize the available data and discuss its usefulness in terms of validating primary 903 Area releases. This limits our discussion to data collected between 1964 and 1969, with some exceptions as noted. A later report will perform a quantitative comparison of measured and modeled concentrations in environmental media that includes all sources of plutonium activity. Rope et al. (1999) contains a detailed description and analysis of all environmental monitoring data, and the material that follows is summarized from this document. Environmental data are available for the following media: ambient air, airborne deposition, vegetation, surface and drinking water, sediment, and soil.

Ambient Air Monitoring

Air monitoring was performed by the site contractor and several other independent agencies. Before 1970, samplers near the RFP were only analyzed for total long-lived alpha activity (TLLa). Monitoring of plutonium in Denver air by the Public Health Service began in 1965. The RFP contractor began onsite ambient air monitoring at a single station in 1952. By early 1953, 10 onsite stations had been established, and in 1969, two additional stations were added.

In the 1950s (particularly 1955–1960), 4-hour gross alpha counts were made. These counts were made 4 hours after collection and included large contributions from natural alpha emitting radionuclides like radon decay products. Beginning in January 1960, 1-week counts and 4-hour counts of alpha and beta activity were performed. The 1-week count was performed 1-week after sample collection, resulting in decay of most of the short-lived radon progeny and, thereby, providing a measure of the long-lived alpha activity collected on the filter. Results were summarized in monthly sampling reports that reported the maximum and minimum average activity levels of all samples for that month. Daily sampling sheets were obtained from October

10, 1964, to December 29, 1971, for S-1 through S-10 samplers (with the exception of S-9 sampler). The minimum detectable concentration quoted by the site contractor was 0.21 counts per minute (cpm), which equates to an activity concentration of 5.5 fCi m^{-3} TLLa (Rope et al. 1999). A conversion factor of 0.038 cpm fCi^{-1} m^3 was used in the calculation. The plutonium activity concentration in ambient air resulting from weapons fallout for the 1965–1970 time frame is around 0.1 fCi m^{-3}, and the long-term average background from natural sources of long-lived alpha activity is 1.4 fCi m^{-3} but can be as high as 7–10 fCi m^{-3} on any given day (Rope et al. 1999).

In 1964, the first indication was found that, barrels containing plutonium-contaminated cutting oil and stored on what is now known as the 903 Area, were leaking and contaminating the underlying soil (Meyer et al. 1996). Suspension of this soil by wind and man-made disturbance was detected in 12 onsite samplers, particularly the S-8 sampler located east of the 903 area. This airborne source is believed to have dominated the activity measured at onsite and offsite sampling locations from 1964 to the present. Annual average concentrations of TLLa in samplers S-1 through S-51 samplers in 1969 (the year of highest measured concentration) ranged from 4–185 fCi m^{-3}. With the exception of S-7 and S-8 samplers, most samplers had annual average concentrations at or slightly above the minimum detectable concentration of 5.5 fCi m^{-3}. Data from the S-8 sampler during this period were used to calibrate 903 Area releases and cannot be used for model validation.

Deposition Measurements

Deposition measurements were made using gummed film beginning in 1954. Early tests of the method were conducted from 1954–1955. Routine monitoring was conducted from 1963–1965 at sampling sites that encircled the Building 771 stack and out to a distance of about 1 km. Unfortunately, sampling was not performed during major releases (1968 and 1969) from the 903 Area, and samplers were not installed downwind from the 903 Area. A gummed film program was started again in 1970 at several onsite and numerous offsite locations. The startup time of this later monitoring is outside the period in which the primary 903 Area releases occurred. Therefore, it is of little use for validating primary 903 Area releases.

Vegetation Monitoring

Vegetation is the only media for which a significant number of plutonium-specific measurements were made before 1970. This medium may, therefore, be important in terms of validating source terms and environmental transport modeling. Monitoring of vegetation began before the site was operating as part of a preoperational background study. Initial monitoring began in 1952, but it was ended in 1953 because of technical problems. Vegetation monitoring resumed after the 1957 fire. Routine monitoring began in 1963 and continued to 1970. These measurements consisted of gross alpha analyses of samples collected at 55 to 65 locations on a 2000-ft (610-m) grid and 44 locations off the grid. With the exception of handwritten data tabulations for six onsite locations that we obtained from a collection of documents at the RFP called the Environmental Master File, none of the reports obtained thus far contain onsite vegetation data for the 1963–1970 time period. The Environmental Survey Reports present the average and maximum values for all samples collected within a given distance from the plant.

These data are potentially useful for model validation. However, prediction of concentrations on vegetation requires an additional level of modeling to compute deposition and retention and vegetative surfaces. With this additional level of modeling comes additional uncertainty. Furthermore, concentrations of plutonium on vegetation are highly variable and depend on the local soil conditions (i.e. moisture content, amount of litter) and the type of vegetation (i.e. sagebrush, grass, or small trees) modeled. The spatial resolution of the environmental transport model does not differentiate soil conditions or vegetation types. Moreover, these details were typically not recorded in the environmental measurements. Therefore, we expect comparisons to be mainly of general spatial and temporal trends, and prediction uncertainty is expected to be quite large (a factor of 10–100).

Surface and Drinking Water Monitoring

Water samples have been collected in the vicinity of Rocky Flats and analyzed for radioactivity since 1951, before operations began, and monitored routinely throughout the 1950s and 1960s. Surface water features within and surrounding the RFP include five creeks, numerous holding ponds, and three reservoirs that are used for drinking water. While the database of surface water measurements is extensive, most of the measurements focused on monitoring liquid effluent discharges to surface water. This monitoring has little relevance to measurements of activity deposited from airborne plumes in surface water. In addition, it would be difficult to separate activity from airborne sources from that originating from plant effluent. Therefore, at this time we do not consider surface and drinking water monitoring data particularly useful for model validation.

Sediment Sampling

Sediment sampling may be useful for model validation because sediments, like soil, are a sink in which activity may accumulate over time. Routine monitoring of sediment for radionuclides was conducted by the RFP contractor in the early 1950s and 1970s. Generally, however, that routine monitoring involved few sampling sites, undocumented methods, and infrequent reporting. Therefore, the data are of limited usefulness. Studies that were more comprehensive were performed from 1969–1992 by numerous agencies including the U.S. Environmental Protection Agency (EPA), Colorado State University, Pacific Northwest Laboratory, and Environmental Measurements Laboratory. Plutonium-239/240, ^{137}Cs, ^{241}Am, and naturally occurring radionuclides were analyzed during these studies. Measurements over this time period have allowed for evaluating temporal trends of radioactivity in this medium because sediment layers can be age-dated. Unfortunately, the airborne component of this activity may be somewhat obscured by liquid effluent discharges and accidental releases. For example, in 1972 reconstruction of some of the holding ponds led to increases in measured activity in sediment in Walnut Creek and Great Western Reservoir. Later studies revealed that the activity in Great Western Reservoir could have two components: atmospheric fallout and waterborne releases from the RFP. The atmospheric component was linked by age-dating the sediments to the time when high releases from the 903 Area occurred. Similar studies on Stanley Lake also indicated high plutonium concentrations that correspond to the time of highest 903 Area releases.

Based on these observations, reservoir sediments appear to be useful for model validation for 903 Area releases. This is not done in this report. Sediment provides a sink in which deposited activity is held tightly and can be dated, based on the analysis of sediment cores and knowledge of sedimentation rates.

Soil

Soil represents a significant sink for plutonium deposited from airborne plumes. Plutonium is relatively insoluble (compared to other radionuclides like radium and uranium) and immobile under most conditions, thereby, allowing it to accumulate in the upper soil layers. Many sampling studies of plutonium in soil around the RFP have been performed. In the early 1970s, several researchers (Poet and Martell 1972; Krey and Hardy 1970) published results showing a well defined plume of plutonium extending eastward from the RFP. Other researchers have expanded upon this work and have provided an extensive database of soil concentration measurements in addition to plutonium inventory analysis (Little 1976; Litaor 1993, 1995; Webb et al. 1994). In Phase I, these data were used to estimate plutonium releases from the 903 Area. Soil measurements will be an important part of the model validation process for the dose reconstruction project. While sources other than the 903 Area may have contributed to the observed plume of plutonium in soil extending east of the plant, it is believed that their contribution is minor. This fact makes soil concentration measurements an important data source for model validation of 903 Area releases.

ENVIRONMENTAL TRANSPORT MODELING

Offsite exposure to plutonium from releases that occurred as a result of suspension of contaminated soil from the 903 Area were investigated in Phase I and summarized in a previous section. Airborne releases were considered to be the principal transport pathway and inhalation the major pathway of exposure. In this section, we describe our approach to estimating atmospheric dispersion of plutonium released from the 903 Area and the uncertainty associated with concentration estimates in the model domain. Dispersion calculations were segregated into two types: those that are treated discretely and those that are treated on an annual average basis. The later case includes the baseline releases and the remainder of the 24 highest S-8 sampler days (19 days) not included in discrete events.

For discrete events, the 26-hour time integrated concentration with uncertainty was estimated by sampling from the distribution of release estimates and coupling these with RATCHET simulations that incorporate uncertainty in the meteorological parameters, wind speed, wind direction, stability class, and Monin-Obukhov length. These simulations used hourly averaged meteorological records obtained from the NCAR recording stations. Source terms were provided for 24 of the 26 hours simulation. Two additional hours were added on the end of the simulation to allow the plume to dissipate in the model domain.

For baseline releases, annual average dispersion factors or χ/Q values (air concentration divided by source term) were calculated deterministically using a surrogate meteorological data set spanning the years 1989–1993. These χ/Q values (s m^{-3}) were multiplied by distributions of annual release quantities (Ci s^{-1}) to yield concentration estimates in the model domain. Uncertainty in the dispersion factors was accounted for by several multiplicative correction

factors applied stochastically to the results. Distributions of airborne concentrations were then used with exposure scenarios and the risk coefficients to calculate lifetime cancer incidence risk for hypothetical receptors in the model domain.

Atmospheric Model Selection

Five atmospheric transport models considered for use in this study were evaluated in Rood (1999a): (1) the Terrain-Responsive Atmospheric Code (TRAC) (Hodgin 1991), (2) the Industrial Source Complex Short Term Version 2 (ISC) (EPA 1992), (3) Regional Atmospheric Transport Code for Hanford Emission Tracking (RATCHET) (Ramsdell et al. 1994), (4) TRIAD (Hicks et al. 1989), (5) and INtegrated PUFF dispersion code (INPUFF2) (Petersen and Lavdas 1986). The purpose of the model comparison study was to determine what models, if any, performed best in the Rocky Flats environs for a given set of modeling objectives. These data, along with other studies, were used to establish the uncertainty one might expect from a model prediction.

Model evaluations were based on how well predictions compared with measured tracer concentrations taken during the Winter Validation Tracer Study (WVTS) conducted in February 1991 at the RFP (Brown 1991). The study consisted of 12 separate tests: 6 tests were conducted during nighttime hours, 4 during daytime hours, and 2 during day-night transition hours. For each test, an inert tracer (sulfur hexafluoride) was released at the RFP at a constant rate for 11 hours from a 10-m high stack located on the southern boundary of the RFP industrial area. Two sampling arcs, 8 and 16 km from the release point, measured tracer concentrations every hour for the last 9 hours of each test period. Seventy-two samplers were located on the 8-km arc, and 68 samplers were located on the 16-km arc. Predicted concentrations were then compared to the observed tracer concentrations at each of the samplers.

We acknowledge that the release conditions of the WVTS are substantially different from the 903 Area release conditions. Most notably, releases from the 903 Area involved particulates subject to dry deposition and gravitational settling, whereas an inert tracer was released in the WVTS. Removal mechanisms that include dry and wet deposition are included in all the models evaluated. These processes are represented in the models by depleting the plume according to the physical properties of the material emitted to the atmosphere and its residence time in the model domain. The dispersion and diffusion aspects of the models are identical to those used for a conservative tracer. We do not believe the differences between the WVTS release characteristics and effluent properties from the 903 Area substantially detract from the overall conclusions reached in the WVTS model comparisons (Rood 1999a). Therefore, we used the results in Rood (1999a) along with other factors as a basis for selecting a model.

Modeling objectives for the comparison study were based on the premise that identifying locations of individual receptors on an hour-by-hour basis was unlikely. Instead, it was more likely to identify receptors (hypothetical or real) who were present at a fixed location for the duration of a release event. The minimum time scale of historical release events at RFP ranged from 6–10 hours to several days. Release events modeled for the WVTS were 9 hours in duration. If we assume the receptor is fixed for a time period of at least 9 hours, then the time-averaged concentration (9-hour average) is an appropriate modeling objective rather that comparing hourly average concentrations. Therefore, models were evaluated based on their performance in predicting time-averaged concentrations at fixed sampler locations in the model

domain (9-hour average concentration at each sampler paired with the corresponding predicted value). Data sets for the time-averaged concentration were limited to only those points where the predicted (C_p) and observed (C_o) concentration pair were greater than the time-averaged minimum detectable concentration.

Fifty percent of the time-averaged model predictions were within a factor of 4 of the observations. Predicted-to-observed ratios (C_p/C_o) ranged from 0.001 to 100 and tended to be higher at the 16-km arc than the 8-km arc. Geometric mean C_p/C_o ratios ranged from 0.64 (TRAC) to 1.5 (ISC), and GSDs ranged 4.4 (RATCHET) to 6.5 (ISC). The RATCHET model had the highest correlation coefficient for the 8-km (0.67) and 16-km (0.58) sampling arc followed by TRIAD and INPUFF2 (Figure 2). Qualitatively, the predictions made by the RATCHET model appear to match the observations best. The slope of the regression line was closest to that of the perfect correlation line (solid line in Figure 2).

The results reported in Rood (1999a) indicated that no one model clearly outperformed the others. However, the RATCHET, TRIAD, and INPUFF2 models generally had lower variability (indicated by lower GSDs of C_p/C_o ratios) and higher correlation coefficients compared to those of the ISC and TRAC models. It is desirable in a study such as this to choose a model that has the least amount of variability when comparing model predictions to observations. In addition, the model selected should have a level of complexity that is consistent with available data. The TRAC model is the most complex in terms of its treatment of the atmospheric dispersion process in complex terrain, but the study showed that it performed no better than the other models. In addition, the meteorological data needed to fully use the capabilities of the TRAC model are lacking for the time frame of interest (1964–1969). The straight-line Gaussian plume model, ISC, tended to overpredict concentrations and was also limited to only one meteorological recording station in the model domain. Available meteorological data for this study period included two meteorological recording stations: one at the RFP and the other at Denver Stapleton International Airport. Therefore, a model that can include multiple meteorological recording stations in the model domain is desirable. The use of multiple meteorological recording stations allows for a spatially varying wind field in the model domain.

The RATCHET, INPUFF2, and TRIAD models performed comparably and were considered viable candidates for atmospheric dispersion estimates. Of these models, RATCHET and TRIAD were chosen for more detailed evaluation because both allow for spatially varying wind fields.

There are advantages and disadvantages to using either model for dispersion calculations. The TRIAD model is capable of incorporating meteorological data on a user-defined time scale while RATCHET uses a fixed, 1-hour increment. Meteorological data from the NCAR recording stations were digitized every 5 minutes; therefore, the TRIAD model would appear better suited for the calculation because it could incorporate the finer resolution of the meteorological data. However, Denver Stapleton International Airport data were recorded every hour, so this advantage was lost in terms of predicting wind vectors at that distance. In addition, model comparisons using the WVTS data set showed that RATCHET performed equally as well, or if not better than TRIAD, using 1-hour average meteorological conditions. RATCHET also has several other features that make it desirable. These features include

- Spatial varying surface roughness lengths and mixing heights
- Algorithms to compute plume depletion and deposition are included (deposition must be computed outside the TRIAD code) and are spatially variable across the model domain
- Random sampling routines that facilitate Monte Carlo uncertainty calculations.

We chose the RATCHET model to perform the calculations based on its performance in the WVTS model comparison (Rood 1999a) and the features of the code stated previously. Features of the RATCHET model are summarized in Table 4.

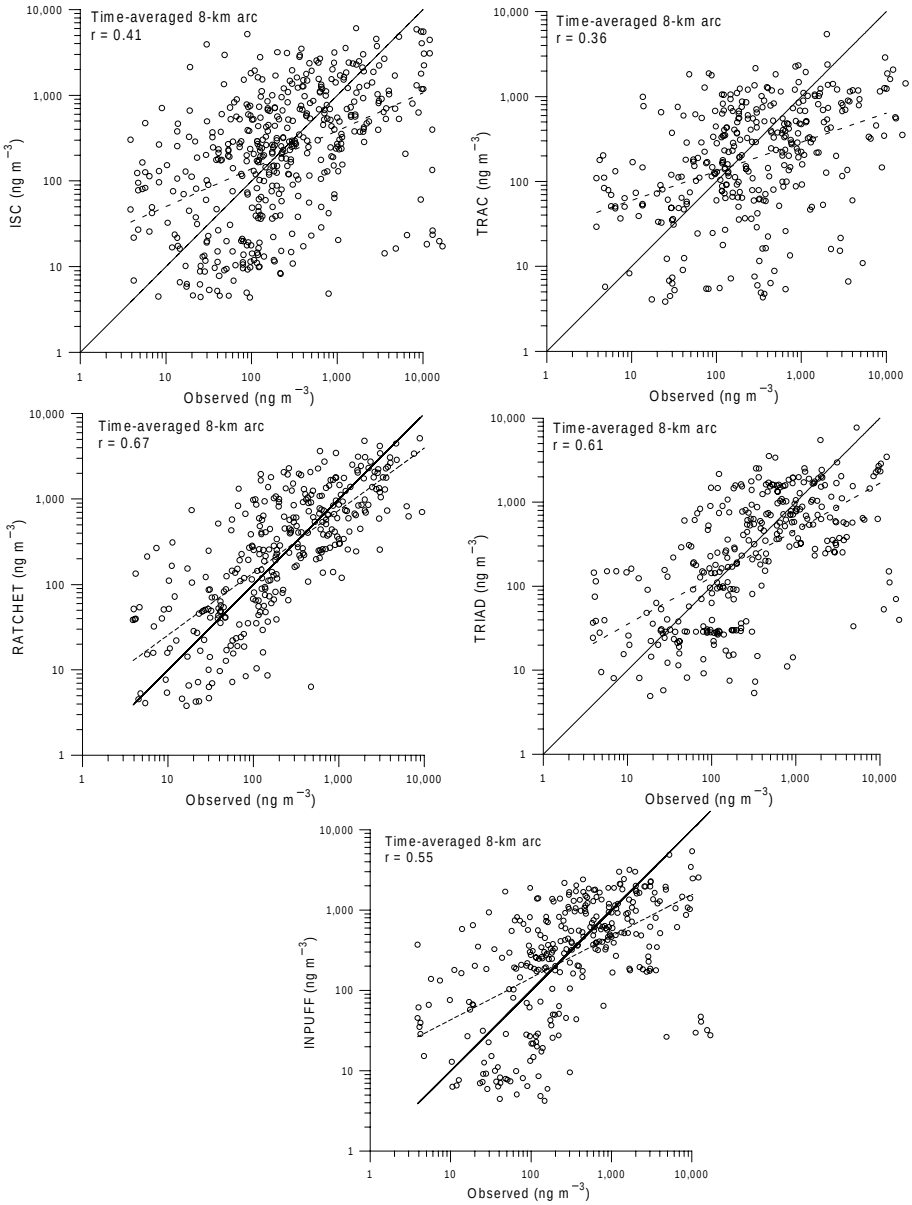

Figure 2. Nine-hour average observed concentrations as a function of predicted values for the five models compared using the Winter Validation Tracer Study data set. Correlation coefficients were for the log-transformed data. The solid line represents perfect correlation between predicted and observed values. The dashed line represents the log-transformed regression fit.

Table 4. Features of the RATCHET Model

Feature	Representation in RATCHET
Domain area[a]	2,200 km^2
Node spacing[a]	2,000 m
Source term	Hourly release rates
Meteorological data	Hourly
Surface roughness	Spatially varying
Wind fields	$1/r^2$ interpolation (r = the radial distance from the observation)
Topographical effects	None explicit[b]
Wind profile	Diabatic
Stability	Spatially varying based on wind, cloud cover, and time of day
Precipitation	Spatially varying based on three precipitation regimes with different precipitation rate distributions
Mixing layer	Spatially varying based on calculated values for each meteorological station
Plume rise	Briggs' equation (Briggs 1969, 1975, 1984)
Diffusion coefficients	Based on travel time and turbulence levels
Dry deposition	Calculated using resistance model
Wet deposition	Reversible scavenging of gases, irreversible washout of particles
Model time step	15 minute maximum, 15 second minimum
Output frequency	Time integrated for the modeling segment
Uncertainty	Options available for Monte Carlo simulation within the code

[a] Modified from the original RATCHET specification for use at Rocky Flats.
[b] Terrain differences are not a model input. However, topographical influence on the wind field may be accounted for by incorporating multiple meteorological stations in the model domain.
[c] RATCHET was modified to accommodate time-integrated concentrations for the modeling segment. The original code output time-integrated concentrations daily.

Model Domain and Receptor Grid

The model domain (Figure 3) encompasses a 2200 km^2 area (50 km north-south × 44 km east-west). The domain extends 28 km south, 12 km west, 22 km north, and 32 km east from the RFP. Most of the Denver metropolitan area and the city of Boulder are included in the domain. The domain was limited in its western extent because few receptors are present and most of the contaminant plumes traveled east and southeast of the plant.

RATCHET uses two modeling grids. Hourly meteorological records are used to estimate wind speed and direction, stability, and precipitation on the environmental grid in addition to surface roughness features. The concentration grid has spacing one-half that of the environmental grid. Ground-level concentrations and deposition are output at each of these grid nodes. The environmental grid was set at 23 nodes east-west and 26 nodes north-south, with a grid spacing of 2000 m. The concentration grid has 45 nodes east-west and 51 nodes north-south, with a spacing of 1000 m. The southwest corner of the model domain has the universal transverse mercator (UTM) coordinates 470850 E and 4387050 N. Release points are defined by distances (in kilometers) from an arbitrary reference node. The reference node for the environmental grid was (7,15) and (13,29) for the concentration grid. Both the environmental and concentration

reference node have the UTM coordinates of 482850 E and 4415050 N. Topographic contours were based on an elevation grid spacing of 100 m. Major roadways and water features were digitized from U. S. Geological Survey 1:100,000 digital line graphs.

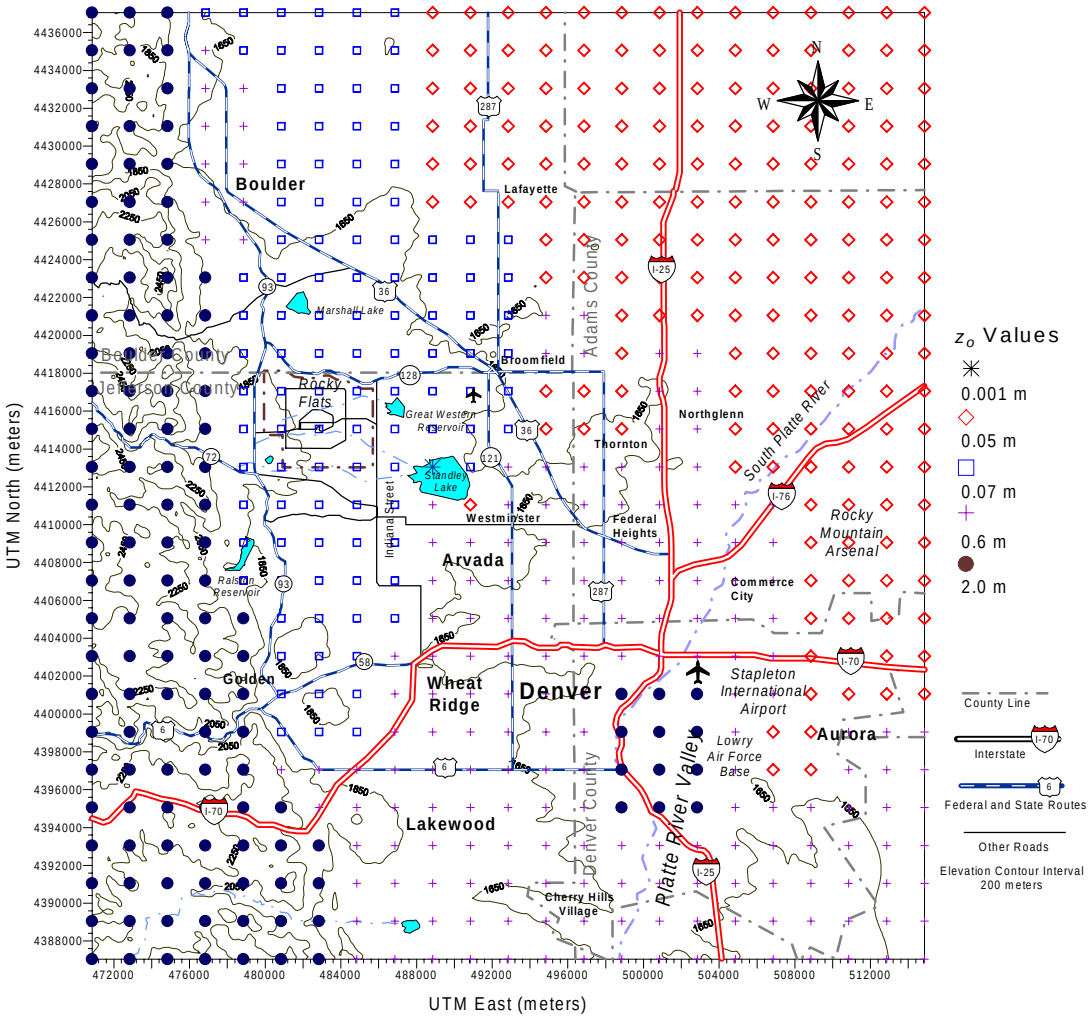

Figure 3. RATCHET environmental modeling grid and roughness length values (z_o). Symbols represent grid nodes and the z_o value assigned to the node.

Figure 3 was generated using U. S. Geological Survey 7.5-minute digital elevation models.

Meteorology

Rocky Flats meteorological data for its operational period (1953–1989) are sporadic, incomplete, and of questionable quality. Requests for meteorological data from the RFP were initially made by ChemRisk during Phase I of the project. ChemRisk was able to locate two letters from Dow Chemical to Dr. Roy Cleare, Executive Director of the Colorado Department of Health, dated March 20, 1970, that contained wind speed and direction for varying time increments during the 1957 and 1969 fire incidents. Computer diskettes containing wind speed, wind direction, and precipitation measurements from October 1968 to May 1969 were also obtained. These data were hourly observations taken approximately 15 minutes before the top of

the hour and do not represent hourly average readings. Although these data appeared to be climatologically reasonable, no records of instrument calibration or audits of the information were found. Parameter resolution was very coarse (for example, wind direction resolution was 45 degrees). Original records, including the strip recording charts, were not located for the period from 1952–1983.

An extensive data search was initiated in 1994 by *RAC* researchers to locate missing data and interview personnel who were involved with measurements at the site. No new data from the RFP were recovered, but several personnel reported problems with the recording instrumentation at the RFP, such as the measured wind direction being off by 180 degrees. In 1984, a 61-m tower was constructed near the southern boundary of the RFP industrial area at UTM coordinates 482064 E, 4414963 N. Meteorological instrumentation was installed at 10-, 25-, and 61-m heights. Data recorded at this station include wind speed, wind direction, temperature, and other parameters (such as, heat flux and standard deviation of wind direction). These instruments were coupled with digital data recorders that allowed data to be taken continuously and processed and stored on a 15-minute interval. Operation of the tower began in 1984, and data recording adhered to strict quality assurance standards.

In 1994, the RFP hired a subcontractor to compile, screen, validate, and analyze historical climatological data (DOE 1995). A draft report, issued in February 1995, contained monthly and annual summaries of wind speeds, wind directions, precipitation, temperature, and other parameters for the years 1953–1993. While these data are of interest and may be important for some aspects of modeling, they lacked the resolution required for detailed atmospheric transport modeling.

Development of the 903 Area source term demanded detailed meteorological records of wind speed and direction for specific days. At the suggestion of a member of the Health Advisory Panel (HAP) overseeing this study, *RAC* queried the NCAR as a possible source of meteorological data from the Front Range winds. A primary station has existed since the 1960s atop Table Mesa, just west of the city of Boulder. To facilitate experiments designed to study wind patterns, other stations were temporarily located at various points east of Boulder and north of the RFP in 1968 and 1969. The station designated as Kent, which is located about 10 km north of the RFP (Figure 4) appeared to best represent RFP conditions (Weber et al. 1999). Meteorological data were obtained in the form of strip charts. These strip charts were digitized in 5-minute increments and used to calculate 903 Area releases for the 24 highest S-8 sampler days. Details of the acquisition and processing of the NCAR meteorological data are presented in Weber et al. (1999). Hourly conditions of wind speed, wind direction, and stability class were calculated from the 5-minute data. These data are presented in Appendix J of Weber et al. (1999) and were used in the RATCHET simulations for discrete events. Meteorological data used in the 903 Area simulations are summarized in Table 5.

Data from Denver Stapleton International Airport covering the 24 highest S-8 sampler days were also obtained and used in conjunction with the Kent data for air dispersion calculations. These data were instantaneous measurements and not hourly averages as was typical of all airport data before the Automatic Surface Observation Site system was installed at most major airports. The Denver Stapleton International Airport meteorological station was located 24 km east and 14 km south from the center of the model domain (the RFP). These data included measurements of wind speed, wind direction, cloud cover, and precipitation. It is known that meteorological conditions in the Denver metropolitan area can differ significantly from those at

Rocky Flats (DOE 1980). Therefore, it is unreasonable to use meteorological data from Denver alone for simulations involving releases from Rocky Flats. In these simulations, initial plume trajectories are primarily influenced by the wind direction at Rocky Flats. Only after plume elements are transported to the Denver metropolitan area are trajectories and dispersion influenced by meteorological conditions present in Denver.

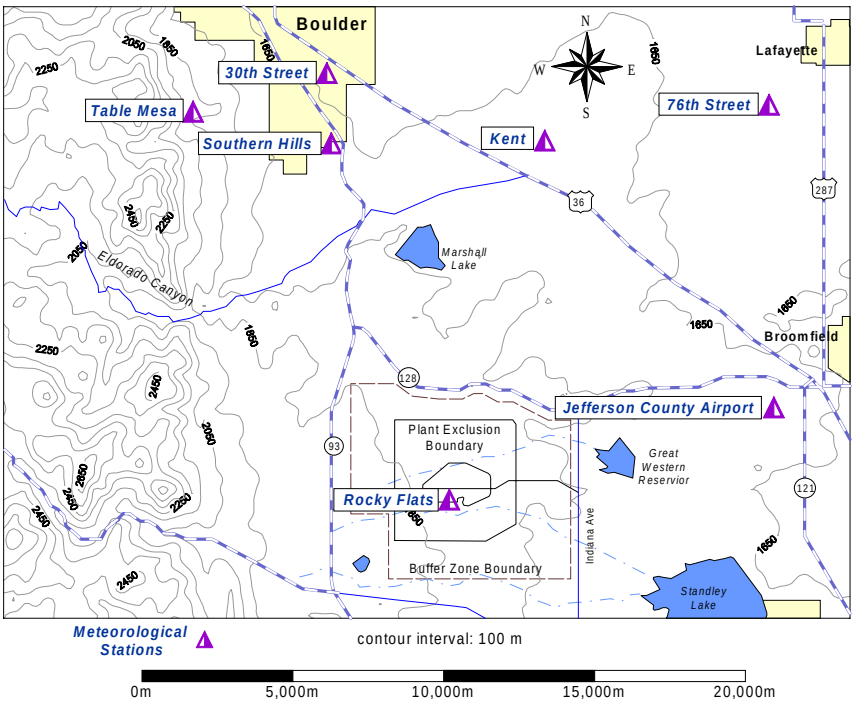

Figure 4. Location of NCAR, Rocky Flats, and Jefferson County Airport Meteorological recording stations. Except for Table Mesa, the NCAR stations were temporary.

Baseline releases required meteorological records spanning the entire period of interest (1964–1969). These data for this time period (1964–1969) were not available from either RFP or NCAR. Therefore, we relied on a technique often used in prospective analysis and in retrospective analysis when historical records are lacking. This technique uses compilations of recently acquired meteorological data as a surrogate for past or future conditions and typically only applies to assessments of long-term (>1 year) dispersion conditions. Federal regulations have stated a 5-year database is adequate for predicting annual-average air quality impacts at a site (CFR 1996). The uncertainty section of this report discusses how representative this 5-year data set is for earlier time periods. This technique was used to estimate annual average dispersion conditions for routine releases of plutonium from the RFP (Rood 1999b) using meteorological data from 1989 to 1994 taken at RFP and Denver Stapleton International Airport. This same data set was used in dispersion calculations of baseline releases.

Table 5. Summary of Meteorological Data Used in 903 Area Simulations

Data set	Years of Available Data	Application to RATCHET modeling
NCAR data at the Kent Station	1968–1969	Used in the simulation of the 6 discrete events
Jefferson County Airport	1964–present	Used to obtain cloud cover and ceiling height data for discrete and baseline releases
Denver Stapleton International Airport	1953–present	Used in baseline and discrete events. Cloud cover data from Denver was used when Jefferson County Airport was closed.
RFP data from 61-m Tower at the 10-m level	1984–present	Used a 5-year (1989–1993) data set to calculate annual average χ/Q values for baseline releases.

Data Processing

Rocky Flats meteorological data from 1989–1993 were obtained in electronic format from the Rocky Flats meteorologist (Carey Dickerman). Only data from the 10-m level were used in the simulations. Each record represented the average over a 15-minute recording period and included wind speed and direction, temperature, heat flux, and standard deviations of these parameters. Processed data suitable for use in EPA's ISC code were also obtained for the same time frame. These data included stability class estimated by the lateral turbulence and wind speed method (standard deviation of the horizontal wind direction fluctuations) as described in EPA (1987) and mixing height estimates. The mixing heights were derived from linear interpolation for each 15-minute period from the rawinsonde data furnished routinely every 12 hours by the National Weather Service for Denver Stapleton International Airport. These data were used as default mixing-layer depths in RATCHET for both the baseline releases and discrete simulations. Mixing-layer depths are calculated hourly within RATCHET at each active meteorological recording station using a methodology described by Zilitinkevich (1972). The calculated or default value is selected based on the relative magnitude of the calculated and default values, the stability, season, and time of day. The larger of the two is selected for the meteorological recording station for the given hour. A multiple linear regression technique is then used to provide a smooth spatial variation in mixing-layer depth across the model domain.

Stability classes were calculated separately for the RFP and Denver Stapleton International Airport meteorological recording stations using the general classification scheme discussed in Pasquill (1961), Gifford (1961), and Turner (1964). This typing scheme employs seven stability categories ranging from A (extremely unstable) to G (extremely stable) and requires estimates of cloud cover and ceiling height. Cloud cover and ceiling height data for the 24 highest S-8 sampler days were obtained from Jefferson County Airport and Denver Stapleton International Airport when the airport Jefferson County Airport was closed.

Hourly average wind speed and direction were calculated from the raw RFP meteorological data and the 5-minute NCAR Kent data using the protocol described in EPA (1987). An arithmetic average of the wind direction was computed first, and it was then segregated into 1 of 36, 10-degree increments as required by RATCHET. The average wind speed for the hour was

computed by taking the average of the four, 15-minute data segments. Hourly precipitation records from Denver Stapleton International Airport were assumed to be consistent over the entire model domain and were segregated into integer values as required by RATCHET (see Table 6). No precipitation was recorded for the discrete days.

Atmospheric Transport Model Parameters

This section describes the input parameters that were selected for the RATCHET model for simulations involving transport and dispersion of plutonium released from the 903 Area. These parameters include surface roughness length, topography, dry and wet deposition, gravitational settling, diffusion coefficients, release parameters (location and area of release), and model control parameters (number of puffs per hour and computational options).

Surface Roughness Length

Roughness elements (such as trees and buildings) and small-scale topographic features (such as rolling hills) have a frictional effect on the wind speed nearest the surface. The height and spacing of these elements will determine the frictional effects on the wind. These effects are directly related to transport and diffusion and affect atmospheric stability, wind profiles, diffusion coefficients, and the mixing-layer depth. The surface roughness length parameter is used to describe these roughness elements and is a characteristic length associated with surface roughness elements (Table 6). In RATCHET, estimates of the surface roughness length are defined for each node on the environmental grid (Figure 2). In our simulations, we selected a value of 0.6 m to represent residential and urban environs. Farmland, which is predominant in the northeast part of the model domain, was assigned a value of 0.05 m. Range and open land, consisting of rolling grass hills, were assigned a value of 0.07 m. Nodes that encompass the range and farmland designation were selected based on the topographic contours and land use maps. The foothills and downtown Denver were assigned a value of 2.0 m, and large open water bodies (e.g., Standley Lake) were assigned a value of 0.001 m.

Table 6. Typical Surface Roughness Lengths for Different Land Use, Vegetation, and Topographic Characteristics[a]

Land use, vegetation, and topographic characteristics	Surface roughness length, z_o (m)
Level grass plain	0.007–0.02
Farmland	0.02–0.1
Uncut grass, airport runways	0.02
Many trees/hedges, a few buildings	0.1–0.5
Average, North America	0.15
Average, U.S. Plains	0.5
Dense forest	0.3–0.6
Small towns/cities	0.6–2.5
Very hilly/mountainous regions	1.5+

[a] Source: Stull (1988), Figure 9.6.

Topography

The RATCHET model does not explicitly address terrain differences within the model domain. Instead, topography and topographic effects on transport and diffusion are reflected in the surface roughness lengths and observed wind velocity data that are affected by topographical features. Topography in the model domain (see Figure 2) can be characterized by three major features: the north-south trending Colorado Front Range foothills in the western part of the model domain, the southwest to northeast trending Platte River Valley located in the southeast part of the model domain, and rolling hills and flat farmland that is predominant in the central and northeastern part of the model domain. The topography generally slopes east from Rocky Flats, dropping 200 m in elevation to the Platte River Valley. The surface roughness lengths reflect these features as stated in the previous section. Observed meteorological data are lacking in most of the model domain and are woefully inadequate to characterize wind fields in the foothills region. However, meteorological observations at Denver Stapleton International Airport do capture the air movement within the Platte River Valley, which is noticeably different from that at the RFP (DOE 1980). Therefore, to a limited extent, topography is accounted for in the model simulation. The use of a complex terrain model would also suffer from the lack of meteorological data, especially in the foothills region according to demographic data compiled in Phase I (ChemRisk 1994c).

Dry and Wet Deposition

The rate of deposition of small particles on surfaces in the absence of precipitation is proportional to the concentration of material near the surface. The proportionality constant between the concentration in air and the flux to the ground surface is the dry deposition velocity. The current generation of applied models estimates deposition using an analogy with electrical systems as described by Seinfeld (1986). The deposition is assumed to be controlled by a network of resistances, and the deposition velocity is the inverse of the total resistance. Resistances are associated with atmospheric conditions; physical characteristics of the material; and the physical, chemical, and biological properties of the surface. Originally, RATCHET was designed to calculate deposition from small particles (≈ 1μm) and reactive gases. For these small particles, gravitational settling is negligible and therefore, RATCHET excluded this process in the deposition velocity. Because particle size for 903 Area releases a substantially larger than submicron particles, gravitational settling needed to be included. We replaced the deposition model in RATCHET with one that includes gravitational settling. This model is based on the work of Slinn and Slinn (1980) and Pleim et al. (1984). We have used the formulation as presented in the ISC3 code (EPA 1995) in out formulation. The approach is similar to that used in RATCHET, but includes the effects of gravitational settling.

The total resistance including gravitational settling effects in is made up of three components: aerodynamic resistance, surface-layer resistance, and transfer resistance. Thus, the dry deposition velocity (v_d, m s^{-1}) is calculated using

$$v_d = \frac{1}{r_a + r_d + r_a\, r_d\, v_g} + v_g \qquad (1)$$

where

r_a = aerodynamic layer resistance (s m^{-1})
r_d = deposition layer resistance (s m^{-1})
v_g = gravitational settling velocity (m s^{-1}).

Note that for large settling velocities, the deposition velocity approaches the settling velocity, whereas, for small settling velocities, v_d tends to be dominated by the r_a and r_d resistance terms.

The lowest few meters of the atmosphere can be divided into two layers: a fully turbulent region where vertical fluxes are nearly constant, and the thin quasi-laminar sublayer. The resistance to transport through the turbulent, constant flux layer is aerodynamic resistance. It is usually assumed that the eddy diffusivity for mass transfer within this layer is similar to that for heat. The atmospheric resistance formulation is based on Byun and Dennis (1995) and for stable conditions is given by

$$ra = \frac{1}{k\,u_*}\left(\ln\frac{z_d}{z_o} + 4.7\frac{z}{L}\right) \tag{2}$$

and for unstable conditions by

$$r_a = \frac{1}{k\,u_*}\left(\ln\frac{\left(\sqrt{1+16\left(z/|L|\right)}-1\right)\left(\sqrt{1+16\left(z_o/|L|\right)}+1\right)}{\left(\sqrt{1+16\left(z/|L|\right)}+1\right)\left(\sqrt{1+16\left(z_o/|L|\right)}-1\right)}\right) \tag{3}$$

where

u_* = friction velocity (m s^{-1})
k = von Karman constant (0.4)
L = Monin-Obukhov length (m)
z = height above ground surface (m)
z_o = surface roughness height (m)
z_d = deposition reference height (m)

The deposition reference height (z_d) is assigned a fixed value of 1.0 m in ISC3. We found that under conditions where z_o is greater than 1.0 m, negative deposition velocities were calculated. To alleviate this problem, we set z_d to 1.0 m + z_o. This change has little impact for small z_o values and results in positive deposition velocities for z_o's greater than 1.0 m as is found in the foothills.

The deposition layer resistance was taken from the approach proposed by Pleim et al. (1984) and modified to include Slinn's (1982)estimate for the inertial impaction term.

$$r_d = \frac{1}{\left(Sc^{-2/3} + 10^{-3/St}\right)u_*} \tag{4}$$

where

Sc = Schmidt number ($Sc = \upsilon/D_B$)
υ = viscosity of air (0.15 cm^2 s^{-1})
D_B = Brownian diffusivity of the particle in air (cm^2 s^{-1})
St = Stokes number ($St = v_g/g\,[u_*^2/\upsilon]$, dimensionless)

g = acceleration due to gravity (981 cm s^{-2})

Stokes law gives the gravitational settling velocity (cm s^{-1}) for particles less than 30 µm as

$$v_g = \frac{C_c\, d^2\, g\rho}{18\mu_{air}} \tag{5}$$

where

C_c = the Cunningham slip correction factor (dimensionless)
d = physical particle diameter (cm)
μ_{air} = dynamic viscosity of air (1.78×10^{-4} g s^{-1} cm^{-2})
ρ = particle density (2.65 g cm^{-3} for soil).

For particle sizes less than several microns, the Cunningham Slip correction factor is approximately 1.0. Figure 5 presents gravitational settling velocity as a function of particle size. The Brownian diffusivity (cm s^{-1}) of the particle in air is given by

$$D_B = 8.09 \times 10^{-10}\, \frac{C_c\, T_a}{d} \tag{6}$$

where

T_a = air temperature (°K)

Each hourly release estimate was broken down by four particles sizes: <3-µm, 3–10-µm, 10–15-µm, and 15–30-µm AED. Risk calculations used the first three size classes because particles >15-µm AED are not assumed to be respirable. Implementation of gravitational settling in RATCHET involved adding Equations 1–6 to the deposition algorithm. Other aspects concerning gravitational settling are discussed in the "Source Characterization" and "Prediction Uncertainty" sections of this report.

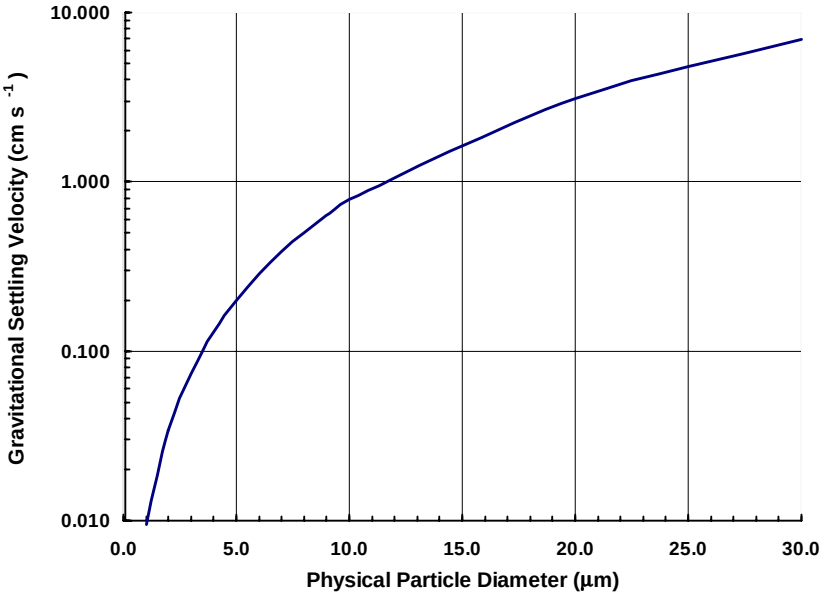

Figure 5. Gravitational settling velocity as a function of the physical particle diameter for soil (ρ = 2.5 g cm^{-3}).

Wet deposition of small particles in RATCHET is modeled using a washout coefficient and assuming irreversible collection of particles as the precipitation falls through the puffs. No precipitation was recorded in the model domain during the 24 highest S-8 sampler days; therefore, this process is irrelevant for these releases. For baseline releases, precipitation measured at the Denver Stapleton Airport was assumed to be constant throughout the model domain because precipitation records at the RFP are lacking.

The following expression, discussed in Slinn (1984), is used to compute the washout coefficient in RATCHET:

$$\Lambda = \frac{C\,E\,P_r}{0.35\,P_n^{1/4}} \tag{7}$$

where
Λ = washout coefficient (hr^{-1})
C = empirical constant assumed to have a value of 0.5
E = average collision efficiency assumed to be 1.0
P_r = precipitation rate (mm hr^{-1})
P_n = normalized precipitation rate (P_r)/ (1 mm hr^{-1}).

The normalized precipitation rate is a dimensionless quantity that represents the precipitation rate normalized to 1 mm h^{-1}. During periods of snow, the washout coefficient for particles is computed by

$$\Lambda = 0.2\,P_r \quad . \tag{8}$$

Precipitation rates in RATCHET are separated into six classes: three for liquid and three for frozen precipitation (Table 7). These classes are the similar to those reported by most airport meteorological recording stations.

Table 7. Precipitation Rates and Washout Coefficients Used in RATCHET

Precipitation type	Precipitation rate (mm hr^{-1})	RATCHET precipitation code	Washout coefficient (hr^{-1})
No precipitation	0.0	0	0.00
Light rain	0.1	1	0.254
Moderate rain	3.0	2	3.26
Heavy rain	5.0	3	4.78
Light snow	0.03	4	0.006
Moderate snow	1.5	5	0.3
Heavy snow	3.3	6	0.66

Diffusion Coefficients

The RATCHET model estimates diffusion coefficients directly from statistics for atmospheric turbulence. In most cases, the statistics describing atmospheric turbulence (i.e., standard deviation of the horizontal and vertical wind direction fluctuations) are not routinely measured at most meteorological recording stations. However, RATCHET makes use of atmospheric conditions that are either measured or calculated from routine meteorological data to

estimate the turbulence statistics. The parameters wind speed, atmospheric stability, and surface roughness are used to estimate the turbulence statistics. The general form of the equation used in RATCHET for estimating the horizontal diffusion coefficient (σ_r) for the first hour following release is

$$\sigma_r = 0.5\sigma_v\, t \tag{9}$$

where

σ_v = crosswind component of turbulence (m s^{-1})
t = travel time.

After the first hour, the horizontal diffusion coefficient is given by $\sigma_r = c_{sy}\, t$, where c_{sy} is a proportionality constant with dimensions of meters per second. Gifford (1983) has shown the value of c_{sy} distributed between 0.14 to 1.4, with a median value of 0.5. For our simulations, we used the median value of 0.5.

The general form of the equation for estimating the vertical diffusion coefficient (σ_z) near the source is

$$\sigma_z = \sigma_w\, t\, f_z(t) \tag{10}$$

where

σ_w = standard deviation of the vertical component of the wind (m s^{-1})
$f_z(t)$ = nondimensional function related to the travel time and turbulence time scale.

As a practical matter, diffusion coefficients in RATCHET are calculated in increments to avoid problems associated with spatial and temporal changes in conditions.

Source Characterization

Estimated atmospheric releases of $^{239/240}$Pu attached to soil particles <30-µm AED from the 903 Area are documented in Weber et al. (1999) and are summarized in a previous section. Release estimates were further discretized into four particle size classes: <3-µm, 3–10-µm, 10–15-µm, and 15–30-µm AED. The first three particles classes represent potentially respirable particles. Separate source terms were calculated for each of these three classes. The last size class was ignored for risk calculations because these particles are not respirable. However, the 15–30-µm AED class was included in deposition calculations, the results of which will be discussed in another report dealing with comparisons of model predictions with environmental monitoring data.

Source terms for the 6 highest S-8 sampler measurement days were generated by the 903 Area source term model. One thousand realizations of the code were performed resulting in 1000 estimates of hourly releases for each of the three size fractions of interest. For each realization, the total release for a given size fraction was parsed into hourly release rates using

$$Q_i = \frac{\left(\frac{u_i}{u_*}\right)^{\gamma}}{\sum_{i=1}^{n}\left(\frac{u_i}{u_*}\right)^{\gamma}} Q_{total}\; f \tag{11}$$

where

Q_i = release rate for the i^{th} hour (Ci h^{-1})
u_i = wind speed for the i^{th} hour (m s^{-1})
u_* = threshold friction velocity (m s^{-1})
γ = wind speed exponent
Q_{total} = total release (all particle sizes) over the measurement period (Ci)
n = number of hours in a measurement period
f = fraction of particles within a given size fraction.

Equation (11) was implemented in the 903 Area source term code. The terms, u_*, f, and γ were sampled once during a Monte Carlo realization. A total release quantity (over the measurement period) was then calculated. This release quantity was then parsed into hourly release rates by size fraction using Equation (11). In the RATCHET simulations, these hourly release rates for each size fraction were read sequentially, and in this way, correlation among particle sizes was maintained. An example of a single realization for the December 5, 1969 release day is illustrated in Figure 6 which shows the hourly release rates for the three size fractions. The RATCHET simulations for discrete events were run for 26 hours, 2 hours longer than the calculated source term. The extra 2 hours were used to transport the remaining plume elements out of the model domain after the source was turned off.

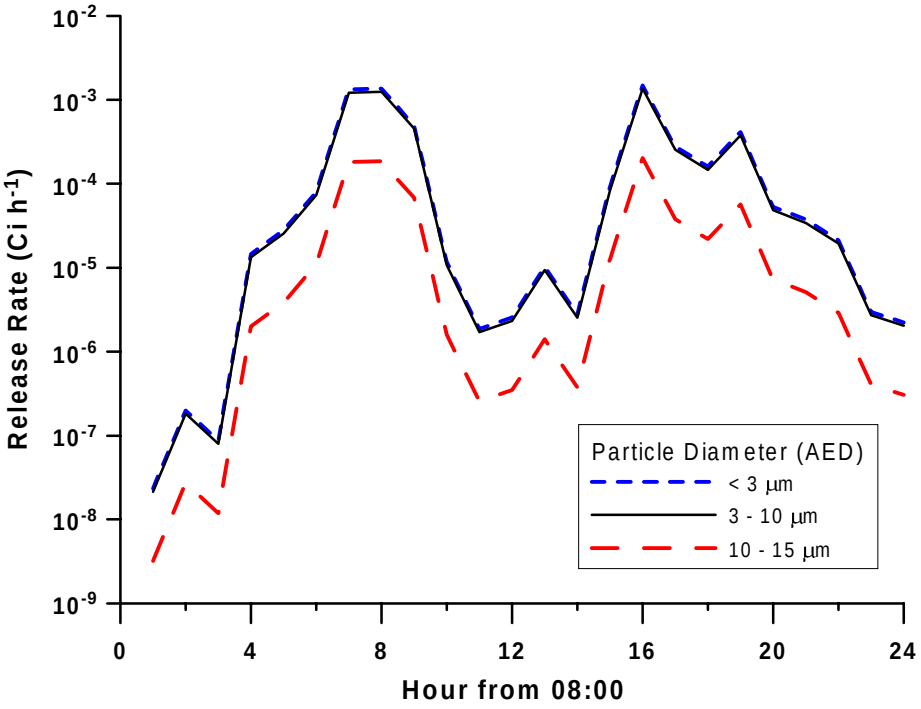

Figure 6. Time-dependent hourly release rates for the three size fractions for December 5, 1968. The graph represents a single Monte Carlo realization.

For baseline releases, annual release quantities were broken down by the size fractions described earlier using a fixed particle size distribution. Release percentiles for the remaining 24 highest S-8 sampler measurement days (excluding the 6 highest S-8 sampler measurement days that were treated discretely) were added to the annual release quantities for their respective year of occurrence. Total annual release quantities were segregated into the three size fractions of

interest by multiplying the total release quantity by the fraction of activity associated with the given size fraction. The fraction of activity in each size fraction was the same as that used to derive the baseline release estimates reported in Weber et al. (1999). The fractions of activity are as follows: 3.5% for <3-µm particles, 7.5% for 3—10-µm particles, and 7.5% for 10—15-µm particles. Releases were assumed constant over the year being modeled. Distributions of release quantities were represented by percentiles in 5% increments for each year in the simulation.

For the 6 highest S-8 sampler measurement days, gravitational settling velocities were calculated stochastically by first selecting a particle diameter (in AED) from a distribution that encompasses the range of diameters for a particular size fraction. The particle size was then converted to its physical diameter given by

$$d_p = \frac{AED}{\sqrt{\rho_s / \rho_u}} \tag{12}$$

where

d_p = physical particle diameter (m)
ρ_s = particle density (2.65 g cm^{-3})
ρ_u = unit particle density (1.0 g cm^{-3}).

The gravitational settling velocity was then calculated using Equation (5). Distributions were assumed to be lognormal based on the distributions used to calculated the risk coefficients and were truncated according to the source-term size range. The GM value was selected to lie midway in the range. The GSD was assumed to be 2.5 for all size ranges and was based on the GSD for the risk coefficients. For the <3-µm size fraction, the GM was assumed to be 1.0 and the minimum diameter was assumed to be 0.5 µm. For gravitational settling calculations, this makes little difference because deposition is dominated by the dry deposition components for these small particles. Table 8 shows the relationship between the source-term-specific particle diameters and the distribution of particle diameters used to compute gravitational settling in the RATCHET simulations.

Table 8. Distributions of Particle Diameters[a] used to Compute Gravitational Settling for the RATCHET Simulations

Source-term particle diameter (µm)	GM of particle diameter[b] (µm)	GSD	Minimum (µm)	Maximum (µm)
<3	1.0	2.5	0.5	3
3–10	6.5	2.5	3	10
10–15	12.5	2.5	10	15

[a] All particle diameters in AED.
[b] Geometric mean of particle diameter distribution used in the RATCHET simulations.

For baseline releases, gravitational settling in RATCHET assumed a fixed value based on the GM of the particle diameter for the three size fractions given in Table 8. Three annual average RATCHET simulations were run, one for each size fraction.

Releases were modeled as occurring over a square source that represented the entire 903 Area (Table 9). Area sources are represented in RATCHET by introducing an initial diffusion coefficient into the calculation. Using the procedure described in Petersen and Lavdas (1986),

the initial horizontal diffusion coefficient (σ_r) is the horizontal dimension of the source divided by 4.3, and the initial vertical diffusion coefficient (σ_v) is the height of the source divided by 2.15. The 903 Area is approximately square with sides measuring about 107 m. Therefore, σ_r was assigned a value of 25 m. Release height (that is, the height of suspended contaminated soil particles above the 903 Area) was assumed to be about 1 m. Therefore, σ_v was assigned a value of 0.5. In practice, downwind concentrations are not particularly sensitive to initial diffusion coefficients when receptors are relatively distant (>3 km) from the source compared to the source dimensions.

Table 9. Release Parameters for 903 Area Releases

Parameter	Value
Release height	1 m
Release area	13,707 m
Initial σ_r	25
Initial σ_z	0.5
UTM east of 903 Area center	483400 m
UTM north of 903 Area center	4415310 m

Other Parameters

Several other parameters in RATCHET influence the accuracy of output and computer runtime. These parameters include the number of puffs per hour, minimum time step, puff consolidation, maximum puff radius, and minimum puff concentration at center. We chose the suggested RATCHET default values for all these parameters except minimum time step and minimum concentration at puff centers (Table 10). Accuracy of the simulation can be improved by using a smaller time step. The RATCHET default was 20 minutes, which we reduced to 10 minutes. The minimum concentration at puff centers was reduced from 1×10^{-13} to 1×10^{-15} to allow dilute plumes to be tracked throughout the model domain. The puff consolidation parameter value combines puffs from the same source when the ratio of the puff centers to the average σ_r is less than the user-input value. The puff consolidation ratio and maximum puff radius (in units of σ_r) were set at RATCHET default values of 1.5 and 3.72, respectively.

Table 10. RATCHET Model Control Parameters

Model parameter	Value
Number of puffs per hour	4
Minimum time step	1 minute
Puff consolidation	1.5
Maximum puff radius (in units of σ_r)	3.72
Minimum concentration at puff centers	1×10^{-15}

Prediction Uncertainty

Prediction uncertainty is the expected uncertainty in model predictions of airborne concentrations of suspended plutonium-contaminated soil in the model domain. The uncertainty in the predicted concentrations accounts for uncertainty in the atmospheric transport model combined with uncertainty in the source term. We have approached the assessment of uncertainty differently for the discrete events and the baseline release events because the manner in which they were modeled differs.

Prediction Uncertainty for Discrete Release Events

Prediction uncertainty for discrete events applies to the 6 highest S-8 sampler days. We employed the random sampling features of RATCHET in these simulations because (1) meteorological data were available for the specific release event and (2) random sampling of meteorological input parameters allows for mass balance of the source term with the contaminant mass in the model domain. RATCHET uses random sampling from specified distributions to represent the uncertainty in meteorological data. Specifically, random sampling is limited to wind directions and wind speeds, stability class, Monin-Obukhov length, precipitation rates, and station mixing-layer depths. This limitation preserves the physically based correlations among other model parameters and variables. Random sampling of precipitation rates was not used because no precipitation fell during the discrete events. Uncertainty in the source term and particle size distributions was handled external to the RATCHET code.

We recognize that we have correlated wind speed, wind direction, and atmospheric stability from the source term calculation only to the extent that these values represent the nominal values used in the RATCHET simulations. For example, the value of the wind speed used for the source term may not be the *exact* same value that was used in a RATCHET realization. In the source term calculation, uncertainty was treated somewhat differently. Instead of varying each of the meteorological inputs according to some predefined distribution, we applied an uncertainty factor to the dispersion calculation that represents uncertainty in the meteorological conditions, deposition and plume depletion algorithms, and transport model formulation. We justify this approach to uncertainty in the RATCHET simulations because meteorological parameters, such as wind speed and direction, tend to show greater variance over larger distances (10–30 km) compared to 190-m distance used to compute transport from the 903 Area to the S-8 sampler. That is, we have assumed the meteorological parameters were reasonably well represented over the short transport distance from the 903 Area to the S-8 sampler. Over greater distances, however, there is greater uncertainty in these parameters and this was accounted for in the RATCHET simulations.

Wind Direction Uncertainty. Uncertainty in the wind direction is addressed in RATCHET by sampling from a uniform distribution whose width depends on the measured wind speed. During calm conditions, the width of the distribution is from 0 to 360 degrees. The distribution narrows as the wind speed increases, until the width of the distribution equals the imprecision in the recorded values (a minimum value of 10 degrees). The method used to vary the width of the distribution in RATCHET is based on a procedure described in Schere and Coates (1992). Other sources of uncertainty in wind directions are not considered by the random-sampling algorithm in RATCHET. These sources of uncertainty include

- Instrument exposures that may cause observed wind direction to differ systematically from the directions that are representative for the region of measurement
- Changes in wind direction with height that may cause elevated plumes to move in a direction that is different from the one predicted from surface observations.

In reference to the last bullet, Elderkin and Gudiksen (1993) studied several of the WVTS nighttime tests in which additional instrumentation was installed and monitored as part of the Atmospheric Studies in Complex Terrain (ASCOT) program. They found dispersion was controlled by multiple scales of motion that created interacting layers, which varied in three dimensions and on an hourly basis. Tracer plumes were mostly confined to a stable drainage layer that followed regional flow features, intermittently interrupted by evolving mountain-canyon flows. Interactions between the surface layer and the mountain-canyon flow layer caused unexpected tracer trajectories that were not anticipated based on conventional surface observations. In all atmospheric model simulations performed for this project, we have assumed the contaminant plumes have remained confined to the surface layers. We acknowledge the possibility that some of the plumes may have been entrained in upper layers as described by Elderkin and Gudiksen (1993). However, we find it impossible to predict with any confidence the trajectory of such entrained material given the lack of meteorological data and the current state-of-the art of atmospheric transport models. In such cases, however, *ground level* atmospheric concentrations of plutonium in the model domain would be substantially lower than current predictions.

Wind Speed Uncertainty. Wind speeds are recorded in some meteorological records as integer values and in a variety of units. For example, the Denver Stapleton International Airport wind speeds are reported to the nearest whole number in units of knots. This imprecision in wind speed measurements is addressed in RATCHET. RATCHET also addresses the additional uncertainty in wind speeds near and below the threshold. However, for our simulations, very few of the measured wind speeds were near this level (about 1 m s^{-1}).

When random sampling of wind speeds is selected, wind speed is drawn from a uniform probability distribution because with a given wind observation there is no reason to assume that the actual speed is more or less likely to be in any part of the range of values. The width of the distribution is two reporting units. For example, if the measured wind speed is 5 m s^{-1}, then the width of the distribution is from 4 to 6 m s^{-1}. When a calm wind is reported, a wind speed between 0 and 1 m s^{-1} is used.

Stability Uncertainty. Atmospheric stability is a fundamental concept in meteorology, but it cannot be calculated directly from the available meteorological data. Therefore, stability must be estimated from the limited data that are available.

Methods of estimating stability classes proposed by Gifford (1961), Pasquill (1961), and Turner (1964) are based on data that are available in routine meteorological observations, such as those taken at airports. These methods form the basis of the procedures that the National Climatic Data Center uses to estimate stability classes from climatological data (Hatch 1988).

Golder (1972) compares stability-class estimates made at five locations using the method proposed by Pasquill and Turner's variation. The results of this comparison, presented in Golder (1972, Figure 3), show reasonable agreement among the hourly stability-class estimates. However, other studies, such as the study of Luna and Church (1972), show that these stability

classes have a much wider range of uncertainty when attempting to estimate turbulence characteristics related to diffusion.

RATCHET allows the user to specify the uncertainty associated with stability-class estimates. This uncertainty is represented by a set of seven conditional cumulative frequency distributions—one conditional cumulative frequency distribution for each stability class. The cumulative frequency distribution represents the possible actual stability class for the one reported stability class. To do this, two different methods of calculating stability were employed: (1) the method described in Turner (1964) and used to define nominal values for stability class and (2) the lateral turbulence and wind speed method (standard deviation of the horizontal wind direction fluctuations) as described in EPA (1987). Stability classes were calculated for 5 years of meteorological data taken at the RFP between 1989 and 1993. This was the same meteorological data set used for baseline release and transport calculations. Conditional cumulative frequency distributions are input through a file containing seven records, one for each stability class (Table 11). Each record contains seven records that are the cumulative probability that the actual stability class is the same as the reported stability class.

For example, the probability that a reported stability class of 1 is actually 1 is 0.934 (see line one column 1). The probability that a reported stability class of 1 may actually be 2 is 0.961 – 0.934 = 0.027. The probability that a reported stability class of 1 may actually be 3 is 0.988 – 0.961 = 0.027. The probability that a reported stability class of 1 may actually be 4 is 1.00 – 0.988 = 0.012 and so on.

Table 11. Conditional Cumulative Frequency Distributions for Stability Class

Stability class	Cumulative frequency that the actual stability class is ≤ the reported stability class						
	1	2	3	4	5	6	7
1	0.934	0.961	0.988	1.000	1.000	1.000	1.000
2	0.565	0.819	0.927	0.996	0.998	1.000	1.000
3	0.268	0.409	0.704	0.955	0.981	1.000	1.000
4	0.072	0.113	0.213	0.895	0.975	1.000	1.000
5	0.000	0.000	0.000	0.597	0.994	1.000	1.000
6	0.000	0.000	0.000	0.339	0.629	1.000	1.000
7	0.000	0.000	0.000	0.110	0.279	1.000	1.000

Monin-Obukhov Length. Stability classes are discrete estimates of atmospheric stability. However, boundary-layer similarity theory uses the reciprocal of the Monin-Obukhov length, which is a continuous variable to represent stability. Figure 2.4 in the RATCHET documentation (Ramsdell et al. 1994), which is based on Golder (1972), provides a basis for converting stability class to Monin-Obukhov length (Figure 7). When random sampling of the reciprocal Monin-Obukhov is selected, RATCHET obtains an appropriate value as needed from a uniformly distributed range of values. The upper and lower bounds of the range are computed from the surface roughness and stability class.

Mixing-Layer Depth. RATCHET computes mixing-layer depth from the friction velocity and Monin-Obukhov length. For stable conditions, the mixing-layer depth is given by

$$H = k\left(\frac{u_* L}{f}\right)^{1/2} \quad (13)$$

where

H = mixing layer depth (m)
k = von Karman constant (~0.4 dimensionless)
u_* = friction velocity (m s^{-1})
L = Monin-Obukhov length (m)
f = Coriolis parameter (s^{-1}).

Pasquill and Smith (1983) indicate that constant values in the range of 0.2 to 0.7 have been suggested in place of the von Karman constant. Weil (1985) suggests constant values in the range of 0.4 to 0.7. For neutral or unstable conditions, the mixing layer depth is estimated using

$$H = \frac{\beta u_*}{f} \quad (14)$$

where β = a dimensionless constant. Zilitinkevich (1972) assumes β is equal to k while Pasquill and Smith (1983) suggests a value in the 0.2 to 0.3 range. Other researchers (Panofsky and Dutton 1984) suggest its range is from 0.15 to 0.25. When random sampling of the mixing depth is selected, RATCHET samples the value of k and β from uniform distributions. The range of k is fixed between 0.2 and 0.7, and the range of β is fixed between 0.15 and 0.3.

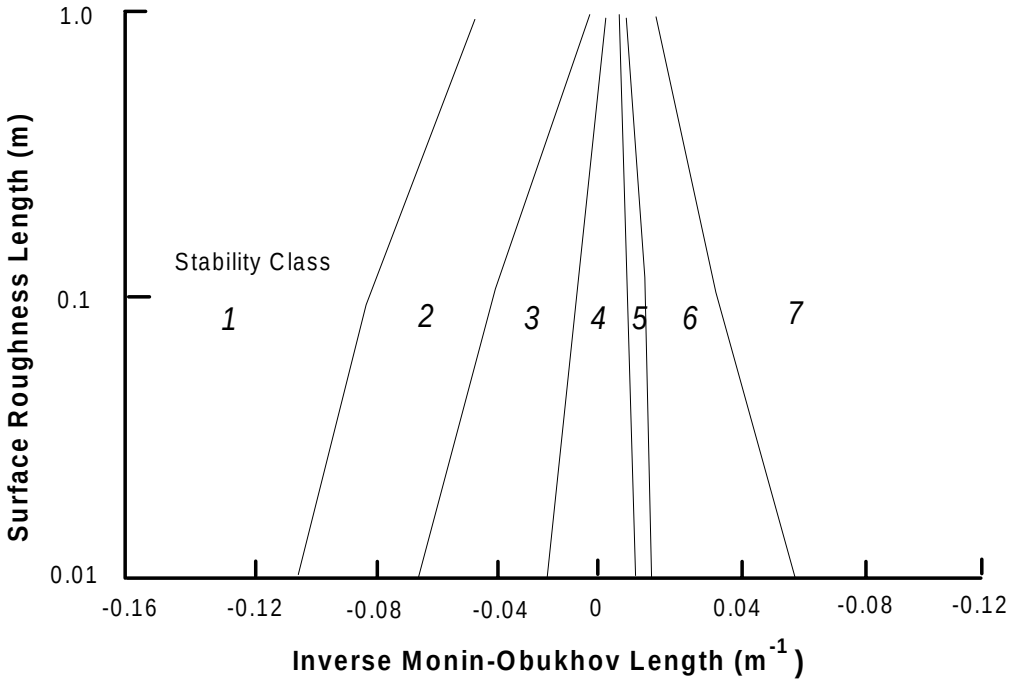

Figure 7. Relationship between stability class and Monin-Obukhov length as a function of surface roughness length (redrawn from Ramsdell et al. 1994).

Integration of Uncertainty Analysis into Model Predictions. The uncertainty analysis for discrete events involved a Monte-Carlo simulation that coupled RATCHET atmospheric transport simulations with distributions of the 903 Area source term for discrete events. For each realization of a discrete event, three RATCHET simulations were generated (one for each of the three size fractions). Each RATCHET Monte Carlo simulation used the same initial random seed numbers for all size fractions. In RATCHET, random number sequences that begin with the same initial seed value are identical. In this way, the stochastic meteorological parameters are correlated among runs for different size fractions. The sampling scheme for a given release event based on 1000 realizations is as follows:

- One thousand realizations of hourly release rates for each particle size were generated by the 903 Area source term model. Release quantities were correlated among the three size fractions. Output was written to files for later use.
- Three RATCHET input files, one for each particle size fraction, were prepared. Each input file used the same initial random number seeds so as to preserve correlation in meteorological parameters among the different size fractions.
- For each size fraction, 1000 realizations of RATCHET were performed. Source terms were read sequentially from the files generated earlier.

Output consisted of 1000 realizations of atmospheric concentrations and deposition at receptor nodes in the model domain. Integration of source term uncertainty into the RATCHET simulations and post-processing of output involved writing a shell program that performed the following tasks: (1) read values from the source-term files and generated a RATCHET source term file, (2) selected a particle size and calculated a gravitational settling velocity, (3) wrote a RATCHET input file and executed the code, and (4) extracted and stored results.

Prediction Uncertainty for Baseline Releases

For baseline releases, we are interested in defining the expected uncertainty in the annual average dispersion estimates within the model domain for each year of the assessment period (1964–1969). The approach we used for baseline releases was to develop distributions of multiplicative correction factors that were applied to each concentration estimate in the model domain. These multiplicative correction factors were developed from field validation data, joint frequency distribution comparisons, and parametric uncertainty analysis. Three components of uncertainty were evaluated:

1. Dispersion uncertainty
2. Meteorology uncertainty
3. Plume depletion uncertainty.

Dispersion uncertainty considers the uncertainty in predicting the annual average concentration of an inert, nonreactive tracer for a specific year, assuming we have the meteorological data for that year. Meteorology uncertainty arises because we used 5-years of meteorological data spanning a recent time period (1989–1993) to calculate an annual average χ/Q values that were applied to years of the assessment period (1964–1969). Uncertainty in plume depletion via dry deposition was considered separately because dispersion uncertainty was based on tracer studies that typically employ inert, nonreactive tracers that have dry deposition velocities that are small

and inconsequential. Uncertainty in plume depletion from wet deposition and gravitational settling was not considered.

Dispersion Uncertainty. Dispersion uncertainty includes two sources: (1) errors in model input and (2) errors in model formulation or in the model itself (i.e., does the model adequately represent the physical process and phenomena it attempts to simulate). For example, suppose we select a location in the model domain and measure the concentration of tracer released from the site for an entire year. Let us assume the uncertainty associated with the measurement is small and inconsequential. Using the meteorological data recorded for that year, we calculate a concentration at the same receptor location using an appropriate atmospheric dispersion model. Assuming our model adequately represents the physical process and phenomena (i.e., if we had the correct inputs to the model, the output would match the observations), the uncertainty associated with the model prediction results from a lack of knowledge about the correct inputs to our model. Propagating these uncertainties through the model calculation provides a distribution of model output. This is termed parameter uncertainty. The output distribution may be compared with measured data to see if model predictions encompass the measurements. Generally, agreement between predictions and observations is achieved when the model adequately represents the processes it attempts to simulate and choices regarding input parameter values have been made correctly.

Model uncertainty arises from the fact that perfect models cannot be constructed, and models often fail to adequately represent the physical process they attempt to simulate. In atmospheric dispersion models, the advection-dispersion process is often oversimplified, and meteorological data required to characterize turbulence in the environment are lacking. In our previous example, the parameter uncertainty may not account for all differences between model predictions and observations if our model does not perfectly represent the physical process. Field validation exercises provide some information about the overall performance of a model and, in turn, model uncertainty. However, these exercises are only partially relevant because field tests are generally not conducted under the same conditions that actual releases occurred.

The RATCHET model incorporates modules to explicitly assess parameter uncertainty. These parameters include wind direction, wind speed, atmospheric stability class, Monin-Obukhov length, precipitation rate, and mixing-layer depths. Other parameters may be assessed by simply varying the input according to some predefined distribution and repeating the simulation a number of times until an adequate output distribution is achieved. We used this approach to evaluate discrete release events. For an annual-average computation, these methods are both time-consuming and computationally intensive. In addition, we lacked the complete meteorological record for the assessment period that is required for such an evaluation. For baseline releases, we ignored the built-in parameter uncertainty in RATCHET and focused our efforts on defining the distribution of a correction factor to be applied to model output. (Parameter uncertainty was only used to evaluate uncertainty in plume depletion and dry deposition.) The correction factor was based on field experiments, considering the relevance of the experiment to actual release conditions and model domain environs. In this approach, we ignored the mass balance features of RATCHET and, instead, treated the model output like that of a straight-line Gaussian Plume model for steady-state releases. The only difference is that plume trajectories are not limited to straight lines.

We began the process of defining the distribution of the correction factor for dispersion uncertainty by reviewing some field studies considered relevant to the assessment question

(Table 12), which is the annual average concentration for each year of the assessment period. The correction factor is defined as the inverse of the distribution of predicted-to-observed ratios [$1/(C_p/C_o)$]. Relevant field studies included a model evaluation using the Rocky Flats WVTS data set (Rood 1999a), validation exercises for RATCHET performed at the Hanford Reservation (Ramsdell et al. 1994), summaries of model validations performed for the Gaussian plume model (Miller and Hively 1987), and other studies reported in the literature. No one study is entirely relevant. Averaging times, release conditions, meteorological conditions, and terrain conditions are different from what we attempted to simulate in this study. Nevertheless, we chose to work with these data, and it is unlikely we will find a field validation experiment that was conducted under the exact conditions of past releases at Rocky Flats. Uncertainty bounds may be expanded to compensate for our lack of knowledge.

An additional study (Carhart et al. 1989) not reported in Table 12 included puff dispersion models that were similar to RATCHET (i.e., MESOPUFF and MESOPLUME). Evaluations were performed using tracer data bases from Oklahoma and the Savannah River Site. Oklahoma data consisted of two experiments measured at 100- and 600-km arcs downwind of a 3-hour perfluorocarbon release. The Savannah River data involved 15 separate experiments, 2 to 5 days in duration, where ^{85}Kr was released from a 61-m stack and measured at points 28 to 144 km downwind from the source. The ratio of the *average* predicted concentration to the *average* observed concentration was between 0.5 and 2. Note that this measure is different than the distribution of individual predicted-to-observed ratios reported in Table 12. There was also a tendency for models to overpredict concentrations in both data sets.

The study considered most relevant to the assessment question involved the RATCHET model using the WVTS data set. While it is true the release conditions for this study differed from those modeled (i.e., point source as opposed to area source); the averaging time differed (i.e., annual average as opposed to 9-hour average); and the source differed (i.e., gas as opposed to particulate)—these data were obtained in the same environs that we are attempting to simulate. Release heights for the 903 Area were generally at ground –level, while the WVTS releases were at 10 m above ground level. Abbott and Rood (1996) also showed that the difference between a point and a 100-m diameter area source (represented by a series of point sources distributed in a circular area) released from a height of 0–19 m is at most 5% along the plume centerline at a distance of 2 km or greater for all combinations of wind speed and stability. We conclude that the major difference between the WVTS data set and our current situation is the averaging time and physical characteristics of the effluent (i.e., gas versus particulate).

The largest range of predicted-to-observed ratios reported in Table 12 involved complex terrain, which suggests models are more sensitive to the local meteorological and terrain conditions than other factors, such as release height and conditions. For example, note the GSD for short-term estimates using the Gaussian plume model at a highly instrumented site for elevated source increases by about 9% from its ground-level counterpart, but the difference between the GSD for flat and complex terrain is almost an order of magnitude.

Table 12. Geometric Mean and Geometric Standard Deviation of Predicted-to-Observed Ratios for Field Studies Relevant to Defining the Correction Factor for Annual Average Concentrations

Model	Averaging time	Receptor distance	Release height	Environment	GM	GSD	Comments
RATCHET[a]	9-hour	8 km	10 m	complex terrain	0.86	4.4	Rocky Flats Winter Validation Study
RATCHET[a]	9-hour	16 km	10 m	complex terrain	1.1	4.3	Rocky Flats Winter Validation Study
RATCHET[b]	28-day	20–80 km	61 m	flat	1.4	2.2	Conducted at the Hanford Reservation
Gaussian Plume[c]	short-term	10 km	ground level	flat - highly instrumented		1.1	P/O ratios ranged from 0.8 to 1.2
Gaussian Plume[c]	short-term	10 km	elevated	flat - highly instrumented		1.2	P/O ratios ranged from 0.65 to 1.4
Gaussian Plume[c]	short -term	—	—	complex terrain		14	P/O ratios ranged from 0.01 to 100
Gaussian Plume[c]	annual average	—	—	complex terrain		3.8	P/O ratios ranged from 0.1 to 10
Gaussian Plume[c]	annual average	10 km	ground-level	flat		1.5	P/O ratios ranged from 0.5 to 2
Gaussian Plume[c]	annual average	10–50 km	ground-level	flat		2.2	P/O Ratios ranged from 0.25 to 4
Gaussian Plume[d]	12-hour	1–5 km	60 m	relatively flat	0.82	3.4	Terrain heights varied by about 50 m
Gaussian Plume[d]	72-hour	1–5 km	60 m	relatively flat	0.67	2.1	Terrain heights varied by about 50 m
Eulerian and Gaussian Plume[e]	annual average	1–1,000 km	0–60 m	relatively flat	0.75	1.5	Gaussian model used for receptors out to 50 km
CTDMPLUS[f]	12 to 72 hour	1 km	—	complex terrain	1.6	2.5	EPA complex terrain model

[a] Source: Rood (1999a).

[b] Source: Ramsdell et al. (1994).

[c] Source: Miller and Hively (1987).

[d] Source: Robertson and Barry (1989).

[e] Source: Simpson et al. (1990).

[f] Source: Genikhovich and Schiermeier (1995).

With the distribution of predicted-to-observed ratios for RATCHET from the WVTS as our starting point, our approach was to modify this distribution based (a) on the differences between the study conditions and those of past releases and (b) our assessment question (i.e., What is the annual average concentration for each year of the assessment period?). We combined data points at the 8- and 16-km distance into a composite set and justified this action based on the evaluations in Rood (1999a) that showed similar GM and GSD values for 8- and 16-km data. In addition, the confidence intervals on the GM and variance of the observed-to-predicted ratio overlapped. The composite distribution had a GM of 0.95 and GSD of 4.4. Predicted-to-observed

ratios are plotted as a function of the number of standard deviations from the mean (normalized to the standard normal distribution) in Figure 8. Note that most of the data points (± 2σ) lie along the line representing the lognormal fit to the data, with the exception of the tails. We, therefore, represent the distribution of predicted-to-observed ratios as a lognormal distribution with a GM and GSD as defined above. Points on the tails, particularly those with predicted-to-observed ratios less than 0.01, were associated with Test 5 (February 9, 1991) at the 8-km arc in the east-northeast sector for the hours 16:00 to 18:00. All models performed poorly for this test. Concentrations in east-northeast sector were grossly underestimated (greater than a factor of 10 difference), and the ground-level contaminant mass at 8 km was also underestimated. Models appeared to have difficulty responding to the transition from daytime to nighttime stability conditions. During the latter hours of the test and under predominately nighttime conditions (18:00–23:00), predicted concentrations showed better agreement with the observations.

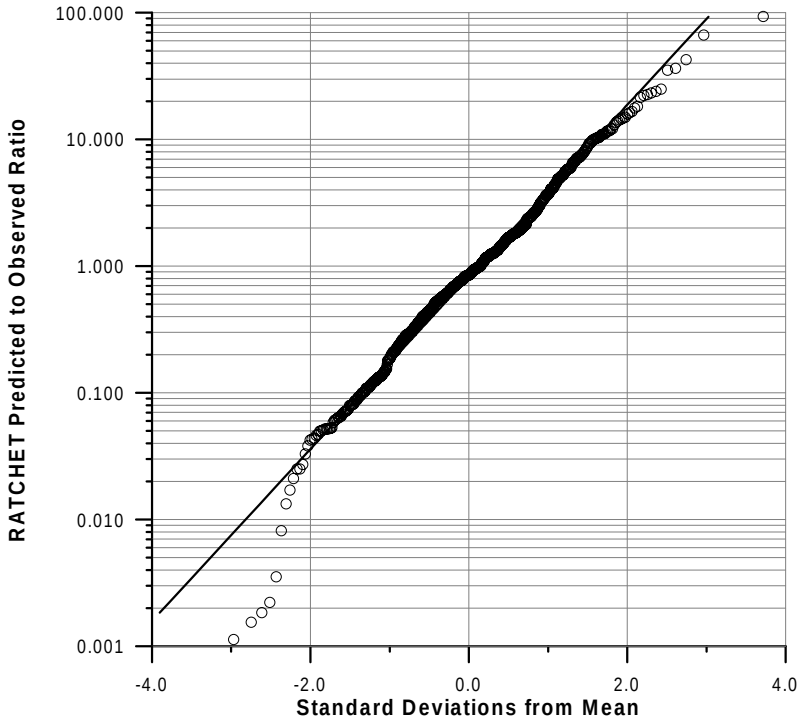

Figure 8. Predicted-to-observed ratios for the RATCHET model as a function of standard deviation from the mean (normalized to a mean of 0 and standard deviation of 1). The solid line represents the lognormal fit to the distribution. Circles represent individual data points.

As stated previously, the major difference between the WVTS data and the assessment question is the averaging time and release height. Averaging time appears to have a large impact on the range of predicted-to-observed ratios encountered. For example, Simpson et al. (1990) reports the GSD of the predicted-to-observed ratio is reduced 38% with an increase in averaging time from 12 to 72 hours (Table 12). Also, note the GSD for the annual average and short-term predicted-to-observed ratio for the Gaussian plume model under complex terrain conditions increases from 3.8 to 14. Validation exercises performed with RATCHET at the Hanford Reservation for an elevated release at distances greater than 20 km showed a slight overprediction by the model (GM = 1.4) and a GSD value of 2.2, which is about 50% smaller

than the GSD for the WVTS data. It is not clear whether these differences are due to averaging time, release height, terrain conditions, or receptor distance. However, based on the other studies reviewed in Table 12, it is likely that the smaller GSD is primarily due to increased averaging time. Key observations relevant to defining the distribution of the correction factor are summarized as follows:

- GSD of predicted-to-observed ratios decrease with increasing averaging time
- GSD of predicted-to-observed ratios increase with increasing terrain complexity
- GSD of predicted-to-observed ratios increase for receptor distances >10 km
- GM of the predicted-to-observed ratio is greater than 1.0 for receptor distances >20 km.

The GSD is expected to fall somewhere between 1.2 and 4.4 based on the data in Table 12. Noting the key observations stated above and the data in Table 12, the following values for GM and GSD were assigned to the predicted-to-observed ratio:

- GSD = 2.2 and GM = 0.95 for receptors <8 km
- GSD = 2.0 and GM = 0.95 for receptors >8 km and <16 km
- GSD = 2.2 and GM = 1.0 for receptors >16 km.

The distribution of predicted-to-observed ratios translates into dispersion correction factors listed in Table 14 in the summary section. The GSD value of 2.2 was the same value calculated for monthly averages using RATCHET at the Hanford Reservation. It may be argued that a lower value is more appropriate because the averaging time is longer. We chose this value because the GSD of monthly average predicted-to-observed ratios will likely be higher for Rocky Flats compared to Hanford because of terrain and particulate deposition complexities. In addition, no annual average predicted-to-observed ratios exist for the Rocky Flats environs. Therefore, uncertainty bounds should be kept large to account for our lack of knowledge. Adjustments in the GSD and GM were also made to account for receptor distance. The GSD was reduced from 2.2 to 2.0 for receptors 8 to 16 km from RFP because the WVTS measurements were made at these distances, and the lower value reflects our greater confidence in uncertainty at these distances. The GM was held at the same value calculated with the WVTS data for receptor distances <16 km and increased to 1.0 for receptor distances >16 km. The GM value was increased to reflect the tendency for models to overpredict at greater distances. Validation studies indicate predicted-to-observed ratios greater than 1.0 (reflecting model overprediction) at distances greater than 20 km. While this may be true, we do not have site-specific data to verify this observation for our model domain. The lower GM predicted-to-observed value will potentially result in model overprediction and, thereby, provide at least a conservative estimate of concentrations at these distances. Correction factor distributions were truncated by a minimum value of 0.01 and a maximum of 1000.

Application of this factor on a year-by-year basis assumes year-to-year annual average concentrations are independent from one another. Analysis of the annual average X/Q values for each year in the 5-year meteorological data set indicated annual average concentrations at some locations are correlated (to some degree) from year-to-year. Ideally, we would like to have meteorological data from the entire assessment period to estimate the year-to-year correlations, but these data are lacking. To account for the unknown year-to-year correlation, we assumed a correlation coefficient of 1.0. This assumption will tend to overestimate uncertainty in the time-integrated concentration (*TIC*), but is justified based on our lack of knowledge about year-to-year

correlations. Details concerning incorporation of this factor in the Monte Carlo uncertainty analysis are discussed in the "Risk Calculations" section of this report.

Meteorology Uncertainty. Meteorology uncertainty arises because we are using 5 years of meteorological data spanning a recent time period (1989–1993) to define an annual average χ/Q value to apply to all previous years for the assessment period (1964–1969). The question is, how well does this 5-year period represent the past? Comparisons of annual average χ/Q values computed with a 5-year data set to the annual average χ/Q values computed using the meteorological data for each specific year were recently performed for the Fernald Dosimetry Reconstruction Project (Killough et al. 1998). Meteorological data from the Cincinnati Airport from 1987 to 1991 comprised the 5-year composite meteorological data set. We then compared annual average χ/Q values computed with these data with the annual average χ/Q value computed for each specific year using the meteorological data for that specific year. The years spanned from 1951 to 1991. Concentrations were calculated at 160 receptors ranging in distance from 1,000 to 10,000 m from the release point. A straight line Gaussian plume model for a 10-m release height was used to generate the χ/Q values. The 5-year composite χ/Q divided by the χ/Q for the specific year (P/O ratio) forms the basis of the upper graph in Figure 9. A similar procedure was applied to the χ/Q values generated for this study and is depicted in the lower graph in Figure 9. However, only the composite period is shown because meteorological data from previous years were not obtained. The lower graph in Figure 9 was generated using the RATCHET model and χ/Q values for 2300 receptors in the model domain. Figure 9 depicts the 5th, 50th, and 95th percentile of the cumulative frequency distribution for all points in the model domain. Note that for the composite period, the spread of the data is similar for both data sets.

As one would expect, the spread is much larger for those years that do not include the 5-year composite data. The long-term trend of these data may not depend strongly on location. If this procedure is applied to the RFP environs using Denver Stapleton International Airport data for instance, the locus of the 50th percentiles is likely to look somewhat different; however, the amplitudes may be similar. Obtaining meteorological data from past years (1964–1969) for Denver Stapleton International Airport and performing the calculations is not a trivial task, and the overall impact on the results may be similar to what is observed at Cincinnati based on a similar spread of these data for the composite period at both locations. For this reason, we chose instead to adapt the Fernald data to our analysis.

The Fernald data were represented by a multiplicative correction factor having a GM of 1.0 and GSD of 1.7. This distribution was developed using the following sampling scheme:

1. Noting from Figure 9 that the maximum range in the GMs is a factor of 2, a GM was randomly selected from a log-uniform distribution with a minimum $2^{-1/2}$ and maximum $2^{1/2}$.
2. Using the GM from step (1) and GSD = 1.61 (the maximum GSD calculated from the ratio of the 5-year composite χ/Q to specific year χ/Q for the 40 years of data), a sample is drawn from a lognormal distribution with these parameters.
3. Values are stored from step (2) and the process is repeated.

This somewhat conservative procedure accounts for the year-to-year variability in the GM of the 5-year composite χ/Q to specific year χ/Q ratio as well as the uncertainty associated with distance and direction from the source. For a sample size of 1000, a lognormal distribution was fitted with a GM = 1.0 and GSD = 1.7.

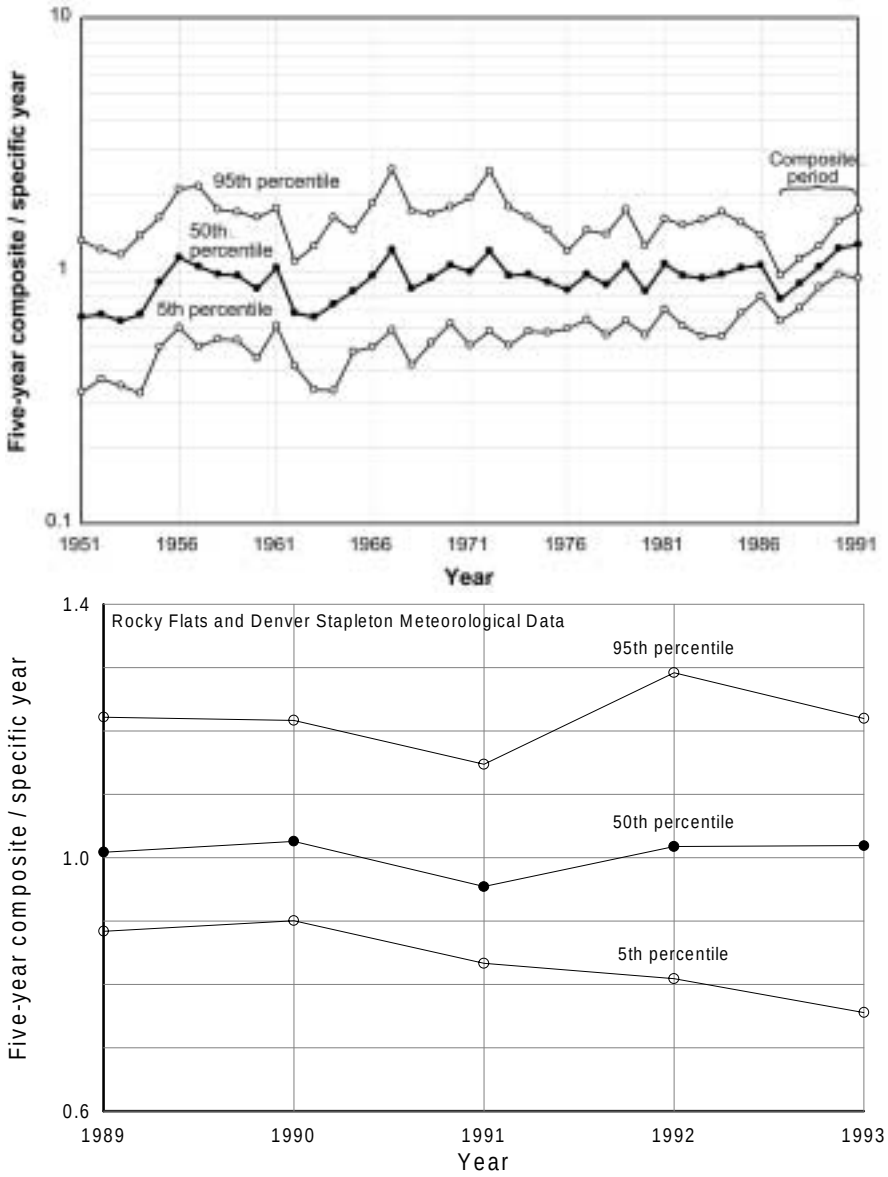

Figure 9. Distributions of P/O ratios for χ/Q calculated with the Cincinnati meteorological data (upper graph) and RFP–Denver Stapleton International Airport meteorological data (lower graph). Predicted (P) corresponds to χ/Q values for a 5-year composite; observed (O) corresponds to the χ/Q values for a specific year (from Killough et al. 1998).

Plume Depletion Uncertainty. One factor not considered in many of the field studies was plume depletion from dry deposition. Most field studies use inert tracers to avoid additional complications involving plume depletion and deposition. Miller et al. (1978) illustrate that plume depletion via dry deposition has little impact on inhalation dose for deposition velocities less than 1.0 cm s^{-1} and release heights greater than 50 m for receptors within 10 km of the release point. For ground-level releases, plume depletion has a greater effect. The ratio of the depleted to nondepleted plume was 0.02 for deposition velocities in the 1.0 cm s^{-1} range and 0.67 for deposition velocities in the 0.1 cm s^{-1} range. Deposition velocities calculated in RATCHET

ranged from 0.3 to 1.0 cm s^{-1}. Therefore, the actual amount of plume depletion would be somewhere between these values. Deposition velocities in the 1.0 cm s^{-1} range are associated with roughness lengths of around 2.0 m, which are limited to the foothills region of the model domain where few receptors are present. For these reasons, the uncertainty in the predicted concentration from plume depletion and deposition is expected to be small for most receptors in the model domain.

Deposition velocity is not an input parameter in RATCHET, but it is calculated (using Equations 1 through 6) for each hour of the simulation. Deposition velocity is a function of the friction velocity, wind speed, roughness height, and a stability correction factor that is a function of the Monin-Obukhov length and wind speed measurement height. Our approach was to vary the Monin-Obukhov length and transfer resistance and calculate alternative values for deposition velocity for a given wind speed and stability classification. Airborne concentrations calculated with alternative values for deposition velocity were compared to the airborne concentrations of the base case. The base case concentrations represent model predictions made using a Monin-Obukhov length that represents the midrange of possible values for a given stability class. (RATCHET uses the midrange of the possible Monin-Obukhov lengths for a given stability class when run in a deterministic mode.)

The random sampling feature in RATCHET was used to vary the Monin-Obukhov length. When random sampling is selected, specific values of the inverse Monin-Obukhov length are obtained from the range of Monin-Obukhov lengths for a given stability class. A random value between 0 and 1 is obtained and used to calculate a value of the inverse Monin-Obukhov length, assuming that the inverse Monin-Obukhov length is uniformly distributed within the range.

Distributions of the transfer resistance must be provided outside the RATCHET code. The rational for the distribution of r_t was based on the distribution of deposition velocities reported in Harper et al. (1995). The 5th, 50th, and 95th percentile values for deposition velocity for 1 μm particles and 5 m s^{-1} wind speed were 0.01, 0.21, and 4.1 cm s^{-1}, respectively. Assuming a lognormal distribution and a 50th percentile r_t value of 100 s m^{-1}, we multiplied the ratio of the 5th/50th percentile and 95th/50th percentile from the distribution of deposition velocities by the 50th percentile transfer resistance value. The 5th percentile for the distribution of r_t was $0.01/0.21 \times 100$ s m^{-1} = 4.8 s m^{-1}. The 95th percentile for the distribution of r_t was $4.1/0.21 \times 100$ s m^{-1} = 1952 s m^{-1}. A lognormal distribution containing 200 individual r_t values was generated in Crystal Ball (Decisioneering 1996) and output to an ASCII file to be used in the uncertainty simulation. The corresponding 5th and 95th percentile deposition velocity calculated using a 5 m s^{-1} wind speed, roughness lengths from 0.001 to 2.0 m, and the midrange value for the Monin-Obukhov length was 0.05 and 1.5 cm s^{-1}, respectively. The range of deposition velocities used in plume depletion uncertainty simulations would be greater because the Monin-Obukhov length was also varied.

A shell program was written to facilitate the plume depletion uncertainty calculations. For each trial, a value of r_t was read from the distribution file created earlier and written to the RATCHET input file. The seed variable for the Monin-Obukhov was also read from the preceding output file and written to the RATCHET input file. The RATCHET code was then called from the shell program and run using meteorological data spanning 1 year (1990) and a unit release rate. Concentrations were output for 156 receptors located 1 to 32 km from the source. Output concentrations were saved, and the process was repeated until all 200 r_t values

were run. A correction factor was calculated for each trial and each receptor. The correction factor is given by

$$CF_{i,j} = \frac{C_{i,j}}{Cb_j} \quad (15)$$

where $CF_{i,j}$ = the correction factor for i^{th} trial and j^{th} receptor, $C_{i,j}$ = the concentration calculated for the i^{th} trial and j^{th} receptor, and Cb_j = the base case concentration for the j^{th} receptor. Correction factors were segregated into bins according to receptor distance. The GM and GSD were then calculated for all CF values within a given bin (Table 13).

These data show a GM near 1.0 and a GSD that increases as a function of receptor distance. As expected, the uncertainty is small, especially near the source, but uncertainty increases at greater receptor distances. The plume depletion uncertainty correction factor was assigned a lognormal distribution with a GM of 1.0 and a GSD that varies with receptor distance as given in Table 13.

Table 13. Plume Depletion Uncertainty Correction Factors

Distance (km)	GM	GSD
4	0.99	1.05
8	1.00	1.09
12	1.01	1.12
16	1.00	1.14
20	1.00	1.16
24	1.00	1.17
28	1.01	1.18
32	1.01	1.18

Summary of Prediction Uncertainty. Three correction factors are applied to our baseline model predictions. The first correction factor accounts for the uncertainty in an annual average concentration of a nonreactive, nondepleting tracer, assuming we have the meteorological data for that year. The second correction factor accounts for the uncertainty associated with using a 5-year composite meteorological data set (1989–1993) to predict the annual average concentrations for years past (1964–1969). The third correction factor accounts for uncertainty in the dry deposition rate and resulting plume depletion for a specific year. The three correction factors are independent of one another and are represented by lognormal distributions. The dispersion correction factor is assumed to be correlated from year to year (correlation coefficient = 1.0). The other correction factors are independent from year-to-year. Table 14 summarizes all three correction factors. Integration of these stochastic factors into the *TIC* estimates is discussed in the "Risk Calculations" section of this report.

Table 14. Summary of Uncertainty Correction Factors Applied to Annual Average Air Concentration Predictions

Receptor distance	Dispersion uncertainty		Meteorology uncertainty		Depletion uncertainty	
(km)	GM[a]	GSD	GM	GSD	GM	GSD
<4	1.1	2.2	1.0	1.7	1.0	1.05
8	1.1	2.0	1.0	1.7	1.0	1.09
12	1.1	2.0	1.0	1.7	1.0	1.12
16	1.1	2.0	1.0	1.7	1.0	1.14
20	1.0	2.2	1.0	1.7	1.0	1.16
24	1.0	2.2	1.0	1.7	1.0	1.17
28	1.0	2.2	1.0	1.7	1.0	1.18
>32	1.0	2.2	1.0	1.7	1.0	1.18

[a] Dispersion uncertainty GM is the inverse of the GM of predicted-to-observed ratios.

Predicted Air Concentrations

Distributions of plutonium concentrations were calculated for 2295 receptor nodes in the model domain. Receptor nodes spacing was 1 km. Eighteen of these receptor nodes were used in subsequent calculations of carcinogenic incidence risk for seven exposure scenarios. Concentrations were calculated separately for the three size fractions: <3 μm, 3–10 μm, and 10–15 μm. This section presents concentration estimates for each release event at the 18 receptor locations that were used in the subsequent carcinogenic risk evaluation. Concentration isopleth maps are also provided for the entire model domain. Results are presented separately for discrete events and baseline releases.

Predicted Air Concentrations for Discrete Events

Distributions of *TICs* for 18 receptor locations in the model domain (illustrated in Figure 10) have been described in terms of their GM and GSD (Tables 14 through 16). These statistics were only used to describe the concentration distributions and not used in the risk calculations. The actual distributions comprising 1000 RATCHET realizations for each size fraction were used instead in the risk calculations to preserve correlation among the size fractions. Geometric standard deviations ranged from 2.7 to 7.9 and were spatially variable. Receptor concentrations near the edge of the plume tended to have greater uncertainty than those near the centerline. Uncertainty in the *TIC* values includes uncertainty in the dispersion estimate and source term. The uncertainty in the dispersion estimate alone was evaluated by running a Monte Carlo simulation for a fixed source term. This was done for the January 7, 1969, date, and GSDs ranged from 1.2 to 3.8. Again, GSDs were spatially variable and tended to be greater near the edge of the plume.

Figure 10 shows the dispersion pattern of the 50th percentile *TIC* for respirable particles (<15 μm) for all discrete events. Dispersion patterns are typical of what we would expect for releases from the RFP during the passage of synoptic weather fronts which was suspected to be responsible for the high wind events. The plume trends east from the RFP until it reaches the western margin of the Platte River Valley located about 10–12 km east of the RFP. At that point,

air movement up and down the Platte River Valley causes the plume to elongate in the northeast-southwest direction. This trend is believed to be due to the influence of the air movement up and down the Platte River Valley and the diurnal pattern of upslope-downslope conditions that characterize the general air movement on the Colorado Front Range environs (Crow 1974). Meteorological data at Denver Stapleton International Airport captures the effect the Platte River Valley has on the general dispersion trends on the Colorado Front Range. The upslope-downslope phenomena is discussed in more detail in the next section.

Table 15. Discrete Event *TIC* Plutonium Concentrations for Particles < 3 μm

Receptor location			<3 μm time-integrated concentration (fCi-h m^{-3}) GM (GSD)					
UTM E (m)	UTM N (m)	Description	05-Dec-68	06-Jan-99	07-Jan-69	30-Jan-69	19-Mar-69	07-Apr-69
485850	4419050	Indiana Street #1	0.78 (3.6)	3.38 (3.7)	32.2 (5.3)	5.20 (4.0)	0.78 (4.5)	0.26 (12.8)
485850	4417050	Indiana Street #2	0.78 (3.7)	8.58 (3.9)	412 (5.8)	3.90 (4.1)	1.04 (4.8)	121 (4.1)
485850	4416050	Indiana Street #3	4.42 (5.6)	9.36 (4.2)	2,092 (3.8)	8.58 (5.3)	5.46 (6.4)	1,074 (3.4)
485850	4415050	Indiana Street #4	314 (3.6)	775 (3.6)	450 (3.6)	4,160 (3.5)	303 (4.2)	1,009 (3.4)
485850	4414050	Indiana Street #5	9.36 (4.0)	139 (3.7)	6.76 (4.4)	14.56 (5.1)	8.06 (5.2)	13.26 (6.2)
485850	4412050	Indiana Street #6	1.30 (3.6)	5.72 (3.5)	3.12 (3.4)	2.34 (4.2)	2.86 (4.8)	0.05 (6.0)
485850	4411050	Indiana Street #7	1.30 (3.6)	4.94 (3.5)	2.34 (3.5)	1.82 (4.3)	0.78 (4.4)	0.05 (5.5)
489850	4409050	Arvada	2.60 (3.5)	5.20 (3.7)	1.56 (3.6)	2.60 (4.1)	1.56 (4.4)	0.26 (4.3)
488850	4401050	Wheat Ridge	2.86 (3.5)	3.12 (3.7)	1.56 (4.4)	0.52 (6.0)	0.26 (4.6)	0.78 (3.6)
491850	4412050	Westminster	8.58 (3.6)	53.0 (3.4)	5.98 (3.4)	11.18 (3.9)	4.16 (4.4)	6.24 (3.8)
492850	4418050	Broomfield	2.08 (3.7)	8.58 (3.5)	223 (3.7)	7.80 (3.8)	1.56 (4.4)	81.9 (3.5)
500850	4416050	Northglenn	10.7 (3.5)	63.7 (3.3)	120 (3.4)	209 (3.5)	10.4 (4.0)	48.1 (3.3)
497850	4412050	Thornton	17.9 (3.5)	71.2 (3.3)	34.6 (3.4)	54.86 (3.5)	7.80 (4.3)	22.9 (3.6)
478850	4426050	Boulder	0.26 (4.1)	1.04 (4.4)	0.26 (4.4)	2.08 (4.3)	0.26 (4.8)	0.00 (--)
492850	4427050	Layfayette	0.78 (3.6)	3.90 (3.7)	5.20 (2.7)	4.94 (4.4)	0.78 (4.5)	0.26 (6.7)
480850	4400050	Golden	0.73 (3.5)	6.73 (3.5)	0.10 (5.1)	0.13 (7.9)	0.16 (5.0)	0.05 (4.3)
505850	4408050	Commerce City	12.7 (3.6)	23.9 (3.2)	44.7 (3.4)	16.90 (3.6)	2.34 (4.1)	19.8 (3.4)
498850	4402050	Denver	10.7 (3.5)	4.94 (3.5)	21.3 (3.6)	1.82 (4.7)	1.04 (4.2)	6.76 (3.4)

Table 16. Discrete Event *TIC* Plutonium Concentrations for Particles 3–10 μm

Receptor location			3-10 μm time-integrated concentration (fCi-h m^{-3}) GM (GSD)					
UTM E (m)	UTM N (m)	Description	05-Dec-68	06-Jan-99	07-Jan-69	30-Jan-69	19-Mar-69	07-Apr-69
485850	4419050	Indiana Street #1	0.520 (4.5)	2.60 (4.4)	25.0 (5.9)	3.90 (4.9)	0.520 (5.5)	0.260 14.4)
485850	4417050	Indiana Street #2	0.780 (4.5)	6.50 (4.5)	320 (6.4)	2.86 (4.9)	0.780 (5.9)	89.4 (4.8)
485850	4416050	Indiana Street #3	3.38 (6.6)	7.28 (5.0)	1,620 (4.5)	6.50 (6.3)	4.42 (6.9)	796 (4.2)
485850	4415050	Indiana Street #4	238 (4.4)	606 (4.3)	348 (4.2)	3,159 (4.3)	236 (5.0)	746 (4.2)
485850	4414050	Indiana Street #5	7.02 (4.9)	108 (4.4)	5.46 (5.0)	10.9 (6.2)	6.24 (6.2)	9.88 (7.2)
485850	4412050	Indiana Street #6	1.04 (4.4)	4.42 (4.2)	2.60 (3.9)	1.82 (5.1)	2.08 (6.1)	0.026 (7.1)
485850	4411050	Indiana Street #7	1.04 (4.5)	3.64 (4.2)	1.82 (4.0)	1.30 (5.2)	0.520 (5.5)	0.026 (6.5)
489850	4409050	Arvada	1.82 (4.4)	3.90 (4.4)	1.30 (4.1)	2.08 (5.0)	1.04 (5.3)	0.260 (5.2)
488850	4401050	Wheat Ridge	2.08 (4.3)	2.34 (4.4)	1.30 (5.1)	0.260 (6.9)	0.260 (5.6)	0.520 (4.4)
491850	4412050	Westminster	6.50 (4.4)	41.3 (4.0)	4.68 (4.0)	8.58 (4.7)	3.12 (5.3)	4.68 (4.6)
492850	4418050	Broomfield	1.56 (4.6)	6.50 (4.2)	172 (4.3)	5.72 (4.6)	1.30 (5.1)	60.6 (4.2)
500850	4416050	Northglenn	8.06 (4.4)	49.7 (3.9)	92.3 (4.0)	158 (4.3)	7.80 (4.8)	35.4 (4.1)
497850	4412050	Thornton	13.5 (4.4)	55.4 (3.9)	26.8 (4.0)	41.6 (4.3)	5.72 (5.2)	16.9 (4.4)
478850	4426050	Boulder	0.26 (5.0)	0.780 (5.2)	0.260 (4.8)	1.56 (5.2)	0.260 (6.0)	0.000 (--)
492850	4427050	Layfayette	0.52 (4.5)	3.12 (4.4)	4.16 (3.0)	3.64 (5.3)	0.520 (5.5)	0.260 (7.7)
480850	4400050	Golden	0.52 (4.4)	5.20 (4.1)	0.078 (5.8)	0.078 (8.9)	0.130 (6.1)	0.026 (5.2)
505850	4408050	Commerce City	9.62 (4.5)	18.7 (3.8)	34.3 (4.0)	12.7 (4.3)	1.82 (5.0)	14.6 (4.2)
498850	4402050	Denver	8.06 (4.3)	3.90 (4.1)	16.1 (4.2)	1.30 (5.5)	0.780 (5.2)	4.94 (4.2)

Table 17. Discrete Event *TIC* Plutonium Air Concentrations for Particles 10–15 μm

Receptor Location			10-15 μm time-integrated concentration (fCi-h m^{-3}) GM (GSD)					
UTM E (m)	UTM N (m)	Description	05-Dec-68	06-Jan-99	07-Jan-69	30-Jan-69	19-Mar-69	07-Apr-69
485850	4419050	Indiana Street #1	0.520 (3.6)	1.82 (3.5)	19.2 (5.2)	2.60 (4.2)	0.260 (4.1)	0.130 13.6)
485850	4417050	Indiana Street #2	0.520 (3.7)	4.68 (3.9)	250 (5.9)	2.08 (4.2)	0.520 (4.5)	82.4 (4.4)
485850	4416050	Indiana Street #3	2.60 (5.5)	4.94 (3.9)	1,267 (3.7)	4.68 (5.3)	2.86 (5.6)	733 (3.6)
485850	4415050	Indiana Street #4	183 (3.6)	443 (3.5)	271 (3.5)	2,406 (3.6)	172 (3.9)	686 (3.4)
485850	4414050	Indiana Street #5	5.20 (4.0)	78.8 (3.7)	4.16 (4.7)	8.06 (4.9)	4.42 (4.8)	9.10 (6.2)
485850	4412050	Indiana Street #6	0.780 (3.6)	3.12 (3.4)	1.82 (3.4)	1.30 (4.4)	1.56 (4.6)	0.026 (6.0)
485850	4411050	Indiana Street #7	0.780 (3.6)	2.60 (3.4)	1.56 (3.4)	1.04 (4.6)	0.520 (4.1)	0.026 (5.4)
489850	4409050	Arvada	1.30 (3.5)	2.60 (3.5)	1.04 (3.6)	1.56 (4.3)	0.780 (3.9)	0.260 (4.2)
488850	4401050	Wheat Ridge	1.56 (3.5)	1.56 (3.6)	1.04 (4.4)	0.260 (6.5)	0.260 (4.2)	0.520 (3.7)
491850	4412050	Westminster	4.94 (3.6)	29.6 (3.4)	3.64 (3.5)	6.240 (3.9)	2.34 (4.0)	4.16 (3.9)
492850	4418050	Broomfield	1.30 (3.7)	4.68 (3.4)	134 (3.6)	4.160 (4.0)	0.780 (3.8)	55.4 (3.7)
500850	4416050	Northglenn	5.98 (3.6)	35.6 (3.2)	71.2 (3.5)	118.8 (3.5)	5.72 (3.6)	32.2 (3.3)
497850	4412050	Thornton	10.1 (3.6)	39.8 (3.2)	20.5 (3.5)	31.2 (3.7)	4.16 (3.9)	15.3 (3.7)
478850	4426050	Boulder	0.260 (4.0)	0.520 (4.1)	0.104 (4.9)	1.04 (4.6)	0.260 (4.7)	0.000 (--)
492850	4427050	Layfayette	0.520 (3.6)	2.08 (3.5)	3.12 (2.9)	2.60 (4.7)	0.260 (4.2)	0.260 (7.0)
480850	4400050	Golden	0.520 (3.5)	3.64 (3.4)	0.078 (4.9)	0.052 (8.4)	0.078 (4.8)	0.026 (4.3)
505850	4408050	Commerce City	7.02 (3.6)	13.3 (3.2)	26.3 (3.5)	9.36 (3.7)	1.30 (3.7)	13.0 (3.5)
498850	4402050	Denver	5.98 (3.4)	2.60 (3.4)	12.2 (3.6)	1.04 (5.0)	0.520 (3.9)	4.42 (3.6)

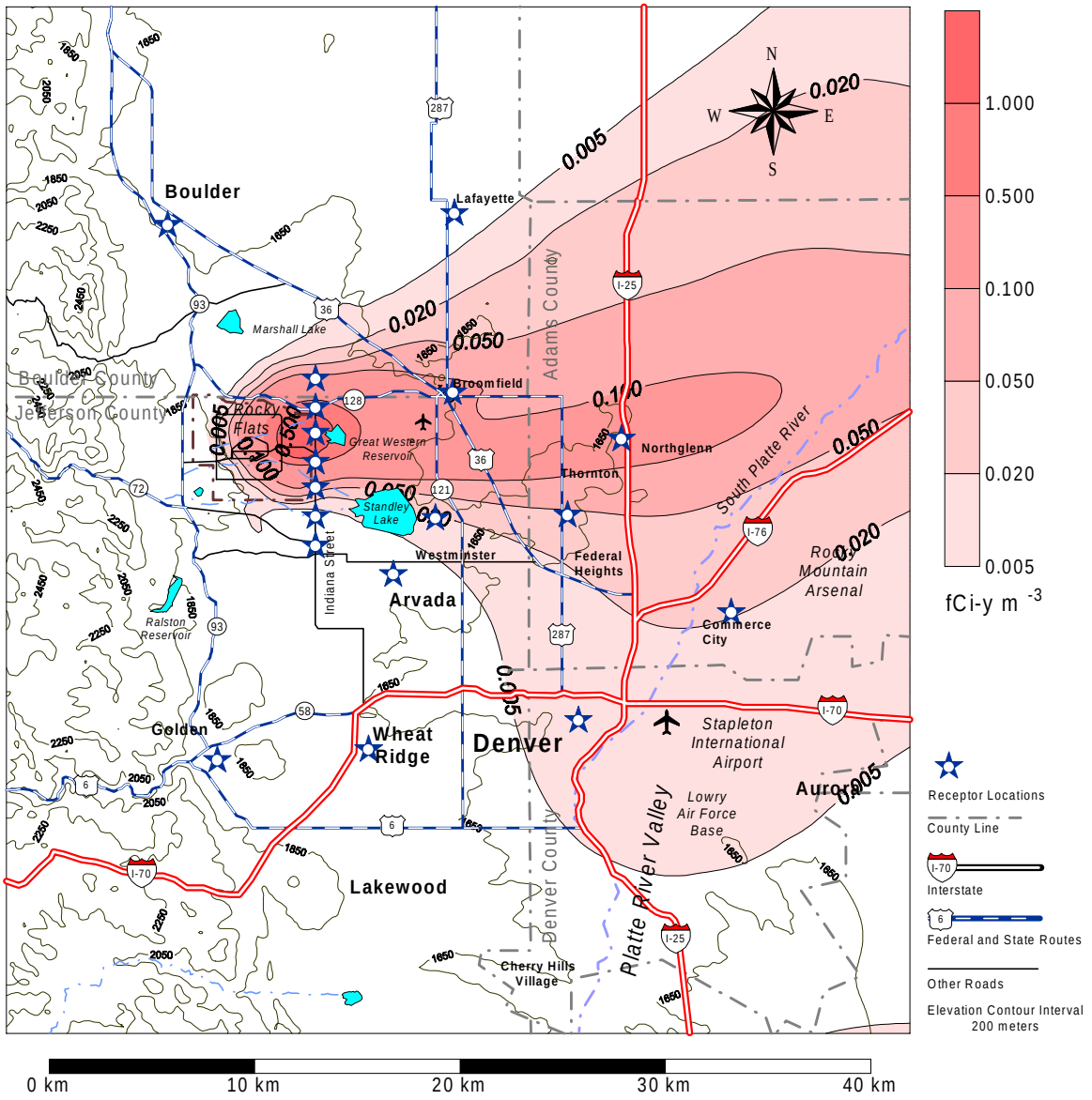

Figure 10. Dispersion pattern of the 50th percentile *TIC* of respirable particles (<15µm) for all six discrete events. Receptor locations are indicated by a star.

Annual Average χ/Q Values for Baseline Release

The procedure and models described in the previous sections were used to calculate an annual average χ/Q for all concentration grid nodes in the model domain (2295 nodes spaced every kilometer). Annual average χ/Q values were calculated separately for each of the three size fractions. Figure 11 illustrates χ/Q values for the 10–15 µm particles. The annual average χ/Q at each of the grid nodes for each year of meteorological data (1989–1993) were computed for a constant unit release (1 Ci s^{-1}). The five χ/Q values at each grid node were then averaged to yield a 5-year composite annual average χ/Q.

The dispersion pattern shown in Figure 11 is characterized by an east-northeast trending ellipsoid shaped plume. Wind roses constructed using RFP data from 1984–1993 (DOE 1995) indicate the predominant wind direction to be from the west-northwest. Higher concentration isopleths near the source trend mostly easterly; however, farther away from the source, concentration isopleths trend to the northeast. The northeast trend is believed to be due to the influence of the Platte River Valley and the diurnal pattern of upslope-downslope conditions that characterize the general air movement on the Colorado Front Range environs (Crow 1974). Downslope conditions typically occur during the evening hours and are characterized by drainage flow of cooler air from the foothills to the plains. Westerly winds predominate, but the direction may be altered by local topography. Upslope conditions are caused by daytime heating and typically result in easterly winds that prevail during the daylight hours with transition from upslope to downslope conditions occurring during the evening and transition from downslope to upslope occurring during the morning. During evening hours under stable conditions, cool air near the surface drains from the Denver metropolitan area down the Platte River Valley (which flows to the northeast) and out to the plains. During daylight hours and after surface heating has eliminated the cooler surface layer, the downslope conditions cease. This is followed by a brief period of relatively calm winds, which in turn is followed by return of air up the valley or upslope conditions. Meteorological data at Denver Stapleton International Airport captures these transitions in the Platte River Valley that are reflected in the χ/Q isopleth maps.

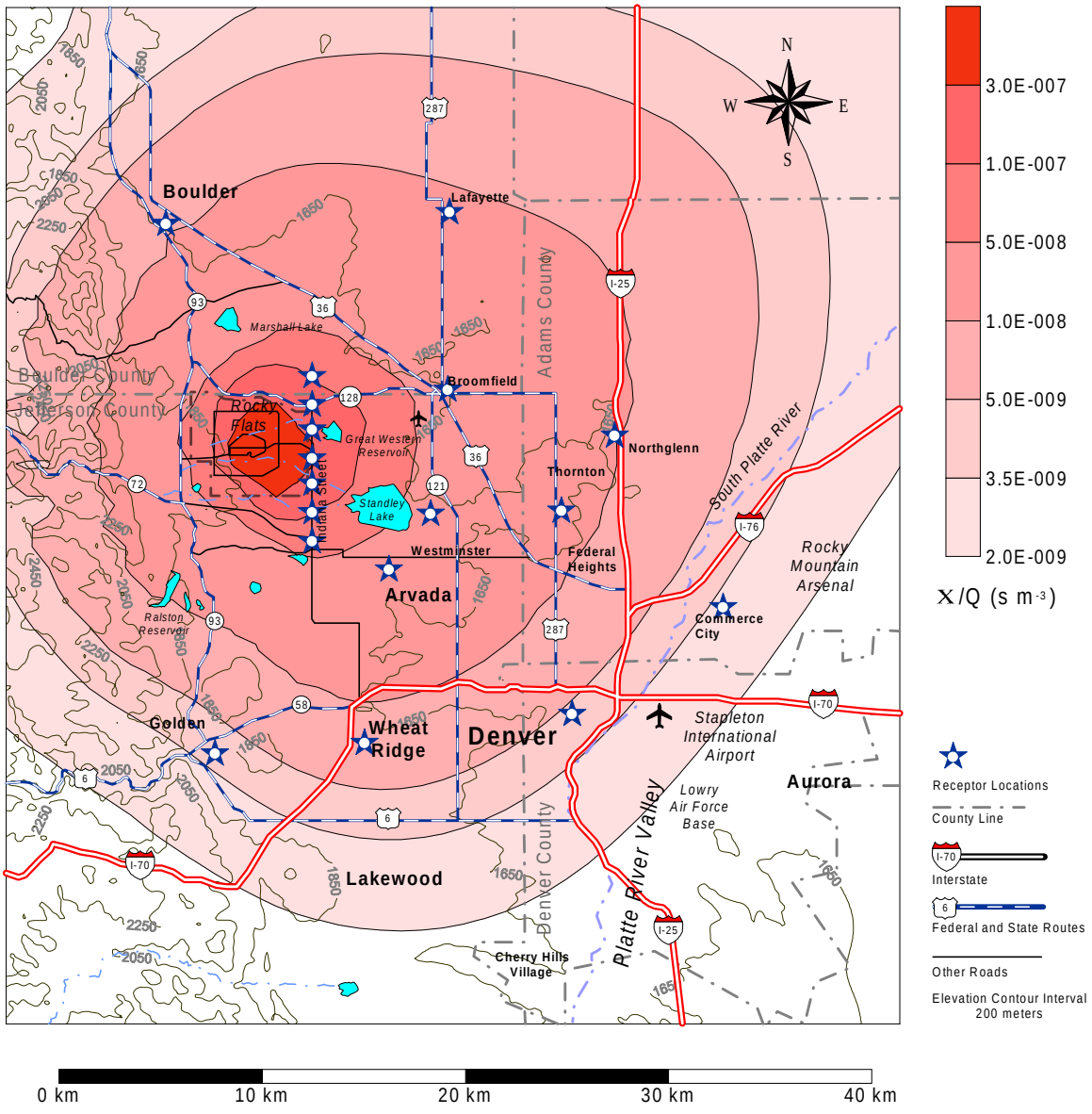

Figure 11. Isopleth map of the annual average χ/Q for 10–15 µm particles using meteorological data from the RFP and Denver Stapleton International Airport from 1989–1993. Receptor locations are indicated by a star.

Time-Integrated Air Concentrations for Baseline Releases

Predicted *TICs* of plutonium at specific receptors were calculated for the years 1964–1969. Uncertainty in the predicted concentration included uncertainty in the dispersion estimate and source term. The *TIC* for the j^{th} size fraction given by

$$TIC_j = CF_1 \sum_{i=1}^{n} CF_2 \; CF_3 \; \chi/Q_j \;\; Q_{i,j} \; \Delta t \qquad (16)$$

where

CF_1 = dispersion uncertainty correction factor,
CF_2 = meteorology uncertainty correction factor,
CF_3 = plume depletion uncertainty correction factor
χ/Q_j = dispersion factor for the j^{th} particle size
$Q_{i,j}$ = annual release of plutonium for the i^{th} year for j^{th} particle size
Δt = 1 year
n = number of years.

The correction factors and the source term (Q) are stochastic quantities. Therefore, the *TIC* is also a stochastic quantity. Note that the corrections factors CF_2 and CF_3 are within the summation symbol and are sampled n times for each Monte Carlo realization. The dispersion correction factor (CF_1) is sampled once for each realization to preserve year-to-year correlation. This procedure was repeated for all three particle-size fractions. Correlation among the size fractions was preserved by using the same random number sequence for sampling source terms and stochastic correction factors for all three Monte Carlo simulations. Time and space correlations among different receptors within the model domain were also preserved by generating distributions of correction factors and source release rates for the number of user-specified realizations at the beginning of the simulation. These values were then used in the same sequence for the 18 receptors in the model domain. The correction factors CF_1 and CF_3 are spatially variable and lognormally distributed. For these correction factors, a set of standard normal deviates for the specified number of realizations was calculated first. These deviates were used in conjunction with the correction factor's GM and GSD for the specified receptor location to calculate a value of the correction factor as given by Equation (17).

$$CF = \exp\left(d \ln(GSD) + \ln(GM)\right) \tag{17}$$

where CF = the correction factors and d = the standard normal deviate. The sampling scheme for 1000 realizations of *TIC* over n years is summarized as follows:

- The source term is sampled 1000 times for each year of the simulation and stored in a random access unformatted file ($1000 \times n$ values).
- The meteorological correction factor is sampled 1000 times for each year of the simulation and stored in a random access unformatted file ($1000 \times n$ values).
- Standard normal deviates are sampled 1000 times for each year of the simulation and stored in a random access unformatted file ($1000 \times n$ values). These values are used to generate a distribution of deposition uncertainty correction factors.
- Standard normal deviates are calculated an additional 1000 times and stored in an array. These values are used generate a distribution of dispersion correction factors that are applied to each *TIC*.
- The *TIC* is calculated 1000 times for each receptor in the model domain using Equation (16). For each receptor, the same sequence of correction factors, standard normal deviates, and source term values are used.
- Meteorological correction factors, standard normal deviates for deposition, and source term values are indexed to each specific year of the simulation. *TIC* values for receptors that are not present during the entire exposure period use correction factors that are indexed to their specific years of exposure.

Random sampling and sorting routines (in FORTRAN) were obtained from Press et al. (1992) Time-integrated concentrations for the 18 receptor locations and three size fractions are presented in Table 18. Concentrations were integrated for all 6 years of the assessment period (1964–1969). The receptor located along Indiana Street at UTM coordinates 485850E, 4415050N had the highest *TIC* for all three size fractions.

Table 18. Time-Integrated Air Concentrations for Baseline Releases

			Time-integrated concentration (fCi-y m^{-3}) GM(GSD)		
UTM E (m)	UTM N (m)	Description	<3 µm	3–10 µm	10–15 µm
485850	4419050	Indiana Street #1	0.086 (2.9)	0.176 (2.9)	0.151 (2.9)
485850	4417050	Indiana Street #2	0.169 (2.9)	0.353 (2.9)	0.310 (2.9)
485850	4416050	Indiana Street #3	0.223 (2.9)	0.470 (2.9)	0.422 (2.9)
485850	4415050	Indiana Street #4	0.258 (2.9)	0.544 (2.9)	0.487 (2.9)
485850	4414050	Indiana Street #5	0.241 (2.9)	0.510 (2.9)	0.461 (2.9)
485850	4412050	Indiana Street #6	0.092 (2.9)	0.191 (2.9)	0.170 (2.9)
485850	4411050	Indiana Street #7	0.076 (2.9)	0.159 (2.9)	0.142 (2.9)
489850	4409050	Arvada	0.029 (2.8)	0.058 (2.8)	0.049 (2.8)
488850	4401050	Wheat Ridge	0.007 (2.8)	0.015 (2.8)	0.012 (2.8)
491850	4412050	Westminster	0.036 (2.8)	0.072 (2.8)	0.061 (2.8)
492850	4418050	Broomfield	0.036 (2.8)	0.073 (2.8)	0.061 (2.8)
500850	4416050	Northglenn	0.011 (2.8)	0.022 (2.8)	0.018 (2.8)
497850	4412050	Thornton	0.014 (2.8)	0.028 (2.8)	0.023 (2.8)
478850	4426050	Boulder	0.009 (2.8)	0.018 (2.8)	0.015 (2.8)
492850	4427050	Layfayette	0.012 (2.8)	0.024 (2.8)	0.019 (2.8)
480850	4400050	Golden	0.004 (2.8)	0.007 (2.8)	0.006 (2.8)
505850	4408050	Commerce City	0.003 (3.0)	0.006 (3.0)	0.005 (3.0)
498850	4402050	Denver	0.004 (3.0)	0.008 (3.0)	0.007 (3.0)

Time-Integrated Air Concentration for All Events

The *TIC* for all events was the sum of the *TIC* for each individual event (baseline plus the six discrete events). Each event was assumed to be independent of one another. Figure 12 shows the dispersion pattern of the 50th percentile *TIC* value for all respirable particles (<15 µm). Note that the baseline and discrete release events both influence the dispersion pattern. The plume is generally elongated in the east-west direction. The 0.005 fCi-y m^{-3} contour line now covers most of the model domain and obliterates the more pronounced northeast-southwest elongation seen in the discrete event plot (Figure 10). With the inclusion of baseline release, the area within the 1.0 fCi-y m^{-3} contour line is now much larger compared to the discrete events. The high-wind events as modeled by the six discrete events are estimated to have been responsible for most of the activity released from the 903 Area. However, high wind speeds also result in greater dispersion, dilution, and depletion within an airborne plume, resulting in lower air concentrations than would be predicted had the same activity been released over a longer period of time and modeled using annual average meteorological data.

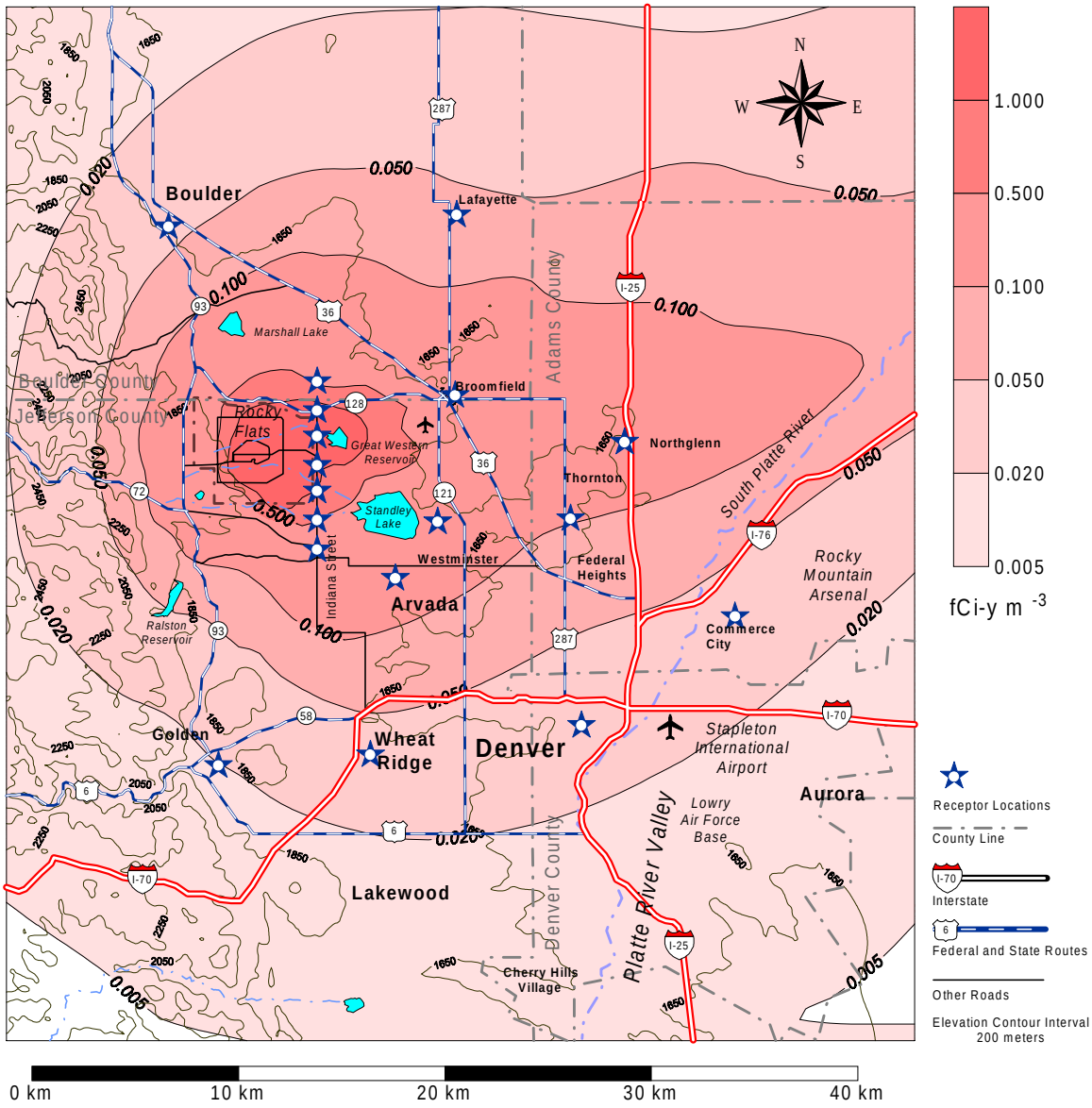

Figure 12. Dispersion pattern of the 50th percentile *TIC* of respirable particles (<15 μm) for all release events. Receptor locations are indicated by a star.

Consider the concentrations predicted in Phase I. The average concentrations for respirable particles near Indiana Street was around 0.5 fCi m^{-3} (see ChemRisk 1994b, Figure 3-18)[4] which yields a 5-year time-integrated value of 2.5 fCi-y m^{-3}. Recall that the source term for respirable particles in Phase I was about the same as Phase II; however, the *TIC* value for Phase I is a factor of 2 to 3 higher than that for Phase II. Consequently, it appears that that while the discrete events may have contributed to most of the releases and offsite contamination, they do yield

[4] There appears to be an error in Figure 3-18. The 5-year average concentration value is reported as 0.005 fCi m^{-3}. Using this average concentration value and the Phase I dose and risk conversion factors yields risk values that are about a factor of 100 too low from what is reported in the Task 8 report (ChemRisk 1994a). We suspect that average concentrations reported in Figure 3-18 are a factor of 100 too low.

proportionally higher concentrations had the activity been released over a longer period (1 year) of time.

EXPOSURE SCENARIOS AND RISK CALCULATIONS

One of the key parts of the Rocky Flats dose reconstruction work is calculating health impacts to people living in the surrounding area from materials released during RFP past operations. Dose reconstruction uses a pathways approach to study the potential radiation doses and health risks of these past releases on the surrounding communities. The pathways approach begins with learning what kinds of and how much materials were released from a facility (source terms) and ends with estimating the health impacts these releases had on the residents in the area. Mathematical models described in the previous section were used to model the transport of plutonium released from the site to the surrounding communities. In this section, we calculate health impacts (incremental lifetime cancer incidence risk) to people living offsite from exposure to these releases.

The risk to a person from exposure to the plutonium released depends upon a number of factors, such as

- Where the person lived and worked in relation to the RFP
- When and how long that person lived near the RFP (for example, during the key release events in 1957 and late 1960s or in the 1970s when releases were smaller)
- The age and gender of the person
- Lifestyle (that is, did the person spend a great deal of time outdoors or doing heavy work on a farm).

Although it is not realistic to calculate individual risks for every resident who may have lived or worked in the Rocky Flats area during its operational history, it is not credible to calculate a single risk that applies to all residents. To consider the many factors that influence exposure, we developed profiles, or exposure scenarios, of hypothetical, but realistic residents of the RFP area for which representative risk estimates could be made. Each scenario represents one individual. These scenarios incorporate typical lifestyles, ages, genders, and lengths of time in the area. The scenarios also specify and vary the home and work locations. These scenarios can help individuals determine risk ranges for themselves by finding a lifestyle profile that most closely matches their backgrounds. The scenarios are not designed to include all conceivable lifestyles of residents who lived in this region during the time of the RFP operations. Rather, they provide a range of potential profiles of people in the area.

We calculated the risks to individuals from 903 Area plutonium releases for seven hypothetical exposure scenarios (Table 19) at 18 separate locations in the model domain. Locations were selected to cover all major population centers. An array of seven receptors was located at the buffer zone fence line along Indiana Street to capture discrete plumes trajectories originating from the 903 Area. As discussed earlier, direct inhalation was the only exposure pathway considered in this assessment. Ingestion of plutonium in water, food, and soil are potential pathways that could have been considered in more detail. However, plutonium compounds are very insoluble and tend to adhere to soil, making them relatively immobile and not readily taken up by plants or accumulated in the edible portions of animal products. Phase I results (ChemRisk 1994a) indicated direct inhalation to be the dominant pathway of exposure

during the period 1964–1969. For the later years (1970–1989), soil ingestion and inhalation of resuspended contaminated soil become a significant component of the total dose because of the accumulation and build up of deposited plutonium in soil and smaller airborne releases. This report deals only with risks from the 903 Area from 1964 to 1969, which are dominated by direct inhalation of suspended activity. Risk from inhalation of resuspended soil activity will be addressed in a later, more comprehensive report that covers all sources of offsite plutonium contamination.

Table 19. Exposure Scenario Descriptions

Exposure scenario	Sex	Year of birth	Year beginning exposure	Year ending exposure	Locations
Rancher	Male	1925	1964	1969	Indiana Street (seven locations)
Office worker	Female	1941	1964	1969	Denver
Housewife	Female	1928	1964	1969	Arvada, Wheat Ridge, Westminster, and Broomfield
Laborer	Male	1943	1964	1969	Thornton, Boulder, and Lafayette
Infant	Female	1968	1968	1969	Northglenn
Child	Female	1963	1964	1969	Commerce City
Student	Female	1953	1964	1969	Golden

Exposure scenarios for the seven hypothetical receptors described in Table 19 were organized according to occupational and nonoccupational activities. Occupational activities include work, school, and extracurricular activities away from the home. Nonoccupational activities include time spent at home doing chores, sleeping, and leisure activities such as watching television. In these calculations, the receptor was assumed to perform occupational and nonoccupational activities at the same location. The age of the receptor and years during which exposure occurred are also considered when calculating exposures. All scenarios, except the infant, assume the individual is exposed for the duration of primary 903 Area releases. The infant is born at the end of 1968 and is exposed in 1969, the year of highest releases.

Breathing Rates and Time Budgets

Each exposure scenario was divided into three types of activities: sleeping, nonoccupational activity, and occupational activity. For the infant and child scenario, occupational and nonoccupational activities are irrelevant; instead, activities were divided into sleeping and two other activities based on the child's age. For the infant, the other two activities were awake sedentary and awake active. For the child scenario, the two other activities were time spent at home (indoors and outdoors) and at preschool and/or day care.

For each activity, time spent at four different exercise levels was assigned. These exercise levels were resting, sitting (sedentary), light exercise, and heavy exercise. Some examples of light exercise are laboratory work, woodworking, housecleaning, and painting. Heavy exercise corresponds to occupations such as mining, construction, farming, and ranching. For each

exercise level, an age- and gender-specific breathing rate was assigned. Breathing rates (Table 20) for persons age 8 and higher were obtained from Roy and Courtay (1991) and for children age 0–7 from Layton (1993).

Table 20. Breathing Rates for Various Exercise Levels as Reported in Roy and Courtay (1991) and Layton (1993)

Gender	Age	Resting ($m^3\ h^{-1}$)	Sitting ($m^3\ h^{-1}$)	Light ($m^3\ h^{-1}$)	Heavy ($m^3\ h^{-1}$)
Male	30–60	0.45	0.54	1.50	3.00
Female	30–60	0.32	0.39	1.26	2.70
Male	18	0.50	0.60	1.58	3.06
Female	18	0.35	0.42	1.32	1.44
Male	16	0.43	0.52	1.52	3.02
Female	16	0.35	0.42	1.30	2.70
Male	15	0.42	0.48	1.38	2.92
Female	15	0.35	0.40	1.30	2.57
Male	14	0.41	0.49	1.40	2.71
Female	14	0.33	0.40	1.20	2.52
Male	12	0.38	0.47	1.23	2.42
Female	12	0.33	0.39	1.13	2.17
Male	10	0.31	0.38	1.12	2.22
Female	10	0.31	0.38	1.12	1.84
Male	8	0.29	0.39	1.02	1.68
Female	8	0.29	0.39	1.02	1.68
Male	3–7	0.24	0.29	0.72	1.68
Female	3–7	0.23	0.27	0.68	1.59
Male	0–3	0.19	0.23	0.58	1.35
Female	0–3	0.14	0.17	0.45	1.02
Average, male[a]	8–17	0.37	0.45	1.28	1.49
Average, female[a]	8–17	0.33	0.40	1.18	2.25

[a] The average female breathing rate from age 8–17 was used for the student.

Time budgets for various receptor activities were also based on Roy and Courtay (1991) (Table 21), but they were modified to fit specific exposure scenarios. The fraction of time spent at a specific exercise level while engaged in a given activity was assigned based on the nature of the activity. For example, the fraction of time spent at the resting exercise level while the receptor slept would be 1.0 and the other exercise levels would be 0. A weighted-average breathing rate was then applied to each activity based on the number of hours spent at each exercise level. For some scenarios (housewife, retiree, and laborer), nonoccupational activities were separated into those performed indoors and those performed outdoors. Although no distinction was made between indoor and outdoor air concentrations, exercise levels for indoor and outdoor activities differed. A time-weighted average breathing rate that included indoor and outdoor activities was calculated and applied to nonoccupational time. Each receptor was assumed to spend 15 days per year away from the Denver metropolitan area and outside the model domain, but each receptor was assumed to be present in the model domain for each discrete event. Plutonium concentrations were assumed to be the same for indoor and outdoor air.

Time-weighted average breathing rates were calculated for the three activities for which each receptor was assumed to be engaged. The time-weighted average breathing rate is given by

$$WBR_j = \sum_{i=1}^{4} BR_i \; f_{i,j} \tag{18}$$

where

WBR_j = time-weighted average breathing rate for the j^{th} activity ($m^3\ h^{-1}$)
BR_i = breathing rate for the i^{th} exercise level ($m^3\ h^{-1}$)
$f_{i,j}$ = fraction of time spent at the i^{th} exercise level for the j^{th} activity.

To summarize, three activities were defined for each exposure scenario: sleeping, occupational, and nonoccupational activities. The location of exposure for occupational and nonoccupational activities was assumed to be the same for all receptors. Four different exercise levels, each with an assigned breathing rate, were distinguished: resting, sitting, light exercise, and heavy exercise. The breathing rate during a given activity was the time-weighted average breathing rate of the four exercise levels.

All receptors were assumed to be present at their respective locations for the duration of each discrete event. Receptors were assumed to go about their typical daily activities and breathe the same as they would on any other day.

Plutonium Intake Calculation

The calculation of the incremental lifetime cancer incidence risk involved three steps:

1. Calculate the *TIC* in air at the point of exposure for each particle size fraction
2. Calculate the amount of plutonium inhaled by the receptor for each particle size fraction
3. Multiply the plutonium intake by a particle-size-specific risk coefficient that relates the incremental lifetime cancer incidence risk to the amount of plutonium inhaled.

Calculation of the *TIC* with uncertainty was discussed in a previous section. Because risk coefficients are particle-size dependent, *TIC* values for different size fractions were stored separately. The risk from each size fraction was then summed to yield the total risk from inhalation.

Uncertainty in risk estimates includes uncertainty in the *TIC* and risk coefficients. Receptors behavior patterns (i.e., the time spent doing different activities at different exertion levels) and their physical attributes (body weight and breathing rate) were considered fixed quantities.

The amount of plutonium inhaled by a receptor for the j^{th} particle size fraction is given by

$$I_j = TIC_j \left(WBR_1\ T_1 + WBR_2\ T_2 + WBR_3\ T_3 \right) \tag{19}$$

where

I_j = intake of plutonium for j^{th} size fraction by the receptor for the exposure period (Ci)
TIC_j = *TIC* for the j^{th} size fraction (Ci-y m^{-3})
$WBR_{1,2,3}$ = time-weighted average breathing rate for occupational, nonoccupational, and sleeping activity ($m^3\ h^{-1}$)
$T_{1,2,3}$ = hours per year for occupational, nonoccupational, and sleeping activity ($h\ y^{-1}$).

Table 21. Time Budgets and Weighted Breathing Rates for the Exposure Scenarios

Scenario	Activity	Fraction of time spent at an exercise level				Hours per day (workweek)	Hours per day (weekend)	Hours per year	Weighted breathing rate ($m^3 h^{-1}$)
		Resting	Sitting	Light	Heavy				
Rancher	Occupational	0.00	0.00	0.25	0.75	8.0	8.0	2800	2.63
	Nonoccupational	0.00	0.50	0.38	0.13	8.0	8.0	2800	1.21
	Sleeping	1.00	0.00	0.00	0.00	8.0	8.0	2800	0.45
	Weighted Daily Average								1.43
Office worker	Occupational	0.00	0.25	0.75	0.00	8.0	0.0	2000	1.04
	Nonoccupational	0.00	0.50	0.38	0.13	8.0	16.0	3600	1.00
	Sleeping	1.00	0.00	0.00	0.00	8.0	8.0	2800	0.32
	Weighted Daily Average								0.786
Housewife	Occupational	0.00	0.13	0.75	0.13	8.0	8.0	2800	1.33
	Nonoccupational								
	Indoor	0.00	0.50	0.38	0.13	4.0	4.0	1400	1.00
	Outdoor	0.00	0.38	0.50	0.13	4.0	4.0	1400	1.11
	Total nonoccupational	0.00	0.44	0.44	0.13	8.0	8.0	2800	1.06
	Sleeping	1.00	0.00	0.00	0.00	8.0	8.0	2800	0.32
	Weighted Daily Average								0.904
Laborer	Occupational	0.00	0.13	0.50	0.38	8.0	0.0	2000	1.94
	Nonoccupational								
	Indoor	0.00	0.50	0.38	0.13	6.0	8.0	2300	1.21
	Outdoor	0.00	0.50	0.25	0.25	2.0	8.0	1300	1.40
	Total nonoccupational	0.00	0.50	0.31	0.19			3600	1.28
	Sleeping	1.00	0.00	0.00	0.00	8.0	8.0	2800	0.45
	Weighted Daily Average								1.16
Infant	Awake–sedentary	0.00	0.71	0.14	0.14	7.0	7.0	2450	0.33
	Awake –active	0.00	0.00	1.00	0.00	1.0	1.0	350	0.45
	Sleeping	1.00	0.00	0.00	0.00	16.0	16.0	5600	0.14
	Weighted Daily Average								0.212
Child	Home								
	Indoor	0.00	0.50	0.42	0.08	6.0	6.0	2100	0.55
	Outdoor	0.00	0.00	0.67	0.33	1.5	1.5	525	1.04
	Total home					7.5	7.5	2625	0.65
	School-indoor	0.00	0.80	0.20	0.00	2.5	2.5	875	0.35
	Sleeping	1.00	0.00	0.00	0.00	14.0	14.0	4900	0.23
	Weighted Daily Average								0.372
Student	Home								
	Indoor	0.00	0.44	0.56	0.00	4.5	8.0	1925	0.83
	Outdoor	0.00	0.00	0.25	0.75	2.5	6.0	1225	1.98
	Total home	0.00	0.22	0.40	0.38	7.0	14.0	3150	1.28
	School								
	Indoor	0.00	0.75	0.25	0.00	6.0	0.0	1500	0.59
	Outdoor	0.00	0.00	0.25	0.75	1.0	0.0	250	1.98
	Total school	0.00	0.38	0.25	0.38	7.0	0.0	1750	0.79
	Sleeping	1.00	0.00	0.00	0.00	10.0	10.0	3500	0.33
	Weighted Daily Average								0.786

The subscripts 1, 2, and 3 refer to occupational, nonoccupational, and sleeping activity, respectively. For discrete events, *TIC* values were converted from units of curies-hour per cubic meter to curies-year per cubic meter by dividing the original quantity by 8760 hours per year. Plutonium intake was calculated for all three respirable size fractions (<3 µm, 3–10 µm, and 10–15 µm) using Equation (19). Correlation among the particle size fractions was maintained by using the distribution of *TIC* values comprised of 1000 realizations for each size fraction, which were determined in the previous step.

Risk Coefficients

Calculation of the lifetime cancer incidence risk requires estimates of risk coefficients. Risk coefficients relate the lifetime risk of cancer incidence to the amount of plutonium inhaled. Plutonium risk coefficients were developed in this phase of the study and are documented in Grogan et al. (1999).

The principal plutonium isotopes of concern at Rocky Flats are ^{239}Pu and ^{240}Pu, which have long half-lives of 24,065 years and 6537 years, respectively. Plutonium emits alpha particles that are relatively heavy and slow, thus, creating short, dense ionization trails. Alpha particles have such weak penetration abilities that they can be blocked by a piece of paper, or the dead, outer layers of the skin. As a result, the major danger from plutonium comes from having it inside your body. For residents in the vicinity of Rocky Flats, plutonium is most likely to have entered the body from breathing air that contained plutonium particles released from the site. After inhalation, plutonium enters the blood and about 80% is transported to the bone or liver where it is retained for years. Following inhalation, the four most highly exposed tissues are bone surface, lung, liver, and bone marrow. These account for more than 97% of the total dose received by infants and adults alike. The dose per unit activity inhaled varies for these four tissues (Table 22). Furthermore, the dose per unit activity (dose conversion factor) also varies depending on the particle size distribution of the inhaled plutonium aerosol (Table 22). Three different particle size distributions are used to characterize the plutonium releases from the 903 Area at Rocky Flats (1-, 5-, and 10-µm AMAD particles). Each of these distributions is assumed to be lognormal with a GSD of 2.5; therefore, each size distribution covers a relatively large range of particle sizes. The 1-µm AMAD particle size distribution results in the largest doses to the tissues per unit intake of activity. This is because the particles penetrate deeper into the lungs and are retained longer. In all cases, the plutonium is assumed to be in the oxide form.

Table 22. Summary of Plutonium Oxide Inhalation Dose Conversion Factors[a]

	Dose conversion factor (µGy Bq^{-1}) [b]		
	1-µm AMAD particles	5-µm AMAD particles	10-µm AMAD particles
Cancer site	GSD = 2.5	GSD = 2.5	GSD = 2.5
Lung	4.4 (1.9)	2.6 (2.7)	1.2 (4.3)
Liver	2.0 (3.0)	0.95 (3.5)	0.42 (4.5)
Bone surface	9.0 (3.0)	4.6 (3.5)	2.1 (4.5)
Bone marrow	0.46 (3.0)	0.22 (3.5)	0.11 (4.5)

[a.] Values for 1-µm AMAD from ICRP 1995; 5 and 10-µm were calculated in Grogan et al. 1999
[b.] Geometric mean (geometric standard deviation).

The incidence of health effects depends on the amount of dose received. There are two main classes of health effects induced by ionizing radiation: deterministic and stochastic effects. Deterministic effects most often follow acute, high dose exposure. The severity of the effect increases with dose above the threshold dose. Below the threshold dose, the effect is not evident; however, subtle minor effects may occur. Deterministic effects cause direct damage to tissues and include effects that most often occur within days to weeks after exposure. For example, these effects can cause reddening of the skin, cataracts, hair loss, sterility, and bone marrow depression after external irradiation. After inhalation of plutonium, deterministic effects may include radiation pneumonitis, pulmonary fibrosis, and lymphopenia, but these conditions occur only after very high doses. The threshold dose for most deterministic effects is at least 0.5 Gy delivered in a short time, and many are much higher (NCRP 1991). For the releases of plutonium that occurred from the site, doses to individuals in the Rocky Flats area were well below the threshold doses. Therefore, deterministic health effects were not possible.

Stochastic effects are assumed to occur randomly at all dose levels, including the lowest doses. The frequency of stochastic effects is dependent on the dose, and the effects usually occur at long intervals after exposure. In a large population exposed to low doses, only a few of the exposed individuals will be affected; most will not. The two principal types of stochastic effects are induced cancer and genetic effects. For exposure to plutonium, the risk of induced cancer is the health effect of most concern; in particular, lung cancer, liver cancer, bone cancer, and leukemia (bone marrow exposure) because these are the tissues that receive the highest doses. Because people exposed to radiation are several times more likely to be affected by an induced cancer than to transmit genetic effects to their children and the plutonium doses to the gonads (ovaries or testes) are small compared to other organs of the body (40 times less than the lung), genetic effects are not an important risk for plutonium exposures. Therefore, they are not considered further.

The alpha particles emitted from plutonium are densely ionizing and the linear energy transfer (LET) to the tissue is high over the short range (about 40 µm) of the alpha particles (thus, the name high-LET radiation). Other radiations, such as gamma rays and x-rays, are less densely ionizing and are termed low-LET radiations. The biological effects of low-LET radiation are better known than those of high-LET radiation. The differences between radiation types are important to the analysis because high-LET radiations are more biologically effective per unit of dose than low-LET radiations. This difference in effectiveness is usually described by the relative biological effectiveness (RBE), which is defined as the ratio of doses from two different radiations to produce the same type and level of biological effect.

Inhalation of plutonium results in the exposure of organs to high-LET radiation. While a few human populations have been exposed directly to large amounts of plutonium and some populations to other radionuclides that emit alpha particles, more groups have been exposed to low-LET gamma radiation and evaluated in more epidemiologic detail. In addition, studies of cancer in animals exposed to both types of radiation and laboratory studies of cellular and other biological endpoints can be used to support human studies. These different sources of information were used in this phase of the study to develop four independent approaches to estimate the risk of cancer because of radiation doses from plutonium deposited in the organs of the human body (Grogan et al. 1999). Three approaches used epidemiologic studies of human populations to derive dose-response relationships, and the fourth used dose-response

relationships from controlled animal experiments. The four independent approaches were used to derive, where possible, risk coefficients for each organ of interest. The coefficients from the different approaches were then combined by weighting each according its intrinsic merit to produce a single risk coefficient with uncertainties for each organ of interest.

The overall mortality risk estimate for each cancer site was adjusted by the lethality fraction to provide lifetime risk estimates for cancer incidence. The influence of gender and age was accounted for in the analyses (see Grogan et al. [1999] for details). The data allowed a distinction to be made between the risks and uncertainties to those under 20 years of age at exposure compared to those 20 and older. The data did not warrant a more detailed analysis. For this reason, the risk coefficients for persons under 20 years of age were applied to the infants and children in the seven hypothetical exposure scenarios.

The GM (50th percentile) and GSDs of the cancer incidence risk coefficient distributions are listed in Table 23. The units reported in Grogan et al. (1999) have been changed from risk per 100,000 persons per unit of activity in kilobecquerels (kBq) to risk per 10,000 persons per unit of activity in microcuries (µCi). These numbers indicate the median number of cases of cancer (fatal and nonfatal) that would be expected to result from 10,000 people all inhaling 1 µCi of $^{239/240}$Pu particles with the defined particle size distribution.

Risk Calculations

Plutonium intake for the three particle sizes (Equation [19]) were multiplied by the risk coefficients (Table 23) and summed across all particle sizes to yield lifetime cancer incidence risk (R_j) for each organ of interest.

$$R_j = \sum_{i=1}^{3} I_i \; RC_{i,j} \tag{20}$$

where

R_j = lifetime cancer incidence risk for the j^{th} organ
I_i = plutonium intake of the i^{th} particle size (Ci)
$RC_{i,j}$ = risk coefficient for i^{th} particle size and j^{th} organ (Ci^{-1}).

Correlation among the particle size fractions was maintained by using the distribution of I values that were comprised of 1000 realizations for each size fraction. Risk coefficients for different particle sizes and organs were also correlated. For each Monte Carlo realization, a standard normal deviate was generated and stored. These deviates were then used to determine a risk coefficient using Equation (17) and substituting the appropriate GM and GSD for the particle size and organ of interest. The total lifetime cancer incidence risk from all organs was calculated by summing the risk across all four organs during each Monte Carlo realization.

Table 23. Lifetime Cancer Incidence Risk Per 10,000 Persons Per 1 µCi of Inhaled $^{239/240}$Pu for the Three Particle Size Distributions Used to Characterize the 903 Area Releases[a]

1-µm AMAD particles (GSD = 2.5)			
Cancer site	Gender	Under 20	20 and older
Lung	male	206 (3.5)	210 (3.4)
	female	206 (3.5)	210 (3.4)
Liver	male	92 (5.2)	49 (5.2)
	female	45 (5.4)	23 (5.4)
Bone surface	male	20 (9.8)	10 (9.8)
	female	10 (10)	5 (10)
Bone marrow	male	2.2 (5.7)	2.2 (5.7)
	female	2.2 (5.7)	2.2 (5.7)
5-µm AMAD particles (GSD = 2.5)			
Cancer site	Gender	Under 20	20 and older
Lung	male	117 (4.3)	119 (4.2)
	female	117 (4.3)	119 (4.2)
Liver	male	46 (5.8)	24 (5.7)
	female	21 (6.0)	11 (6.0)
Bone surface	male	10 (11)	5.2 (11)
	female	4.9 (11)	2.5 (11)
Bone marrow	male	1.0 (6.5)	1.0 (6.5)
	female	1.0 (6.5)	1.0 (6.5)
10-µm AMAD particles (GSD = 2.5)			
Cancer site	Gender	Under 20	20 and older
Lung	male	55 (6.1)	56 (6.0)
	female	55 (6.1)	56 (6.0)
Liver	male	21 (6.7)	11 (6.8)
	female	9.6 (7.0)	5.0 (6.9)
Bone surface	male	4.7 (12)	2.4 (12)
	female	2.3 (13)	1.2 (13)
Bone marrow	male	0.49(7.6)	0.49 (7.6)
	female	0.49(7.6)	0.49 (7.6)

[a] Geometric mean (geometric standard deviation).

INCREMENTAL LIFETIME CANCER INCIDENCE RISK ESTIMATES

This section presents the incremental lifetime cancer incidence risk that includes all release events (discrete and baseline) by organ and receptor. Appendix B contains detailed percentile summaries of risk by release event, receptor, and organ of interest. The lifetime cancer incidence risk was greatest for the rancher scenarios, in particular, the Rancher #4 scenario. The rancher scenarios were located at the buffer zone fence line along Indiana Street. These scenarios were distributed to intercept discrete plumes trajectories originating from the 903 Area. The GM incremental lifetime cancer incidence risk (the total of all organs) for the Rancher #4 scenario (Table 24) was 1.0×10^{-6} and ranged from 4.4×10^{-8} (2.5 percentile) to 3.3×10^{-5} (97.5 percentile) (Figures 13–15). Using the Rancher #4 scenario as an example, the uncertainty in these risk estimates may be interpreted as follows:

- There is a 95% probability that incremental lifetime cancer incidence risk was between 4.4×10^{-8} (2.5% value) and 3.3×10^{-5} (97.5% value).
- There is a 2.5% probability that incremental lifetime cancer incidence risk was greater than 3.3×10^{-5} and a 2.5% probability the risk was less than and 4.4×10^{-8}.

We may also interpret this to mean, given an exposure history and lifestyle similar to that of the Rancher #4 scenario, there is a 97.5% probability that the model-predicted number of cancer cases attributed to inhalation of plutonium originating from the 903 Area would be no greater than 33 persons in a population of 1 million similarly exposed individuals. The organ with the greatest risk was the lung, followed by the liver, bone, and bone marrow.

The magnitude of the lifetime cancer incidence risk was dependent mainly on the location of the receptor. Plumes from the discrete events, which account for most of the 903 Area releases, were confined to a relatively narrow corridor east of the 903 Area. Receptors located outside the plume trajectory generally received little if no exposure. In addition and as noted earlier, the high winds modeled for the discrete events result in greater dilution and dispersion of airborne material, which result in lower air concentrations. Consequently, exposure attributed to baseline releases made up a substantial portion of the overall exposure received by the receptors in the model domain. In general, the discrete events only contributed substantially to exposure of Rancher #2, #3, and #4 scenarios. The release on January 30, 1969 had the highest overall risk for any single release event (see Appendix B) for Rancher #4 scenario. The 5% and 95% risk values for this scenario were 1.6×10^{-8} and 5.5×10^{-6}, respectively, with a 50% value of 3.3×10^{-7}. Releases for January 6 and 7, 1969, resulted in the second and third highest risks for any single event for the Rancher #4 scenario.

The combination of several high release days where plume trajectories were confined to narrow corridors overlain by more-or-less continuous releases makes interpretation of the results difficult and confusing. No one event dominates the risk at any one location. In general, risks were higher for receptors directly east of the 903 Area and decrease with increasing distance. However, exposure to plutonium concentrations from any single discrete event was highly localized, and receptors just a few kilometers from each other could have substantially different exposures.

An almost infinite number of possible exposure scenarios can be defined; in most cases, the risks associated with each scenario will differ. However, the maximum risks will probably be bounded by the risks associated with the rancher scenarios. The scenarios involving the rancher may be considered the maximum exposed individual in the model domain because he was placed at the point of highest concentration outside the RFP buffer zone and remained there for the duration of the primary 903 Area releases. However, it is recognized that ranchers could have been grazing cattle within the current buffer zone and up to the old cattle fence. There were also bunkhouses, or some type of permanent overnight ranch camp, to the northeast within the buffer zone. To increase the risk substantially from our estimates, the air concentrations within the buffer zone would have to be several orders of magnitude greater than outside it. Soil concentrations within the buffer zone are substantially higher than outside it. The high concentrations are attributed to deposition of large, nonrespirable soil particles (30–150-μm AED) suspended from the 903 Area during the high wind events. While suspension and transport of these large particles have contributed to substantially higher soil concentrations in the buffer zone, this does not translate into substantially higher inhalation risk because these particles are not respirable. The resulting risk from inhalation of respirable particles and accounting for

occupancy time within the buffer zone would likely still be in same range as calculated for the rancher scenarios.

Table 24. Lifetime Incremental Cancer Incidence Risk × 10^8 for Baseline and Discrete Release Events

Receptor	Lung[a]	Liver[a]	Bone surface[a]	Bone marrow[a]	Total[a,b]
Rancher Indiana St. #1	6.2 (6.)	1.3 (7.8)	0.26 (13.7)	0.055 (8.6)	7.9 (6.5)
Rancher Indiana St. #2	19 (5.7)	3.9 (7.5)	0.80 (13.2)	0.17 (8.2)	24 (6.2)
Rancher Indiana St. #3	44 (5.)	9.2 (6.8)	1.9 (12.2)	0.40 (7.5)	57 (5.5)
Rancher Indiana St. #4	80 (4.7)	17 (6.4)	3.4 (11.6)	0.73 (7.)	104 (5.1)
Rancher Indiana St. #5	19 (5.9)	3.8 (7.6)	0.78 (13.3)	0.17 (8.3)	24 (6.3)
Rancher Indiana St. #6	6.2 (6.2)	1.3 (8.)	0.26 (13.9)	0.055 (8.8)	7.9 (6.7)
Rancher Indiana St. #7	5.1 (6.2)	1.0 (8.)	0.21 (13.9)	0.045 (8.8)	6.5 (6.7)
Housewife-Arvada	1.3 (5.7)	0.12 (7.8)	0.026 (13.6)	0.011 (8.2)	1.4 (6.)
Housewife-Wheat Ridge	0.37 (5.4)	0.036 (7.4)	0.008 (13.1)	0.003 (7.9)	0.43 (5.7)
Housewife- Westminster	2.1 (5.2)	0.20 (7.2)	0.043 (12.8)	0.019 (7.6)	2.4 (5.5)
Housewife-Broomfield	3.5 (5.)	0.34 (7.)	0.071 (12.6)	0.031 (7.4)	4.0 (5.3)
Infant-Northglenn	0.56 (4.7)	0.11 (6.6)	0.023 (11.8)	0.005 (6.9)	0.72 (5.2)
Laborer-Thornton	2.4 (4.5)	0.50 (6.2)	0.10 (11.4)	0.022 (6.8)	3.1 (5.)
Laborer-Boulder	0.51 (5.8)	0.10 (7.6)	0.022 (13.3)	0.005 (8.3)	0.66 (6.3)
Laborer-Lafayette	0.78 (5.5)	0.16 (7.3)	0.033 (12.9)	0.007 (8.)	1.00 (6.)
Student-Golden	0.17 (5.5)	0.031 (7.4)	0.007 (12.8)	0.002 (7.7)	0.21 (5.9)
Student-Commerce City	0.66 (4.5)	0.13 (6.4)	0.027 (11.5)	0.006 (6.7)	0.84 (5.)
Office Worker	0.40 (4.8)	0.039 (6.7)	0.008 (12.2)	0.004 (7.1)	0.46 (5.1)

[a] Geometric mean (geometric standard deviation).

[b] The total is not the sum of the geometric mean of the individual organs. It is the geometric mean of the sum of the individual organs for 1000 realizations.

It is instructive to compare the Phase I risk results with those of Phase II that are presented in this report. The sector with the highest risk in Phase I was east-southeast from the plant and extending from the buffer zone boundary (Indiana Street) eastward about 5 km to the western margin of Standley Lake (Sector 4B). Recall that median total *respirable* release quantities were about the same (0.34 Ci in Phase I compared to 0.33 to 0.6 Ci in our current estimates). Geometric mean risk estimates were slightly lower in Phase II for a receptor located in the vicinity of Indiana Street. The GM of the maximum risk in Phase II was 1×10^{-6} (Rancher #4 scenario) compared to a best estimate reported in Phase I for a similarly located receptor of 5×10^{-6}. The lower risk for Phase II may be attributed to the reasons stated earlier. That is, in Phase II, most of the respirable activity released was during discrete, high wind events. The incorporation of the high wind events into the transport model resulted in lower *TIC* values than would be calculated had the activity been released over a longer period of time and modeled using annual average meteorological conditions.

However, the uncertainty bounds are greater for the Phase II estimates. Ninety-five percent of the Phase II values cover a range of 3 orders of magnitude, compared to 2 orders of magnitude for Phase I. The greater uncertainty in Phase II is attributed primarily to greater uncertainty in the risk coefficients. For comparison, the Phase II estimated lifetime cancer incidence risks are

within the U.S. Environmental Protection Agency point of departure for acceptable lifetime cancer incidence risk of 1 in 1,000,000 to 1 in 10,000 people.

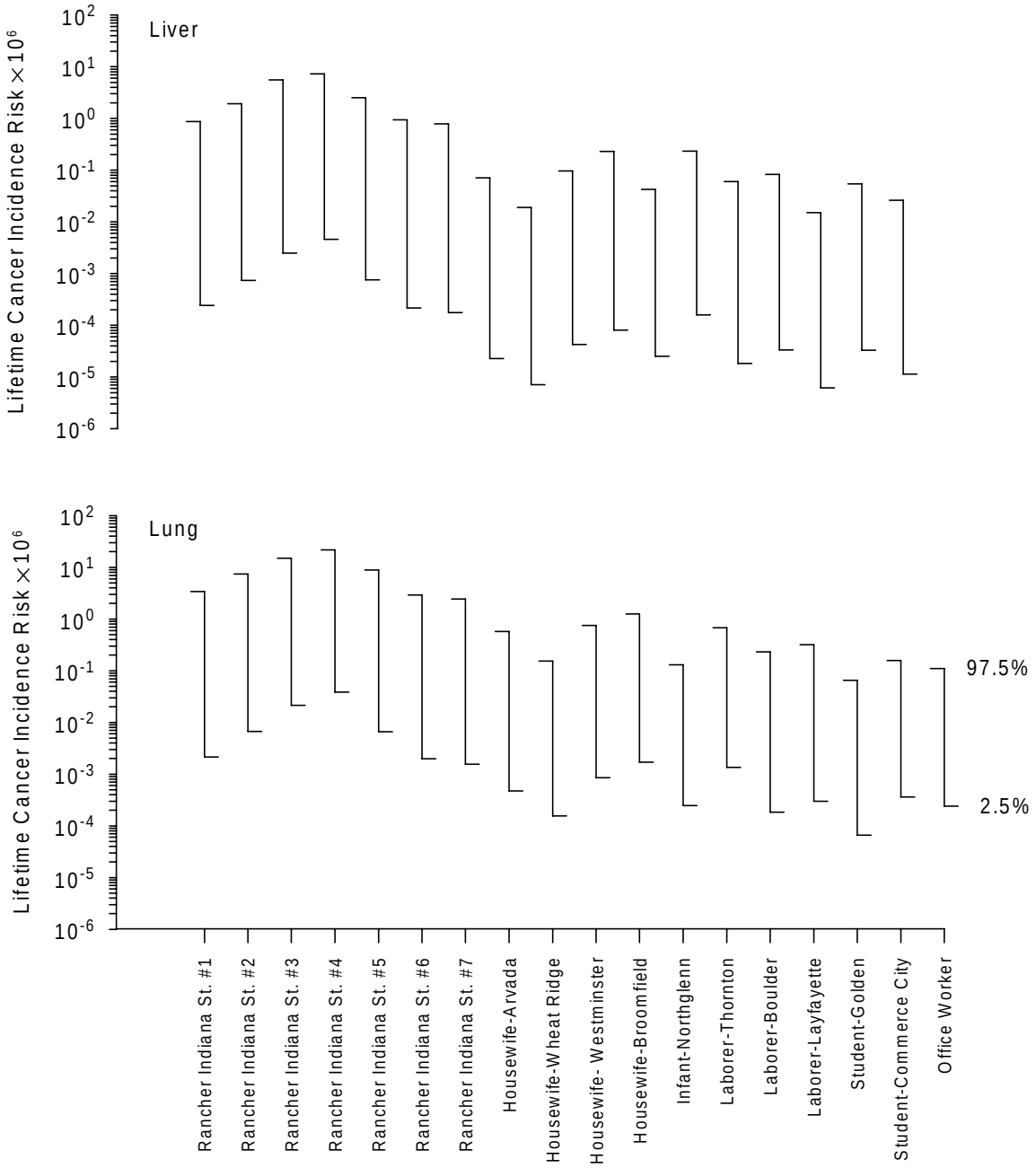

Figure 13. Incremental lifetime cancer incidence risk estimates for the lung and liver for the 18 exposure scenarios. The range of values shown represent 2.5% and 97.5% on the cumulative density function.

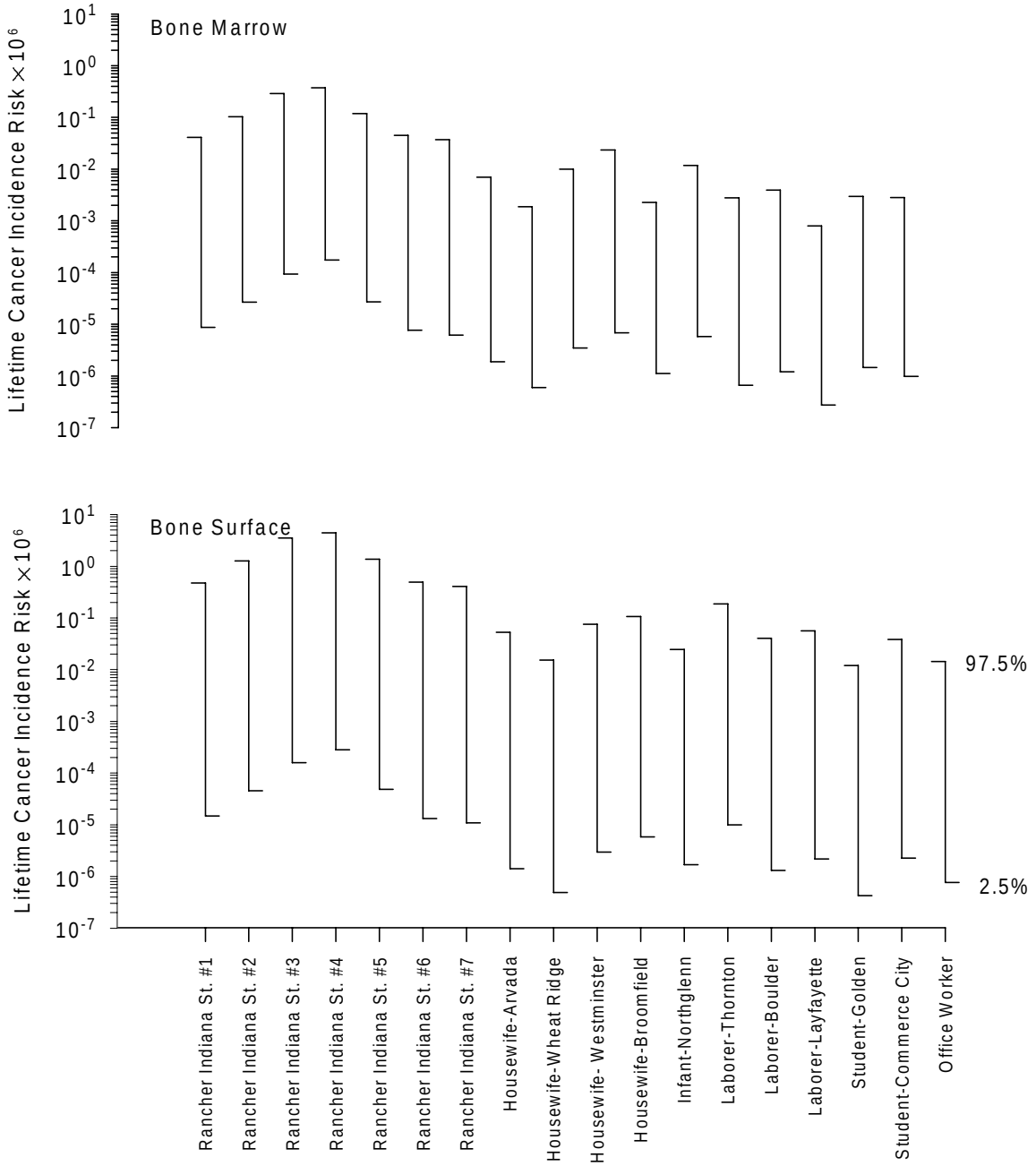

Figure 14. Incremental lifetime cancer incidence risk estimates for bone surface and bone marrow for the 18 exposure scenarios. The range of values shown represent 2.5% and 97.5% on the cumulative density function.

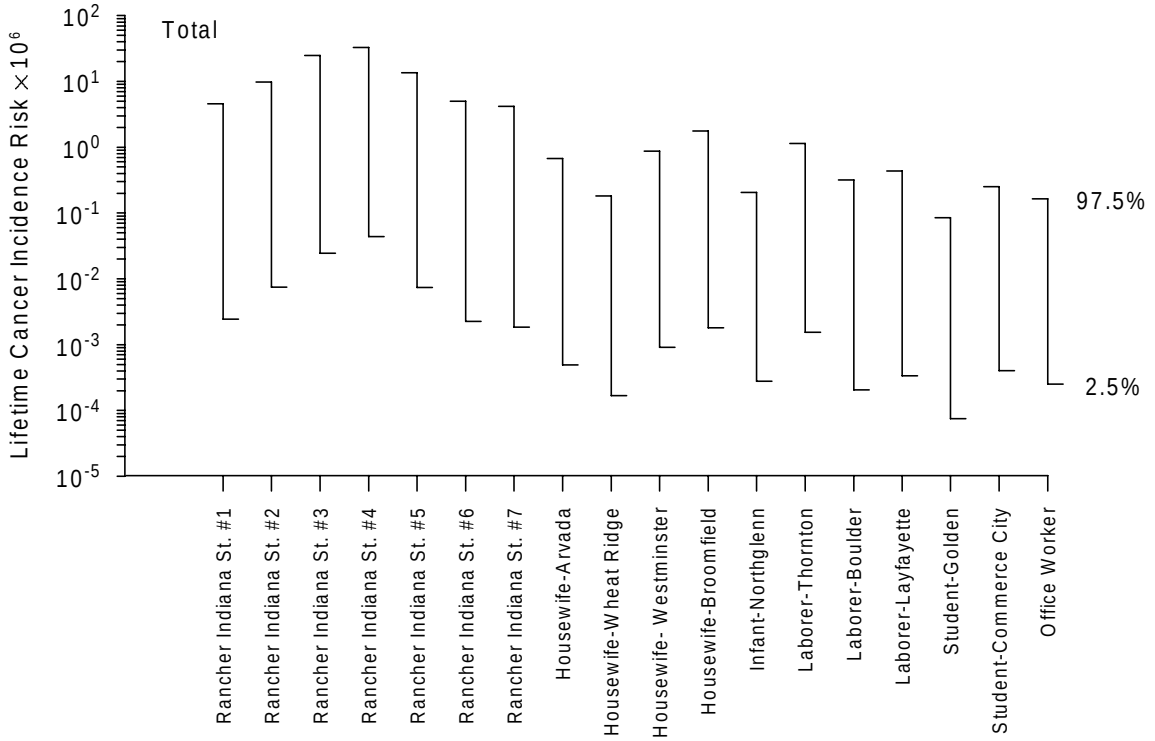

Figure 15. Incremental lifetime cancer incidence risk estimates for all organs for the 18 exposure scenarios. The range of values shown represent 2.5% and 97.5% on the cumulative density function.

REFERENCES

Abbott, M.L. and A.S. Rood. 1996. *Source Group Optimization Program (SGOP): A Program the Groups Emission Sources for Input into Air Dispersion Models*. INEL-96/0376. Idaho National Engineering Laboratory, Idaho Falls, Idaho.

Briggs, G.A. 1969. *Plume Rise*. TID-25075. U.S. Atomic Energy Commission, Washington, D.C.

Briggs, G.A. 1975. "Plume Rise Predictions." *Lectures on Air Pollution and Environmental Impact Analysis.* American Meteorological Society, Boston, Massachusetts. 59–111.

Briggs, G.A. 1984. "Plume Rise and Buoyancy Effects." *Atmospheric Science and Power Production.* DOE/TIC-27601. U.S. Department of Energy, Washington, D.C. 327–366.

Brown, K.J. 1991. *Rocky Flats 1990-91 Winter Validation Tracer Study*. Report AG91-19, North American Weather Consultants, Salt Lake City, Utah.

Byun, D.W. and R. Dennis, 1995. "Design Artifacts in Eulerian Air Quality Models: Evaluation of the Effects of Layer Thickness and Vertical Profile Correction on Surface Ozone Concentrations." *Atmospheric Environment*, (29): 105–126.

Carhart, R.A., A. J. Policastro, M. Wastag, and L. Coke. 1989. "Evaluation of Eight Short-Term Long-Range Transport Models Using Field Data." *Atmospheric Environment* 23 (1): 85–105.

ChemRisk. 1994a. *Dose Assessment for Historical Contaminant Releases from Rocky Flats*. Project Task 8 for Phase I. Prepared for the Colorado Department of Public Health and Environment. ChemRisk, A division of McLaren/Hart, 1135 Atlantic Avenue, Alameda, California 94501. September.

ChemRisk. 1994b. *Exposure Pathway Identification and Transport Modeling*. Project Task 6 for Phase I. Prepared for the Colorado Department of Public Health and Environment. ChemRisk, A division of McLaren/Hart, 1135 Atlantic Avenue, Alameda, California 94501. May.

ChemRisk, 1994c. *Demographic & Land Use Reconstruction of the Area Surrounding the Rocky Flats Plant*. Task 7 for Phase I. Prepared for the Colorado Department of Public Health and Environment. ChemRisk, A division of McLaren/Hart, 1135 Atlantic Avenue, Alameda, California 94501. April.

CFR (Code of Federal Regulations). 1996. *Guidelines for Air Quality Models*. 40 CFR Part 51, Appendix W, August 12, 1996.

Cowherd, C. Jr., G.E. Muleski, P.J. Englehart, and D.A. Gillette. 1985. *Rapid Assessment of Exposure to Particulate Emissions from Surface Contamination Sites*. EPA/600/8-85/002. U.S. Environmental Protection Agency, Office of Health and Environmental Assessment, Washington, D.C. February.

Crow, L.W., 1974. *Characteristic Airflow Patterns near Rocky Flats Plant and Their relationship to Metropolitan Denver*. LWC-143. Report prepared for Dow Chemical USA, Rocky Flats Division, December.

Decisioneering Inc. 1996. Crystal Ball Forecasting and Risk Analysis Software Version 4.0. Boulder, Colorado.

DOE (U.S. Department of Energy). 1980. *Final Environmental Impact Statement, Rocky Flats Plant*. DOE/EIS-0064. April.

DOE. 1995. *Rocky Flats Environmental Technology Site Historical Data Summary*. AV-R-93-08-200. February.

EPA (U.S. Environmental Protection Agency). 1987. *On-Site Meteorological Program Guidance for Regulatory Modeling Applications*. EPA-450/4–87–013, Research Triangle Park, North Carolina.

EPA. 1992. *User's Guide for the Industrial Source Complex (ISC) Dispersion Models Vol. 1, User's Instructions*. EPA-450/4–92–008a. Research Triangle Park, North Carolina.

EPA. 1995. *User's Guide for the Industrial Source Complex (ISC3) Dispersion Models Vol. 1, User's Instructions*. EPA-454/B–95–003b. Research Triangle Park, North Carolina.

Elderkin, C. E. and P. H. Gudiksen. 1993. "Transport and Dispersion in Complex Terrain." *Radiation Protection Dosimetry* 50: 265–271.

Genikhovich, E.L. and F.A. Schiermeier. 1995. "Comparison of United States and Russian Complex Terrain Diffusion Models Developed for Regulatory Applications." *Atmospheric Environment* 29 (17): 2375–2385.

Gifford, F.A. 1961. "Use of Routine Meteorological Observations for Estimating Atmospheric Dispersion." *Nuclear Safety* 2 (4): 47–51.

Gifford, F.A. 1983. "Atmospheric Diffusion in the Mesoscale Range: Evidence of Recent Plume Width Observations." *Sixth Symposium on Turbulence and Diffusion, American Meteorological Society*. Boston, Massachusetts.

Gillette, D.A. 1974. "On the Production of Soil Wind Erosion of Soil: Effect of Wind and Soil Texture." *Atmospheric-Surface Exchange of Particulate and Gaseous Pollutants*. ERDA Symposium Series 38, Oak Ridge Tennessee. 591–609.

Golder, D. 1972. "Relations among Stability Parameters in the Surface Layer." *Boundary-Layer Meteorology* 3(1): 47–58.

Grogan, H.A., W.K. Sinclair, and P.G. Voillequé, 1999. *Assessing Risks of Exposure to Plutonium*. 5-CDPHE-RFP-1999-FINAL(Rev. 1), *Radiological Assessments Corporation*, Neeses, South Carolina. August.

HAP (Health Advisory Panel). 1993. *Health Advisory Panel's Report to Colorado Citizens on the Phase I Study of the State of Colorado's Health Studies on Rocky Flats*. Colorado Department of Health. Denver, Colorado.

Harper, F.T., S.C. Hora, M.L. Young, L.A. Miller, C.H. Lui, M.D. McKay, J.C. Helton, L.H.J. Goossens, R.M. Cooke, J. Pasler-Sauer, B. Kraan, and J.A. Jones. 1995. *Probability Accident Consequence Uncertainty Analysis, Dispersion and Deposition Uncertainty Assessment*. NUREG/CR-6244, U.S. Nuclear Regulatory Commission. Washington, D.C.

Hatch, W.L. 1988. *Selective Guide to Climatic Data Sources*. Key to Meteorological Records Documentation No. 4.11, National Climatic Data Center, Asheville, North Carolina.

Hicks, B.B., K.S. Rao, R.J. Dobosy, R.P. Hosker, J.A. Herwehe, and W.R. Pendergrass. 1989. *TRIAD: A Puff-Trajectory Model for Reactive Gas Dispersion with Application to UF_6 Releases to the Atmosphere.* ERL ARL-168, National Oceanic and Atmospheric Administration, Air Resources Laboratory. Silver Spring, Maryland.

Hodgin, C.R. 1991. *Terrain-Responsive Atmospheric Code (TRAC) Transport and Diffusion: Features and Software Overview*. Report RFP-4516, EG&G Rocky Flats. Golden, Colorado.

ICRP (International Commission on Radiological Protection). 1990. *1990 Recommendations of the International Commission on Radiological Protection* ICRP Publication 60. *Annals of the ICRP* 21, Nos 1–3, Pergamon Press, Oxford.

ICRP. 1994. Human Respiratory Tract model for Radiological Protection. ICRP Publication 66. *Annals of the ICRP* 24, Nos 1–3. Pergamon Press, Oxford.

ICRP 1995. *Age-Dependent Doses to Members of the Public from Intake of Radionuclides: Part 4, Inhalation Dose Coefficients*. ICRP Publication 71. Ann. ICRP 25, Nos 3 & 4. Pergamon Press, Oxford.

Killough, G.G., M.J. Case, K.R. Meyer, R.E. Moore, S.K. Rope, D.W. Schmidt, B. Shleien, W.K. Sinclair, P.G. Voillequé, and J.E. Till. 1998. *Task 6: Radiation Doses and Risk to Residents from FMPC Operations from 1951–1988*. Volume II, Appendices. 1-CDC-Fernald-1998-FINAL (Vol. II). *Radiological Assessments Corporation*. Neeses, South Carolina. September.

Krey, P.W. and E.P. Hardy. 1970. *Plutonium in Soil around the Rocky Flats Plant*. Report HASL-235. Health and Safety Laboratory, U.S. Atomic Energy Commission, New York, New York.

Layton, D.W. 1993. "Metabolically Consistent Breathing Rates for use in Dose Assessment" *Health Physics* 64 (1): 23–36.

Litaor, M.I. 1993. "Spatial Analysis of Plutonium Activity in Soils East of Rocky Flats Plant." In *Environmental Health Physics Proceedings of the Twenty-Sixth Midyear Topical Meeting of the Health Physics Society*. Edited by R.L. Kathren, D.H. Denham, and K. Salmon. Columbia Chapter, Health Physics Society, Richland, Washington. 117–136.

Litaor, M.I. 1995. "Spatial Analysis of Plutonium 239+240 and Americium-241 in Soils around Rocky Flats, Colorado." *Journal of Environmental Quality* 24: 506–516.

Little C.A. 1976. *Plutonium in a Grassland Ecosystem*. Doctoral Dissertation, Department of Radiology and Radiation Biology, Colorado State University, Fort Collins, Colorado.

Luna, R.E. and H.W. Church. 1972. "A Comparison of Turbulence Intensity and Stability Ratio Measurements to Pasquill Stability Classes." *Journal of Applied Meteorology* 11 (4): 663–669.

Meyer, H.R., S.K. Rope, T.F. Winsor, P.G. Voillequé, K.M. Meyer, L.A. Stetar, J.E. Till, and J.M. Weber. 1996. *The Rocky Flats Plant 903 Area Plutonium Source Term Development*.

RAC Report 2-CDPHE-RFP-1996-FINAL. *Radiological Assessments Corporation*, Neeses, South Carolina.

Miller, C.W. and L.M. Hively. 1987. "A Review of Validation Studies for the Gaussian Plume Atmospheric Dispersion Model." *Nuclear Safety* 28 (4): 522–531.

Miller, C.W., F.O. Hoffman, and D.L. Shaeffer. 1978. "The Importance of Variations in the Deposition Velocity Assumed for the Assessment of Airborne Radionuclide Releases." *Health Physics* 34: 730–734.

NCRP (National Council on Radiological Protection and Measurement). 1991. *Some Aspects of Strontium Radiobiology*. NCRP Report No. 110. National Council on Radiological Protection and Measurement, Bethesda, Maryland.

Panofsky, H.A. and J.A. Dutton. 1984. *Atmospheric Turbulence*. New York: J. Wiley and Sons.

Pasquill, F. 1961. "The Estimation of the Dispersion of Windborne Material." *The Meteorological Magazine* 90: 33–49.

Pasquill, F. and F.B. Smith. 1983. *Atmospheric Diffusion*, 3rd Edition. New York: Halsted Press.

Petersen, W.B. and L.G. Lavdas. 1986. *INPUFF 2.0 - A Multiple Source Gaussian Puff Dispersion Algorithm: User's Guide*. EPA-600/8-86/024. Atmospheric Sciences Research Laboratory, U.S. Environmental Protection Agency, Research Triangle Park, North Carolina.

Pleim, J., A. Venkatram, and R Yamartino, 1984. *ADOM/TADAP Model Development Program. Volume 4, The Dry Deposition Module*. Ontario Ministry of Environment, Rexdale, Ontario.

Press, W.H., S.A. Teukolsky, W.T. Vetterling, and B.P. Flannery. 1992. *Numerical Recipes: The Art of Scientific Computing*. New York, New York: Cambridge University Press.

Poet, S.E. and E.A. Martell. 1972. "Plutonium-239 and Americium-241 Contamination in the Denver Area." *Health Physics* 23: 537–548.

Ramsdell, J.V. Jr., C.A. Simonen, and K.W. Burk. 1994. *Regional Atmospheric Transport Code for Hanford Emission Tracking* (RATCHET). PNWD-2224 HEDR. Battelle Pacific Northwest Laboratories, Richland, Washington.

Robertson, E. and P.J. Barry. 1989. "The Validity of a Gaussian Plume Model When Applied to Elevated Releases at a Site on the Canadian Shield." *Atmospheric Environment* 23 (2): 351–362.

Rope, S.K., K.R. Meyer, M.J. Case, H.A. Grogan, D.W. Schmidt, M. Dreicer, T.F. Winsor, and J.E. Till. 1999. *Task 4: Evaluation of Environmental Data for Historical Public Exposure Studies on Rocky Flats*. *RAC* Report No. 1-CDPHE-RFP-1997-Final (Rev. 1). *Radiological Assessments Corporation,* Neeses, South Carolina. August.

Rood, A.S. 1999a. *Rocky Flats Dose Reconstruction Project, Phase II: Performance Evaluation of Atmospheric Transport Models*. *RAC* Report 3-CDPHE-RFP-1996-FINAL(Rev. 1). *Radiological Assessments Corporation,* Neeses, South Carolina. August

Rood, A.S., 1999b. *Estimated Exposure and Lifetime Cancer Incidence Risk from Routine Plutonium Releases at the Rocky Flats Plant. RAC* Report 8-CDPHE-RFP-1997-FINAL(Rev. 1). *Radiological Assessments Corporation*, Neeses, South Carolina, August.

Roy, M. and C. Courtay. 1991. "Daily Activities and Breathing Parameters for Use in Respiratory Tract Dosimetry." *Radiation Protection Dosimetry* 35 (3): 179–186.

Schere, K.L. and C.J. Coates. 1992. "A Stochastic Methodology for Regional Wind-Field Modeling." *Journal of Applied Meteorology* 31 (12): 1407–1425.

Seinfeld, J.H. 1986. *Atmospheric Chemistry and Physics of Air Pollution*. New York: John Wiley and Sons.

Simpson, D., D.A. Perrin, J.E. Varey, and M.L. Williams. 1990. "Dispersion Modeling of Nitrogen Oxides in the United Kingdom." *Atmospheric Environment* 24 (7): 1713–1733.

Slinn, S.A. and W.G.N. Slinn, 1980. "Predictions for Particle Deposition in Natural Waters." *Atmospheric Environment* (14): 1031–1-16.

Slinn, W.G.N., 1982. "Predictions for Particle Deposition to Vegetative Canopies." *Atmospheric Environment* (16): 1785–1974.

Slinn, W.G.N. 1984. "Precipitation Scavenging." In *Atmospheric Science and Power Production*. Edited by D. Randerson. DOE/TIC-27601. U.S. Department of Energy, Washington, D.C. 466–532.

Stull, R.B. 1988. *An Introduction to Boundary Layer Meteorology*. Dordrecht, Netherlands: Kluwer Academic Publishers.

Turner, D.B. 1964. "A Diffusion Model for an Urban Area." *Journal of Applied Meteorology* 3 (1): 83–91.

Webb, S.B., J.M. Stone, S.A. Ibrahim, and F.W. Whicker. 1994. "The Spatial Distribution of Plutonium in Soil Near the Ricky Flats Plant." In *Plutonium and Americium in the Environs of Rocky Flats: Spatial Distribution, Environmental Transport, and Human Exposure, a Report to Dow Chemical Company.* F.W. Whicker and S.A. Ibrahim Principal Investigators. Colorado State University, Fort Collins, Colorado.

Weber, J.M., A.S. Rood, H.R. Meyer, and J.E. Till. 1999. *Development of the Rocky Flats Plant 903 Area Plutonium Source Term. RAC* Report 8-CDPHE-RFP-1998-FINAL(Rev 1). *Radiological Assessments Corporation*, Neeses, South Carolina. August.

Weil, J.C. 1985. "Updating Applied Diffusion Models." *Journal of Climate and Applied Meteorology* 24 (11): 1111–1130.

Whicker, F.W. and V. Schultz. 1982. *Radioecology: Nuclear Energy and the Environment*. Boca Raton, Florida: CRC Press Inc.

Winges, K.D. 1990. *User's Guide for the Fugitive Dust Model*. EPA-910/9-88-202R. U.S. Environmental Protection Agency, Region 10, Seattle, Washington.

Zilitinkevich, S.S. 1972. "On the Determination of the Height of the Ekman Boundary Layer." *Boundary-Layer Meteorology* 3 (2): 141–145.